JUSTUS-LIEBIG-
UNIVERSITÄT
GIESSEN

# Characterization and *S*-glutathionylation of hexokinase from the malaria parasite *Plasmodium falciparum*

**A thesis submitted to the Faculty of Biology and Chemistry (FB 08) in fulfilment of the requirements of the Doctor of Science Degree of Justus Liebig University Giessen, Germany**

**By**

**Tao Zhang**

**from**
**Henan, China**

**June 2013**

# Declaration

I declare that this thesis is my original work and other sources of information have been properly quoted. This work has not been previously presented to obtain any other degree from any other university.

Ich erkläre: Ich habe die vorgelegte Dissertation selbständig und ohne unerlaubte fremde Hilfe und nur mit den Hilfen angefertigt, die ich in der Dissertation angegeben habe. Alle Textstellen, die wörtlich oder sinngemäß aus veröffentlichten Schriften entnommen sind, und alle Angaben, die auf mündlichen Auskünften beruhen, sind als solche kenntlich gemacht. Bei den von mir durchgeführten und in der Dissertation erwähnten Untersuchungen habe ich die Grundsätze guter wissenschaftlicher Praxis, wie sie in der „Satzung der Justus-Liebig-Universität Gießen zur Sicherung guter wissenschaftlicher Praxis“ niedergelegt sind, eingehalten.

Giessen, 11st, June 2013 …….

# Dedication

*To my family*

The thesis was presented for examination on the 17th July 2013 to the Faculty of Biology and Chemistry of the Justus Liebig University Giessen, Germany. This thesis was supervised by Prof. Dr. Katja Becker and Prof. Dr. Tina Trenczek.

**The thesis defense examination committee was composed of:**

**Prof. Dr. Katja Becker**

Biochemistry and Molecular Biology

Interdisciplinary Research Centre (IFZ)

Justus-Liebig-University Giessen

Heinrich-Buff-Ring 26-32, 35392 Giessen

Germany

**Prof. Dr. Tina Trenczek**

Institute of General Zoology and Developmental Biology

Justus Liebig University Giessen

Stephanstr. 24, 35390 Giessen

Germany

**Prof. Dr. Eveline Baumgart-Vogt**

Institute of Anatomy and Cell Biology

Justus Liebig University Giessen

Aulweg 123, 35385 Giessen

Germany

**Prof. Dr. Albrecht Bindereif**

Institute of Biochemistry

Justus Liebig University Giessen

Heinrich-Buff-Ring 58, 35392 Giessen

Germany

# Acknowledgements

I wish to sincerely thank Prof. Katja Becker and Prof. Tina.E.Trenczek for supervising my PhD project. Especially, I would like to thank Prof. Katja Becker, who offered me the opportunity to work in her group and supported me to apply for a PhD degree at JLU. She gave me excellent scientific supervision, continuous encouragement and support during my research work. I also would like to thank Prof. Akhil Vaidya (Drexel University, USA) for the support with the knockout of *Pf*HK in *P. falciparum*.

My sincere gratitude goes to all the distinguished members of Prof. Becker's research group both past and present members (2009-2013). To Dr. Stefan Rahlfs, I would like to thank for his long term patient advising, insightful views and creative discussion. I benefited a lot from his expertise in bioinformatics. I wish to thank Dr. Esther Jortzik for her valuable advice and discussion of enzyme assay and kinetics. Many thanks go to Dr. Sebastian Kehr for making me familiar with the lab work in our group. To Elisabeth Fischer, thanks for the support with the cell culture experiments. Thanks a lot to Michaela Stumpf for the help with crystallization and gel filtration. And many thanks to Timothy Bostick for critically proof-reading my PhD thesis. I would like to thanks all other group members, including Rimma Iozef, Beate Hecker, Karin Fritz-Wolf, Ulrike Burkhard-Zahrt, Lihui Wang, Jipeng Ma, Dennis Matovu Kasozi, Jette Pretzel, Janina Preuss, Franziska Mohring, Jochen Bathke, Kathleen Zocher and Christina Brandstädter for all the help I have gained from you.

I wish to acknowledge the 'China Scholarship Council' (CSC) for the generous financial support throughout my PhD study in Germany.

Finally, I would like to thank all my family members and friends for their support. Their sacrifices and encouragement help me to overcome all the difficulties in my life and give me the courage to pursue my dream.

## List of Publications

1. **Zhang T**, Jortzik E, Rahlfs S, Becker K. (2013). Characterization of hexokinase from malaria parasite *Plasmodium falciparum*. In preparation

……..

2. Han My, **Zhang T,** Zhao Cp, Zhi Jh. (2011). Regulation of the expression of lipoxygenase genes in *Prunus persica* fruit ripening. *Acta Physiologiae Plantarum*. 4: 1345-1352

## Conferences and Scientific Meetings

1. **Zhang T**, Jortzik E, Rahlfs S, Becker K. (**2012**). Characterization and *S*-glutathionylation of hexokinase in *Plasmodium falciparum*. *5th Annual Conference of the International Giessen Graduate School for the Life Sciences (GGL)*, Giessen, September 18th-19th, 2012.

2. **Zhang T**, Jortzik E, Rahlfs S, Becker K. (**2011**). Characterization and *S*-glutathionylation of hexokinase in *Plasmodium falciparum*. *4th Annual Conference of the International Giessen Graduate School for the Life Sciences (GGL)*, Giessen, September 21st-22nd, 2011.

3. **Zhang T**, Jortzik E, Rahlfs S, Becker K. (**2010)**. Characterization and *S*-glutathionylation of hexokinase in *Plasmodium falciparum*. *3th Annual Conference of the International Giessen Graduate School for the Life Sciences (GGL)*, Giessen, September 29th-30th, 2010.

# Summary

Tropical malaria caused by the unicellular apicomplexan parasite *Plasmodium* is still a major threat to human health and welfare in tropical and subtropical regions of the world. In the past decades, both the emergence of antimalarial resistance of *Plasmodium* and insecticide-resistance in the mosquito vector made the situation more and more severe. The progress in developing a malaria vaccine, in identifying new drug targets, and in developing novel antimalarials is slow. Hexokinase represents a central enzyme of glucose metabolism in the malaria parasite *P. falciparum*. Due to the high glucose dependence of the parasite, studying hexokinase can enhance our knowledge of central metabolic processes in *Plasmodium* and contribute to the search for new antimalarial drug targets. In this thesis, I have therefore studied hexokinase (*Pf*HK) from *P. falciparum* including its kinetic properties as well as its redox regulation.

First, *Pf*HK has been successfully cloned, heterologously overexpressed in *Escherichia coli* and purified to homogeneity. Gel filtration indicated that recombinant *Pf*HK is present as a tetramer. Kinetic studies showed relatively low affinities for the substrates glucose and ATP when compared with the human homologues. In contrast to the common 50-kDa hexokinases in other species, *Pf*HK can be inhibited by G6P. Two constructs of GFP fused *Pf*HK (full-length and C-terminally truncated) were generated and revealed that the sub-cellular localization of *Pf*HK is cytosolic in *P. falciparum*. The data furthermore showed that the C-terminal hydrophobic region in *Pf*HK does not seem to lead to membrane association of the protein. In order to obtain crystals of *Pf*HK and solve its three-dimensional structure, more than 500 crystallization conditions were tested. Although no high quality crystals have been obtained so far, the screening seems to be worth of further optimization. To gain first structural insights, a model of *Pf*HK was generated based on the structure of human hexokinase I (PDB ID: 1DGK). Three insertions were found on the surface of *Pf*HK when comparing the structure with its human counterpart, which might provide a basis for selective inhibitor development.

In a second focus of my work, I studied the redox regulation of *Pf*HK, which had been shown to be a target of members of the thioredoxin superfamily and of *S*-glutathionlylation. Thioredoxin-related proteins (thioredoxin 1, glutaredoxin and plasmoredoxin of *P. falciparum*) slightly enhanced the

activity of *Pf*HK. Similar results were obtained with DTT incubation which indicates an underlying reductive mechanism. Furthermore *Pf*HK was inhibited by *S*-glutathionylation, an effect that could be partially reversed by DTT. Different incubation conditions with glutathione were tested and anti-GSH antibodies were used to probe *S*-glutathionylation. After trypsin digestion, a clear mass increase of ~305 Da was observed in several cysteine- containing peptides by MALDI-TOF. *S*-glutathionylation was reproducibly found on $Cys^{21}$, $Cys^{249}$, $Cys^{236}$, and $Cys^{346}$.

Thirdly, to validate *Pf*HK as a drug target in *P. falciparum*, I started to generate a *Pf*HK knockout strain. For this purpose, first a merodiploid strain was constructed which can episomally express *Pf*HK. The transgenic parasites were obtained and in a next step the knockout of endogenous *Pf*HK will be performed.

The experiments performed in this study represent important steps towards characterizing *Pf*HK as a potential target of novel antimalarial compounds.

# Zusammenfassung

Tropische Malaria, die durch den einzelligen Parasiten der Gattung Apikomplexa, *Plasmodium*, verursacht wird, stellt weiterhin eine große Bedrohung für Gesundheit und Wohlergehen der Menschen in tropischen und subtropischen Regionen der Welt dar. In den vergangenen Jahrzehnten haben sowohl die Verbreitung von Resistenzen des Malariaerregers gegen eingesetzte Medikamente, als auch Pestizidresistenzen der Vektormücke die Situation ständig verschlechtert. Der Fortschritt in der Entwicklung von Impfstoffen, in der Identifizierung von neuen Angriffspunkten für Medikamente und in der Entwicklung von neuen Medikamenten gegen Malaria geht nur langsam voran. Die Hexokinase repräsentiert ein zentrales Enzym in dem Glukosemetabolismus des Malariaparasiten *P. falciparum*. Infolge der hohen Glukoseabhängigkeit des Parasiten kann die Erforschung der Hexokinase dazu beitragen, zentrale metabolische Prozesse in *Plasmodium* zu verstehen und neue Ziele für die Entwicklung neuer Medikamente gegen Malaria zu finden. Deshalb habe ich in meiner Arbeit die Kinetik und Redoxregulation der Hexokinase aus *Plasmodium falciparum* untersucht.

Als erstes wurde *Pf*HK kloniert, in *Escherichia coli* heterolog überexprimiert und gereinigt. Die Gelfiltrationschromatografie weist darauf hin, dass die rekombinante *Pf*HK als Tetramer vorliegt. Kinetische Untersuchungen zeigen, im Vergleich zu dem humanen Homolog, eine relativ geringe Affinität zu den Substraten Glukose und ATP. Im Gegensatz zu den üblichen 50-kDa-Hexokinasen in anderen Spezies, kann *Pf*HK durch G6P gehemmt werden. Es wurden zwei Fusionskonstrukte aus GFP und *Pf*HK (full-length und C-terminal verkürzt) hergestellt, die erkennen lassen, dass *Pf*HK im Zytosol von *P. falciparum* lokalisiert ist. Des Weiteren zeigten die Daten, dass die C-terminale hydrophobische Region der *Pf*HK nicht zu einer Membranassoziation des Proteins führt. Um Kristalle der *Pf*HK zu erhalten und die dreidimensionale Struktur aufzulösen, wurden mehr als 500 Kristallisationsbedingungen getestet. Obwohl bisher keine hochqualitativen Kristalle erhalten wurden, Wird es sich lohnen, das Screening weiter zu optimieren. Um erste Kenntnisse über die Struktur zu gewinnen, wurde ein Modell basierend auf der Struktur der humanen Hexokinase I (PDB ID: 1DGK) erstellt. Im Vergleich mit dem humanen Gegenstück wurden drei Insertionen auf der Oberfläche der *Pf*HK gefunden, die eine Basis für die Entwicklung selektiver Inhibitoren darstellen könnten.

Ein zweiter Fokus meiner Arbeit richtete sich auf die Redoxregulation der *Pf*HK, von der gezeigt

wurde, dass sie ein Angriffspunkt von Mitgliedern der Thioredoxinsuperfamilie und der *S*-Glutathionylierung ist. Thioredoxin-verwandte Proteine (Thioredoxin 1, Glutaredoxin und Plasmoredoxin von *P. falciparum*) erhöhen leicht die Aktivität der *Pf*HK. Ähnliche Ergebnisse wurden durch die Inkubation mit DTT erhalten, was dafür spricht, dass ein reduktiver Mechanismus zugrunde liegt. Des Weiteren wurde die *Pf*HK durch *S*-Glutathionylierung gehemmt, einen Effekt, der teilweise durch DTT reversibel ist. Es wurden verschiedene Inkubationsbedingungen mit Glutathion getestet und anti-GSH-Antikörper genutzt um die *S*-Glutathionylierung zu untersuchen. Nach dem Trypsinverdau wurde eine Masse von ~305 Da in verschiedenen Cystein-enthaltenden Peptiden durch MALDI-TOF beobachtet. *S*-Glutathionylierung wurde reproduzierbar in $Cys^{21}$, $Cys^{249}$, $Cys^{236}$ und $Cys^{346}$ gefunden.

Drittens, um *Pf*HK als Ziel für Medikamente gegen *P. falciparum* zu validieren, habe ich angefangen einen *Pf*HK knockout-Stamm herzustellen. Für diesen Zweck wurde zunächst ein merodiploider Stamm konstruiert, der episomal *Pf*HK exprimiert. Die transgenen Parasiten sind vorhanden und in einem nächsten Schritt wird der knockout des endogenen *Pf*HK durchgeführt werden.

Die Experimente, die in dieser Studie durchgeführt wurden sind wichtige Schritte auf dem Weg zur charakerisierung der *Pf*HK als Ziel für neuartige Antimalariamittel.

# Table of Contents

**Declaration** ..... **I**

**Dedication** ..... **II**

**Acknowledgements** ..... **IV**

**List of Publications** ..... **V**

**Conferences and Scientific Meetings** ..... **V**

**Table of Contents** ..... **X**

**List of Figures** ..... **XIV**

**List of Tables** ..... **XVI**

**List of Abbreviations** ..... **XVII**

**Introduction** ..... **1**

**1.1 Malaria** ..... **1**

1.1.1 Life cycle of *Plasmodium falciparum* ..... 3

1.1.2 Control of malaria ..... 5

1.1.2.1 Development of chemotherapeutics ..... 5

1.1.2.2 Development of a malaria vaccine ..... 6

1.1.3 Glucose metabolism of *P. falciparum* in the human blood stage ..... 8

**1.2 Rationale of the study** ..... **10**

1.2.1 Hexokinase ..... 10

1.2.1.1 Isoforms of hexokinase ..... 11

1.2.1.2 Structure of hexokinase ..... 13

1.2.1.3 Hexokinase in humans ..... 17

1.2.1.4 Hexokinase in *Plasmodium falciparum* ..... 21

1.2.2 Protein *S*-Glutathionylation ..... 23

1.2.3 Genetic manipulation of *Plasmodium falciparum* ..... 25

**1.3 Objective of the study** ..... **26**

1.3.1 Hexokinase from *P. falciparum* ..... 26

1.3.2 *S*-Glutathionylation of *Pf*HK ..... 27

1.3.3 Knockout of *Pf*HK ..... 27

**2. Materials** ..... **28**

**2.1 Chemicals ..... 28**

**2.2 Antibodies ..... 30**

**2.3 Antibiotics ..... 30**

**2.4 Enzymes ..... 30**

2.4.1 Restriction Enzymes ..... 30

2.4.2 DNA Polymerase ..... 31

2.4.3 Other enzymes ..... 31

**2.5 Biological materials ..... 31**

2.5.1 Plasmids ..... 31

2.5.2 *E. coli* strains ..... 31

2.5.3 *Plasmodium falciparum* strain ..... 32

**2.6 Kits ..... 32**

**2.7 Materials of affinity chromatography ..... 32**

**2.8 Medium for *E. coli* culture ..... 32**

**2.9 Instruments ..... 33**

**2.10 Protease inhibitors ..... 34**

**2.11 Buffers and solutions ..... 34**

2.11.1 Buffer for DNA electrophoresis ..... 34

2.11.2 Buffer for extraction of *P. falciparum* parasites ..... 34

2.11.3 Buffer for HK assay ..... 35

2.11.4 Buffer for protein purification ..... 35

2.11.5 Buffer for SDS-PAGE electrophoresis ..... 35

2.11.6 Western blot buffer ..... 36

2.11.7 Stock solutions ..... 36

**3. Methods ..... 36**

**3.1 General methods ..... 36**

3.1.1 Preparation of competent cells ..... 36

3.1.2 Cleavage of double stranded DNA by restriction endonucleases and ligation ..... 37

3.1.3 Transformation of competent cells ..... 37

3.1.4 SDS-polyacrylamide gel electrophoresis ..... 37

3.1.5 Western blot....38

3.1.7 Determination of protein concentration....40

**3.2 *Pf*HK methods....40**

3.2.1 Cloning of *Pf*HK....40

3.2.2 Heterologous overexpression of *Pf*HK....42

3.2.3 Optimization of the heterologous overexpression of *Pf*HK....42

3.2.4 Purification of *Pf*HK....42

3.2.5 Optimization of *Pf*HK purification....42

3.2.6 Gel filtration of *Pf*HK....43

3.2.7 Western blot using anti-His antibody to identify *Pf*HK....43

3.2.8 *Pf*HK kinetic assay....43

3.2.8.1 Determination of $K_m$ values for ATP and glucose....43

3.2.8.2 *Pf*HK's pH and buffers profile....44

3.2.8.3 Feedback inhibition with ADP and G6P....45

3.2.8.4 Test for HK activity in full blood and *P. falciparum*-infected RBC....45

3.2.9 *Pf*HK regulation by *P. falciparum* redox proteins....46

3.2.10 *S*-Glutathionylation of *Pf*HK....46

3.2.11 Deletion mutant of *Pf*HK....47

3.2.11.1 Mutagenesis PCR....47

3.2.11.2 Heterologous overexpression of truncated *Pf*HK....48

3.2.12 GFP construction of full-length and truncated *Pf*HK....49

3.2.12.1 *P. falciparum* cell culture....50

3.2.12.2 Synchronization....50

3.2.12.3 Parasite transfection....51

3.2.12.4 Immunofluorescence imaging....51

3.2.12.5 Western blot analysis....51

3.2.13 *Pf*HK knockout....52

3.2.13.1 Construction of the merodiploid strain....52

3.2.14 *Pf*HK crystal screening....56

## 4. Results 57

**4.1 *Pf*HK characterization....57**

4.1.1 Sequence alignment and phylogenetic tree....57

4.1.3 Cloning, heterologous overexpression and purification of recombinant *Pf*HK....59

4.1.4 *Pf*HK oligomerization studies....60

4.1.4 Test of buffers, pH and salt for *Pf*HK ..... 64

4.1.5 *Pf*HK kinetic studies ..... 64

4.1.6 *Pf*HK product inhibition ..... 67

4.1.7 Redox regulation of *Pf*HK ..... 67

4.1.8 *S*-Glutathionylation of *Pf*HK ..... 69

4.1.9 Inhibition of *Pf*HK by compounds with antimalarial activity ..... 72

**4.2 *Pf*HK localization ..... 72**

**4.3 Activity of HKs in *P. falciparum*-infected erythrocytes ..... 73**

**4.4 Crystallization and structure prediction of *Pf*HK ..... 75**

**4.5 *Pf*HK knockout ..... 79**

4.4.1 Generation of a *Pf*HK merodiploid strain ..... 79

4.4.2 Knockout of *Pf*HK in both wild type and merodiploid Dd2 strains ..... 79

**5 Discussion ..... 80**

**5.1 Hexokinase in *Plasmodium falciparum* ..... 80**

**5.2 Structure analysis of *Pf*HK for estimating the potency as antimalarial drug target ..... 85**

**5.3 Cysteine residues of *Pf*HK as the target of redox regulation and *S*-glutathionylation. ..... 87**

**6 References ..... 89**

# List of Figures

Figure 1.1: Worldwide distribution of countries at risk of malaria .....1

Figure 1.2: Life cycle of malaria .....4

Figure 1.3: Vaccine candidates targeting different life cycle stages .....7

Figure 1.4: Carbon flow through the metabolic network of *P. falciparum* .....9

Fig 1.5: Scheme depicting the hypothesis of hexokinase evolution. .....13

Fig 1.6: Structure of yeast hexokinase with open (A) and closed (B) conformations. .....14

Fig 1.7: Stereoview of the monomer and dimer of hexokinase I in humans. .....15

Fig 1.8: Active site of the C-terminal half of monomeric hexokinase I. .....16

Figure 1.9: Scheme of the allosteric regulation in hexokinase I monomer .....17

Figure 1.10: Tumors harness a multitude of genetic, epigenetic, transcriptional and post-translational strategies for enhanced expression and function of hexokinase II. .....20

Figure 1.11: Mitochondrial-bound hexokinase II plays a major role in preventing tumor apoptosis. .....21

Figure 1.12: Scheme depicting different pathways leading to the formation of protein S-glutathionylation .....24

Figure 3.1: Transfer stack in semi-dry Western blot .....39

Figure 3.2: Schematic diagram of the primer design for site-directed mutagenesis .....48

Figure 3.3: Structure of GFP fusion construction of the *PfHK* gene in *pARL-2a+* .....49

Figure 3.4: The *PfHK* gene in the *pLN* vector. .....53

Figure 3.5: Scheme of the dual-plasmid attB×attP recombination .....54

Figure 3.6: Structure of the pUF-1 vector .....55

Figure 4.1: Multiple sequence alignment of *Pf*HK with six hexokinases from other species .....58

Figure 4.2: Radial phylogenetic tree generated by using the neighbour-joining method based on the results of multiple sequence alignments of HKs from various species. .....59

Figure 4.3: Purification and gel filtration result of recombinant *Pf*HK. .....60

Figure 4.4: *Pf*HK tetramer structure in the presence of 4 mM DTT .....61

Figure 4.6: Michaelis-Menten, Lineweaver-Burk, Eadie-Hofstee, and Hanes graphs of *Pf*HK with glucose and ATP. .....65

Figure 4.7: The double reciprocal plots of *Pf*HK for the reaction with ATP and glucose as substrates. .66

Fig 4.8: Inhibition of *Pf*HK by G6P. .68

Fig 4.9: Inhibition of *Pf*HK by ADP. .68

Figure 4.11: Activity of *Pf*HK after incubation with redox proteins and DTT. .69

Figure 4.12: Western blot of glutathionylation of *Pf*HK. .70

Figure 4.13: Glutathionylated cysteins in *Pf*HK as detected by mass spectrometric analysis .71

Figure 4.14: *Pf*HK incubated with different concentrations of oxidized glutathione at 4 °C overnight. .71

Figure 4.15: *Pf*HK incubated with different concentrations of oxidized glutathione at room temperature .71

Figure 4.16: Reversibility of the glutathionylation of *Pf*HK. .72

Figure 4.17: The images of subcellular localization of *Pf*HK. .73

Figure 4.18: Activities of HKs in RBC lysates .74

Figure 4.19: Western blots of infected and uninfected RBC using antibodies against *Pf*TrxR (A) and *Pf*GluPho (B) .75

Figure 4.20: Image of the crystal screening .76

Figure 4.21: The predicted secondary structure of *Pf*HK. .77

Figure 4.22: The *Pf*HK models and details of substrate binding sites .78

Figure 4.23: Western blot of the episomal *Pf*HK. .79

Figure 5.1: Schematic representation of a random mechanism of *Pf*HK. .83

Figure 5.2: Comparison of human hexokinase type I (yellow) (amino acids 16 to 459) and a model of *Pf*HK (blue) (amino acids 29 to 488) .87

# List of Tables

Table 1.1: Targets for antimalarial chemotherapy .....5

Table 1.2 The molecular dimensions of hexokinases .....13

Table 3.1: Composition of SDS-PAGE gels. .....38

Table 3.2: Primers for HK-GFP constructs .....49

Table 3.3: Primers for knockout constructs .....55

Table 4.1: Optimization of the buffers used for heterologous overexpression of *Pf*HK .....61

Table 4.2: Optimization of the heterologous overexpression of *Pf*HK .....62

Table 4.3: Optimization of the purification of heterologously overexpressed *Pf*HK .....63

Table 4.4: Kinetic parameters of *Pf*HK. .....67

Table4.5: Promising conditions for crystallization screening. .....76

Table 5.1: Summary of kinetic parameters of hexokinase .....82

# List of Abbreviations

| | |
|---|---|
| ACTs | Artemisinin-based combination therapies |
| ART | Artemisinin |
| ATM | Artemether |
| ATP | Adenosine triphosphate |
| APS | Ammonium persulfate |
| BSA | Bovine serum albumin |
| CQ | Chloroquine |
| DHFR | Dihydrofolate reductase |
| dNTP | Deoxynucleotide triphosphate |
| DMSO | Dimethyl sulfoxide |
| DNA | Deoxyribonucleic acid |
| DNase | Deoxyribonuclease |
| DTT | 1, 4-Dithiothreitol |
| *E. coli* | *Escherichia coli* |
| EDTA | Ethylenediaminetetraacetic acid |
| FPLC | Fast protein liquid chromatography |
| HK | Hexokinase |
| $H_2O_{dd}$ | Double distilled water |
| IPTG | Isopropyl-β-D-thiogalactopyranoside |
| kDa | Kilodalton |
| LB | Lysogeny Broth Medium |
| NADH | β-Nicotinamide adenine dinucleotide, reduced disodium salt |
| Ni-NTA | Nickel nitrilotriacetic acid |
| OD | Optical density |
| PBS | Phosphate buffered saline |
| PCR | Polymerase chain reaction |

| | |
|---|---|
| PEG | Polyethylene glycol |
| *Pf* | *Plasmodium falciparum* |
| PMSF | Phenylmethylsulfonylfluoride |
| PVDF | Polyvinyl difluoride |
| RBC | Red blood cells |
| SDS | Sodium dodecyl sulphate |
| SDS-PAGE | Sodium dodecyl sulphate – polyacrylamide gel electrophoresis |
| TB | Terrific Broth medium |
| TEMED | N,N,N',N'-Tetramethylethylenediamine |
| WHO | World Health Organisation |
| µg | Microgram |
| µl | Microliter |
| µM | Micromolar |

# Introduction

## 1.1 Malaria

The malaria parasite causes a life-threatening tropical disease via the bite of infected mosquitoes and still plagues tropical and sub-tropical regions. Because of its high morbidity and mortality, malaria is a great endemic infectious disease and a major disease burden in these countries, as are HIV and tuberculosis (Mechai *et al*., 2012). According to the WHO 2012 report, malaria caused an estimated 219 million illnesses and 660,000 deaths in 2010, having fallen by more than 25% since 2000 (WHO, 2012). Approximately 80% of cases and 90% of deaths were estimated to occur in Africa, with children under five years of age and pregnant women most severely affected; 90% of the cases are caused by *P. falciparum* (Murray *et al*., 2012; WHO, 2012).


**Figure 1.1: Worldwide distribution of countries at risk of malaria (WHO 2011)**

"*Mal' aria*," which means bad air in Italian and was associated with marshy areas, has been noted for more than 4,000 years and has probably influenced to a great extent human populations and human history (CDC 2013). People have struggled unremittingly with this ancient, preventable, and treatable disease. In 2700 B.C., the symptoms of malaria were described in ancient Chinese medical writings. In Europe malaria also became widely recognized in Greece by the 4$^{th}$ century B.C., and it was

responsible for the decline of many of the city-states' populations. By the age of Pericles, there were extensive references to malaria in literature, and depopulation of rural areas was recorded (CDC 2013). In the development of malaria parasitology, many events are remarkable from the end of the 19th century. Charles Louis Alphonse Laveran, a French army surgeon, firstly discovered the parasites in the blood of the patients suffering from malaria in 1880, and he was awarded the Nobel Prize in 1907. During the same period, Camillo Golgi, an Italian neurophysiologist, devoted himself to the differentiation of species of malaria in 1886. Ronald Ross demonstrated and solved malaria transmission in 1887 and was awarded the Noble Prize in 1902. Finally the complete sporogonic cycle of *P. malaria* was demonstrated in 1899 by an Italian team (CDC 2013).

In order to fight against malaria, people have applied more than 1,277 plant species from 160 families as herbal medicines over thousands of years (Willcox *et al.*, 2004). The *qing hao* plant and cinchona bark as the representative herbal medicines are used to extract artemisinins and quinine, which are the potent and effective drugs today. In some poor, rural areas with malaria epidemics, these traditional medicines are still a choice to exploit as affordable and effective treatment (Willcox *et al.*, 2004). In the antimalarial chemical synthesis, chloroquine (resochin) was discovered by a German, Hans Andersag, in 1934 at Baye IG and was established as an effective and safe antimalarial in 1946 by British and U.S. scientists (CDC website 2013). Until now artemisinin-based combination therapies (ACTs) are the pillars of first-line treatment of malaria cases.

The Global Malaria Eradication Program was initiated by the WHO in 1955, relying on chloroquine for prevention and treatment as well as DDT for vector control (WHO, 1999). This program achieved success in eliminating malaria from North America, the Caribbean, Central-South America, Europe, and parts of Asia (Carter *et al.*, 2002). However, this strategy of massive and rapid application of DDT to interrupt transmission of the disease, regardless of geography and epidemiology, failed to interrupt transmission completely in many countries, and malaria resurged to previous levels (Feachem *et al.*, 2008). After the emergence of chloroquine-resistant *Plasmodium* parasites and DDT-resistant *Anopheles* mosquitoes (Brito, 2001), the eradication program was abandoned in 1972. With the spread of chloroquine resistance from the early 1970s, the situation began to deteriorate slowly and progressively. At the same time, malaria mortality doubled or more in most parts of Africa (Trape *et al.*, 2002). To combat this worsening situation, many organizations initiated several programs to control or eliminate this public health problem. In 1992, the global strategy for malaria control was adopted by a

Global Ministerial Conference on Malaria. The strategy has four elements: to provide early diagnosis and prompt treatment; to plan and implement selective and sustainable preventive measures, including vector control; to detect early, contain, or prevent epidemics; and to strengthen local capacities in basic and applied research (Dr. B.S. Kakkilaya's Malaria Web Site 2006). The Roll Back Malaria (RBM) program, which was started in 1998 by the World Health Organization, the United Nations Development Program, the United Nations Children's Fund, and the World Bank, focused on establishing a global partnership to control malaria effectively (WHO Malaria report 2012). The aim of this program was to halve the global malaria burden of risk, morbidity, and mortality by 2010 (Hay *et al*., 2004). In 2007, the Bill & Melinda Gates Foundation renewed a call, originally set forth by the WHO in 1955, for malaria eradication. And in 2011, the UN Secretary-General declared a goal of reducing malaria deaths to zero by 2015 (Murray *et al*., 2012). Achieving this ambitious goal requires the development of new tools to monitor, prevent, and treat malaria.

### 1.1.1 Life cycle of *Plasmodium falciparum*

Malaria is a parasitological disease caused by protozoan parasites of the genus *Plasmodium* from the phylum *Apicomplexa*. There are five *Plasmodium* species, *P. falciparum*, *P. knowlesii* (Collins, 2012; Singh *et al*., 2004), *P. malariae*, *P. ovale*, and *P. vivax*, which cause human malaria. *P. falciparum* and *P. vivax* are the two predominant species responsible for most malaria infection (WHO, 2011). *P. falciparum* is the most lethal one, which causes over 90% of deaths in Africa (WHO, 2012). All five of these *Plasmodium* species exhibit a similar complex life cycle with slight differences, composed of different stages and multiple forms that inhabit multiple cell types including the vertebrate host (human) and invertebrate vector (*Anopheles* mosquito) (Figure 1.2). The malaria infection begins with a bite from an infected *Anopheles* female mosquito. Normally more than 25 sporozoites in the saliva of a mosquito are inoculated into the subcutaneous tissue and then migrate into the blood stream. Via the circulatory system, sporozoites invade the hepatocytes in the liver, initiating liver stage development (the pre-erythrocytic phase). This stage lasts about 6 days. After asexual replication, thousands of merozoites are released into the blood stream and invade erythrocytes beginning asexual blood stage development (erythrocytic phase). Notably, *P. vivax* and *P. ovale* are capable of undergoing a dormant period instead of asexual replication within hepatocytes. Within the erythrocytes, the parasites live in the cytosol and develop their own plasma membrane. From the young trophozoites, called the ring

stage due to its morphology, the parasites develop into mature trophozoites within 24 hours after invasion. Approximately 36 hours after invasion, parasites develop into the schizont stage, which is indicated by repeated nuclear division without cellular segmentation. Later the schizonts develop and form merozoites in the erythrocytes. About 48 hours after invasion, the mature merozoites rupture the erythrocytes and spread into the bloodstream to invade new erythrocytes, reinitiating a new round of the erythrocytic life cycle. The asexual blood stage of *Plasmodum* parasites is responsible for all the clinical manifestations and the pathology associated with malaria. To transmit malaria, a few parasites in the form of blood-stage merozoites develop into macrogametocytes (female) and microgametocytes (male), which are ingested into the mosquito gut when a female mosquito bites an infected human. Gametogenesis can be induced by several factors, such as a sudden drop in temperature, a rise in pH, or the metabolites within the mosquito. The male gametocyte develops into eight flagellated microgametes, which escape from the enclosing erythrocytes (exflagellation). Macrogametes can be fertilized by microgametes and form motile zygotes (ookinetes). This zygote then resembles a wart on the outside of the mosquito gut and develops an oocyst when it traverses the peritrophic membrane and epithelium of the mosquito midgut. Numerous threadlike sporozoites are released after oocyst maturation and rupture. The sporozoites quickly migrate to the salivary glands and start the next round of infection once the mosquito bites a human. Normally the mosquito becomes infectious two weeks after ingesting gametocytes from an infected human.

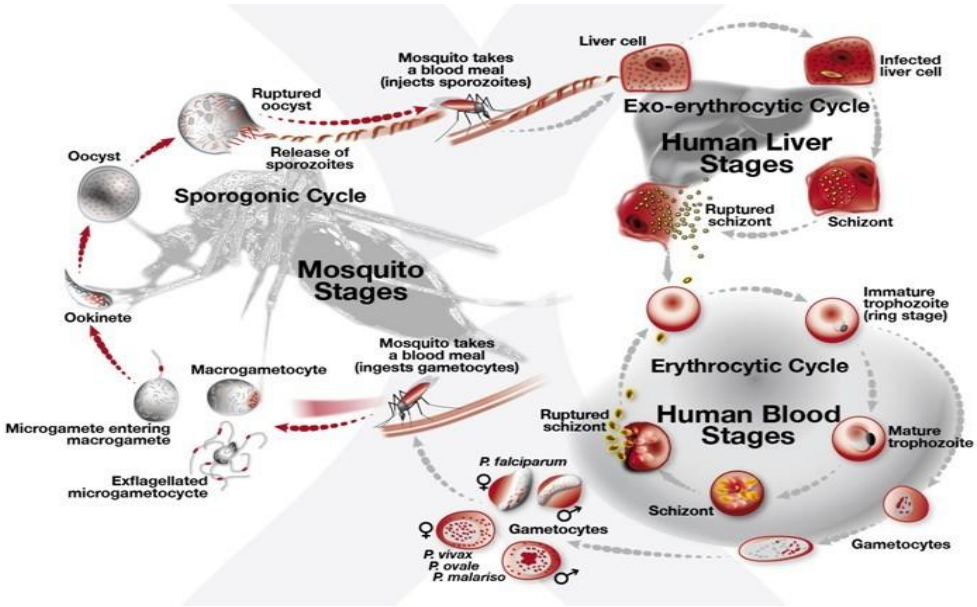


**Figure 1.2: Life cycle of malaria (EVI website 2013)**

### 1.1.2 Control of malaria

After the first Global Malaria Eradication Program which was abandoned in 1972, the situation of malaria in some parts of the world (especially in Africa) progressively deteriorated, and antimalarial resistance emerged (Trape, 2001). In order to control the havoc wrought by malaria, antimalarial chemotherapy is still the predominant treatment, but the development of an effective vaccine would bring a more promising future.

#### 1.1.2.1 Development of chemotherapeutics

Through several decades fighting against malaria, antimalarial chemotherapy by drugs can be divided into a few classes: quinolines, antifolates, artemisinins, atovaquone, pyrimethamine, and their derivatives. After decades of research, understanding of the action site of antimalarial drugs has increased remarkably (Table 1.1).

| Target location | Pathway/mechanism | Target molecule | Examples of therapies | |
|---|---|---|---|---|
| | | | Existing therapies | New compounds |
| Cytosol | Folate metabolism | Dihydrofolate reductase | Pyrimethamine, proguanil | Chlorproguanil |
| | | Dihydropteroate synthase | Sulphadoxine, dapsone | |
| | Glycolysis | Thymidylate synthase | | 5-fluoroorotate |
| | | Lactate dehydrogenase | | Gossypol derivatives |
| | | Peptide deformylase | | Actinonin |
| | Protein synthesis | Heat-shock protein 90 | | Geldanamycin |
| | Glutathione metabolism | Glutathione reductase | | Enzyme inhibitors |
| | Signal transduction | Protein kinases | | Oxindole derivatives |
| | Unknown | $Ca^{2+}$-ATPase | Artemisinins | |
| Parasite membrane | Phospholipid synthesis | Choline transporter | | G25 |
| | Membrane transport | Unique channels | Quinolines | Dinucleoside dimers |
| | | Hexose transporter | | Hexose derivatives |
| Food vacuole | Haem polymerization | Haemozoin | Chloroquine | New quinolines |
| | Haemoglobin hydrolysis | Plasmepsins | | Protease inhibitors |
| | | Falcipains | | Protease inhibitors |
| | Free-radical generation | Unknown | Artemisinins | New peroxides |
| Mitochondrion | Electron transport | Cytochrome *c* oxidoreductase | Atovaquone | |
| Apicoplast | Protein synthesis | Apicoplast ribosome | Tetracyclines, clindamycin | |
| | DNA synthesis | DNA gyrase | Quinolones | |
| | Transcription | RNA polymerase | Rifampin | |
| | Type II fatty acid bio-synthesis | FabH | | Thiolactomycin |
| | | FabI/PfENR | | Triclosan |
| | Isoprenoid synthesis | DOXP reductoisomerase | | Fosmidomycin |
| | Protein farnesylation | Farnesyl transferase | | Peptidomimetics |
| Extracellular | Erythrocyte invasion | Subtilisin serine proteases | | Protease inhibitors |

**Table 1.1: Targets for antimalarial chemotherapy (Fidock, et al. 2004)**

The quinoline family, which comprises chloroquine, amodiaquine, quinine, mefloquine, etc., used to be the gold standard for the treatment of malaria with its efficacy, low toxicity, and affordability (less than US $0.20 for a three-day adult treatment course) (White, 1996). These drugs acts by binding to heme moieties and interfering with heme detoxification in infected erythrocytes (Fitch, 2004). Because of the abuse, only a decade later the first report of chloroquine-resistant strains of *P. falciparum* came out

(Wellems *et al*., 2001). To date ACTs have become the mainstay of malaria control (WHO, 2010) because of their beneficial properties such as rapid action and a broad spectrum. The ACT combination therapies are the first choice of treatment of malaria cases. There are five recommended combinations available currently: artemether-lumefantrine, artesunate-amodiaquine, artesunate-mefloquine, artesunate-sulfadoxine-pyrimethamine, and dihydroartemisinin-piperaquine (WHO, 2012). In spite of the emergence of resistance in *P. falciparum* in Southeast Asia (Anderson *et al*., 2010), the ACTs still contribute to over 90% worldwide clinical efficacy (WHO, 2012). Current evidence suggested that the mechanism of ART and derivates is to cleave the endoperoxide bridge, leading to alkylation of essential biomolecules (O'Neill *et al*., 2004).

For decades, the rise of resistant *P. falciparum* strains interrupted the efficacies of almost all antimalarial drugs. The mechanism was not clearly understood. Recent research found that the mutation of transporters was a major contributor to drug resistance, and three transporters are focused on: the chloroquine-resistance transporter *Pf*CRT, the multi-drug resistance-associated protein *Pf*MRP, and the multi-drug-resistant transporter 1 *Pf*MDR1 (Sanchez *et al*., 2010). The multiple polymorphic alleles of *pfcrt* are related to different levels of chloroquine resistance (Sa *et al*., 2009). The *Pf*MRP was demonstrated to transport multiple antimalarial drugs out of the parasites (Raj *et al*., 2009). Single nucleotide polymorphisms of *pfmdr1* encoding an ATP-binding cassette (ABC) transporter and a homolog of P-glycoprotein in humans regulate drug susceptibility (Reed *et al*., 2000; Sidhu *et al*., 2005).

In the challenging situation of combating malaria, novel drugs are desperately needed. The new antimalarial drugs must meet the requirement of rapid efficacy, minimal toxicity, and low cost (Fidock *et al*., 2004). However, traditional drug development strategies hardly meet these desires. Therefore, an effective vaccine against malaria would offer the prospect of malaria elimination.

#### 1.1.2.2 Development of a malaria vaccine

To control, prevent and eradicate malaria, a safe, effective, and affordable malaria vaccine is a vital milestone. Then natural immunity to malaria can be acquired via repeated malaria infection. This immunity to human malaria is largely mediated by IgG antibodies, but the specific antigens that these antibodies target are difficult to pinpoint (Hviid, 2007). This immunity response is generally short-lived, possibly because malaria infections hinder the development of B cell memory (Dorfman *et al*., 2005).

Although the acquisition of natural immunity response seems to appears only at blood stages of malaria, the development of a malaria vaccine is focused on three life cycle stages: the sporozoite and liver stage (pre-erythrocytic vaccines), the asexual blood stage (blood stage vaccines), and the sexual gametocyte/gamete stage (transmission blocking vaccines) (Ashley *et al*., 2012).

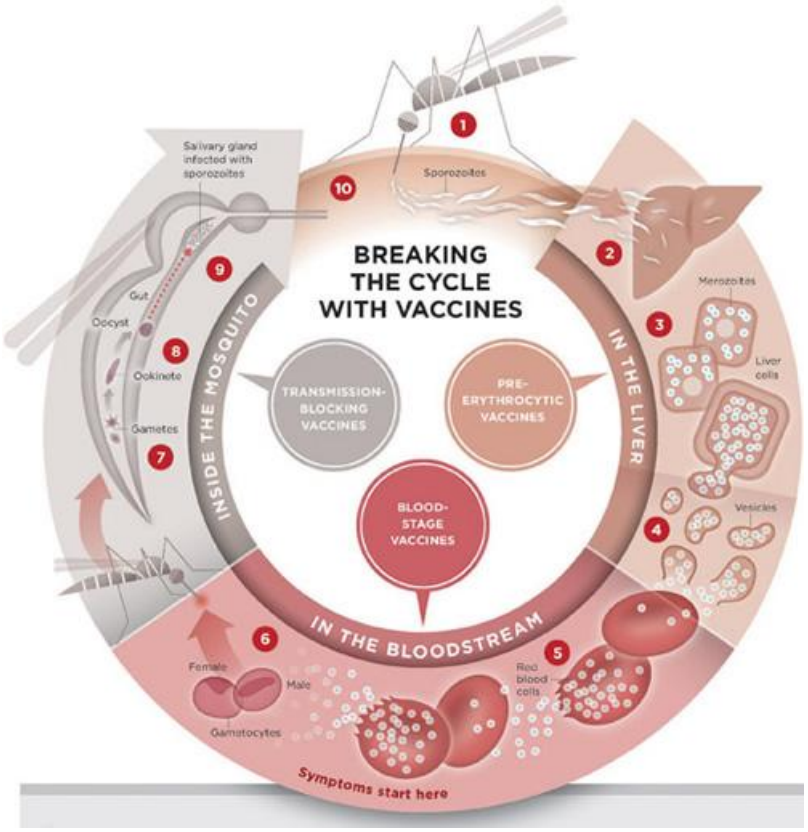


**Figure 1.3: Vaccine candidates targeting different life cycle stages (MVI 2013)**

The pre-erythrocytic vaccines aim to elicit an immune response in order to prevent infection or attack the infected hepatocytes at the liver stage, where parasites enter or mature in hepatocytes. The circumsporozoite protein (CSP) is a promising target, because strong immunity response can be elicited during natural exposure or vaccination (Calvo-Calle *et al*., 2005). RTS vaccine, which shows the best result of immunity so far, is fused to the amnio-terminal portion of HBsAg with portions of the *P. falciparum* CSP polypeptide. However, the protection of clinical malaria has only been 56% until now (Patterson *et al*., 2008).

Besides the pre-erythrocytic vaccines, the blood stage vaccines target *Plasmodium* at its most destructive stage (the rapid replication of the organism in erythrocytes). The blood-stage vaccines aim to decrease the number of parasites (the merozoites) in the blood to reduce the severity of disease. Up

until now, the candidate antigens in the blood stage are composed of merozoite surface protein 1-3 (MSP1-3), apical membrane antigen 1 (AMA-1), erythrocyte-binding surface antigen 175 (EBA-175), glutamate-rich protein (GLURP), ring-infected erythrocyte surface antigen (RESA), and serine repeat antigen 5 (SERA5) (Ashley *et al.*, 2012). The evidence shows that low concentrations of anti-basigin antibodies of conserved merozoite ligands can block the invasion of malaria completely (Crosnier *et al.*, 2011). Transmission-blocking vaccines (TBVs) seek to interrupt the life cycle of malaria by inducing antibodies to prevent the parasite from maturing in the mosquito. These vaccines would not prevent human infection by malaria or attenuate the symptoms of disease, but they would limit the transmission by mosquitoes. Research of *Pf*s25, a protein expressed on the surface of the zygote and ookinete form of the parasites, showed that high anti-*Pf*s25 IgG titers and sera from immunized mice inhibited the transmission of *P. falciparum* to the mosquito in mice (Goodman *et al.*, 2011).

Despite recent progress, the development of a malaria vaccine is still as complex as ever. In order to achieve the long-term goal of over 80% efficacy against malaria, there is still a long way to go (Nussenzweig *et al.*, 2011).

### 1.1.3 Glucose metabolism of *P. falciparum* in the human blood stage

Glucose, the most important and abundant nutrient in human serum, is essential for the asexual stage of *P. falciparum* to survive and multiply (Kirk, 2001). The intra-erythrocytic parasites possess a significantly streamlined carbon metabolic network in which the TCA cycle plays a minor role and derives most of its energy from glucose fermentation (Kirk *et al.*, 1996; van Dooren *et al.*, 2006). After infection, the parasites increase glucose consumption 50 to 100-fold at the most metabolically active trophozoite and schizont stages (Roth, 1990). After a couple hours of glucose starvation, *P. falciparum* parasites appeared as shrunken, rounded bodies with pyknotic nuclei and failed to recover viability via glucose re-supplementation (Babbitt *et al.*, 2012). Besides extreme glucose dependence, the glucose metabolism of *P. falciparum* is also quite different from the human host.

The transport of glucose into erythrocytes is mediated by the human glucose transporter and the *Plasmodium* glucose transporter (*Pf*HT) with relatively high affinities ($K_m$ <1 mM) (Geary et al., 1985). The utilization of glucose in parasites can be catalogued into the core conserved components of carbon metabolism: glycolysis and the pentose phosphate pathway (PPP). The intermediate of glycolysis and the PPP can be integrated into lipid biogenesis, glycosylation, and at least some

components of citric acid metabolism (Olszewski *et al*., 2011).

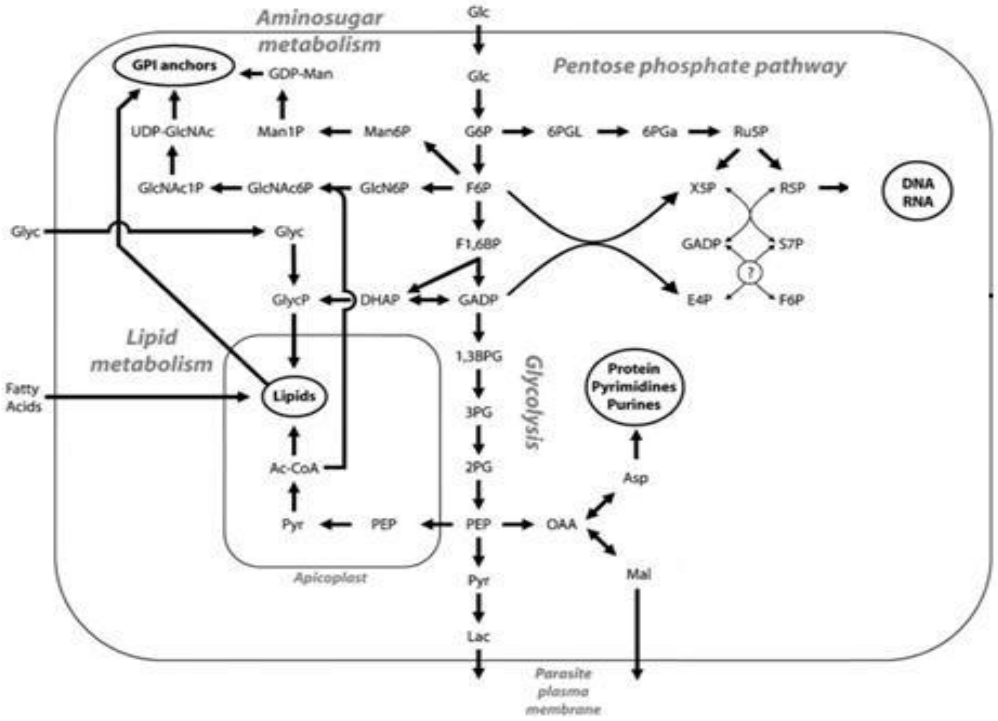


**Figure 1.4: Carbon flow through the metabolic network of *P. falciparum* (Olszewski et al., 2011)**

Based on numerous classical experiments, the Embden-Meyerhof-Parnas (EMP) pathway has been verified to be central to carbon metabolism in blood stage *Plasmodium* parasites. This glucose-to-lactate convention provides ATPs for energy and metabolic intermediates, which involves other physiological process such as ribose synthesis, lipid metabolism, and amino sugar metabolism. By completely sequencing the *P. falciparum* genome, it was shown that the parasites possess all the enzymes found in glycolysis. Due to rapid multiplication and the absence of a functional citric acid cycle in *P. falciparum*, the huge requirement of ATP must be obtained by a mass of glucose fermentation. With voracious glucose assimilation, *Plasmodium* glycolysis consumes and incompletely oxidizes approximately 60-70% of glucose to lactic acid (Jensen *et al*., 1983). This large consumption of glucose by parasites and excretion of lactic acid to the host correlate with the metabolic complications (lactic acidosis and hypoglycemia) of malaria.

The pentose phosphate pathway is another critical and conserved glucose metabolism pathway in *Plasmodium*, which oxidizes glucose-6-phosphate to ribose for nucleic acid synthesis and NADPH for redox regulation and as a cofactor for biosynthetic reactions. Due to the high metabolic rate of their

rapid growth and multiplication in erythrocytes, *Plasmodium* parasites demand a large amount of ribose and are confronted with continuous oxidative stress from the large quantities of toxic redox-active byproducts (Becker *et al.*, 2004). Hence a highly efficient PPP is essential for the asexual stages of the parasites. In investigations, the activity of this oxidative pathway in infected erythrocytes increased 78-fold at the trophozoite stages (Atamna *et al.*, 1994). The parasites contribute 82% of this activity, and the erythrocytes' PPP is also up-regulated 24-fold to levels roughly similar to those observed when subjecting uninfected erythrocytes to oxidative stress (Olszewski *et al.*, 2011). It seems that the active PPP is important for both parasites and their host blood cells to eliminate the toxicity of reactive oxidative species. After all, maintaining the host erythrocytes' survival is required to sustain the parasites' viability.

As *Plasmodium* parasites rely on glucose, the utilization of glucose and the enzymes involved in glucose metabolism have been studied over many years and have the potential to contribute to the development of new anti-malarial drugs directed e.g. against the glucose transporter (*Pf*HT1) or the rate-limiting enzyme in the PPP (glucose-6-phosphate dehydrogenase-6-phosphogluconolactonase).

## 1.2 Rationale of the study

With the tardy progression of vaccine development and the rapid emergence of both antimalarial drug and insecticide resistance, the situation of malaria is becoming increasingly severe. In reports, there is no more clinical and parasitological response to the malaria of ART-resistant strains which can resist almost all antimalarial drugs. In response to this dire situation, research and identification of new drug candidates is becoming more urgent. From the inspiration of anti-cancer therapy and the rigid dependence on glucose, this glucose utilization of *Plasmodium* parasites could be a promising target of antimalarial drugs. *Plasmodium* hexokinase which contributes to the first step of glucose utilization is an ideal target to disturb the glucose metabolism of the parasites. Also, the whole genomic sequencing of *Plasmodium falciparum* reveals that there is only one isoenzyme of *Pf*HK, that and it exists as a single copy in the genome. The investigation of catalytic mechanism and post-translational regulation of *Pf*HK may provide the hints for a novel anti-malarial drug.

### 1.2.1 Hexokinase

In a large part of prokaryotic cells and all eukaryotic cells hexokinase as the pacemaker of glucose

metabolism starts the initial step of intracellular glucose utilization by phosphorylating glucose to form glucose-6-phosphate (G6P). After phosphorylation the imported glucose can be trapped in the cytoplasm, entering different metabolic pathways. The subsequent metabolic fates of G6P may vary in different types of cells and under different physiological conditions. Hexokinase prefers glucose as the primary substrate and can also phosphorylate other hexoses, as the recommended name of ATP:D-hexose 6-phosphotransferase (EC 2.7.1.1 indicates). Only a few species, especially bacteria, are known to possess the enzyme specific for glucose, which is called glucokinase (ATP:D-glucose 6-phophotransferase, EC 2.7.1.2) (Ureta *et al.*, 1987). In different species hexokinases differ in molecular mass and tissue distribution, and these enzymes normally exist as a mixture of isoenzymes that again have different kinetic characteristics and molecular masses. The differential expression of isoenzymic forms of hexokinases may be an important factor in determining the pattern of glucose metabolism in cells. Besides the function of glucose phosphorylation, many studies have proved that the different isoforms of hexokinases are involved in a series of metabolic regulations and physiological processes.

#### 1.2.1.1 Isoforms of hexokinase

The first system with multiple hexokinases was demonstrated in yeast with three isoenzymes: hexokinase $P_I$ and $P_{II}$ and glucokinase (Kaji *et al.*, 1961). From then on the isoenzymes of hexokinases have been successively found in different species. More than two isoforms of hexokinases have been found and examined in green plants and several invertebrate species (Jang *et al.*, 1997; Ureta *et al.*, 1987). In mammals, the hexokinase isoforms were first reported in rodent livers (Viñuela *et al.*, 1963; Walker, 1963) and seem to be a characteristic of all animals. In human tissues these isoenzymes were also verified (Brown *et al.*, 1967; Rogers *et al.*, 1975). Furthermore, the hexokinases in vertebrate species have been characterized in four isoenzymes, named hexokinase types I, II, III, and IV (Katzen *et al.*, 1965) on the basis of their electrophoretic mobility; hexokinase IV is commonly called 'glucokinase' because of its substrate specificity.

The molecular mass of most native hexokinases in different species is 50 kDa or 100 kDa, and the subunits also exist with the molecular mass of 50 kDa or 100 kDa (Table 1.2 ). There are some smaller molecular mass hexokinases that were found in eubacteria, i.e., 24 kDa subunits in *E. coli* (Fukuda *et al.*, 1984) and *S. mutans* (Victoria *et al.*, 1982), 33 kDa subunits in *Z. mobilis* (Scopes *et al.*, 1985) and

*B. stearothermophilus* (Hengartner *et al*., 1973), and a large amont of other bacterial sugar kinases with molecular masses from 32 kDa to 37 kDa. The oligomers of these isoenzymes are commonly monomers or dimers. In fungi and invertebrates, the hexokinases are formed as monomers of 50 kDa molecular mass, althought in a few cases they are dimerized, as glucokinase in *Drosophila*. Veterbrates have hexokinases of 100 kDa monomers, which can also dimerize when co-crystallized with substrates, with the exception of glucokinase, which is only 50 kDa and does not dimerize. The monomer molecular masses of hexokinases in all species can statistically fall in the geometric series 25:50:100, apart from the 35-kDa hexokinases in bacteria. Thus, according to a hypothesis shown in Fig 1.5, hexokinases in present-day organisms may have been derived from the ancestor of the 25-kDa enzyme still present in bacteria (Ureta *et al*., 1987). It was supposed that genes of 50-kDa hexokinases in fungi and invertebrates came from the duplication and fusion of ancestral genes, and another gene duplicated and fused to produce a gene of hexokinase of 100-kDa in vertebrates. For this tempting assumption, there is good evidence for the duplication and fusion from the hexokinase of 100-kDa. In vertebrates, the rise of 100-kDa hexokinase might correspond to the acquisition of new functions, with a new allosteric site responsible for the significant inhibition by glucose 6-phosphate. For example, hexokinase I in rats, twice the size enzyme of yeast hexokinase, only has one catalytic site, which is located in the C-terminal half, and each domain is structurally related to yeast hexokinase. The mutation of the residues in the N-terminus that correspond to catalytic residues in the C-terminus did not influence the activity of this enzyme; glucose 6-phosphate could strongly inhibit the enzyme's activity, but not the activity of yeast hexokinase. However, further research on the 51 kDa C-terminal fragment from the digestion of hexokinase I by typsine revealed that the regulation by glucose 6-phosphate can also take place at the C-termial half (White *et al*., 1989). The same result was reported for the C-terminus of human hexokinase I: the inhibition by glucose 6-phosphate was exactly as the complete hexokinase (Magnani *et al*., 1992). Then the view of the evolutionary relationship between the hexokinases adjusted accordingly to accept that the sensitivity to glucose 6-phosphate arose before gene duplication and fusion. According to this, the ancestor of mammalian hexokinases is more similar to starfish hexokinase than the yeast enzyme, which is the 50-kDa hexokinase inhibited by glucose 6-phosphate (Mochizuki, 1981; Mochizuki *et al*., 1980).

| Taxon | Organism | Isoenzyme | Molecular mass (kDa) | |
|---|---|---|---|---|
| | | | Native | Subunit |
| Archaea | *P. furiosus* | Glucokinase | 93 | 47 |
| Bacteria | *B. stearothermophilus* | Glucokinase | 67 | 34.5 |
| | *S. mutans* | Glucokinase | 41 | 24 |
| | *E. coli* | 'Glucokinase' | 49 | 24.5 |
| Fungi | *Sac. cerevisiae* | $P_I$, $P_{II}$ | 102 | 51 |
| | *Sac. cerevisiae* | 'Glucokinase' | aggregates | 51 |
| Protozoa | *Try. brucei* | Hexokinase | 295 | 50.3 |
| Plants | Wheat germ | $L_I$, $L_{II}$ | 50 | 50 |
| | Wheat germ | $H_I$, $H_{II}$ | 100 | |
| Nematodes | *Hymenolepsis diminuta* | Hexokinase | 98 | |
| | *Ascaris suum* | Hexokinase | 100 | 100 |
| Insects | *Drosophila* | Hexokinase A | 47 | 47 |
| Echinoderms | Starfish | Hexokinase | 50 | 50 |
| Chordates | Lamprey | Hexokinase | 90 | 90 |
| | Rat | Hexokinase A | 98 | 98 |
| | Rat | Hexokinase B | 96 | 96 |
| | Rat | Hexokinase C | 99.5 | 98 |
| | Rat | Hexokinase D | 49 | 49 |

**Table 1.2 The molecular dimensions of hexokinases (Cardenas et al., 1998)**

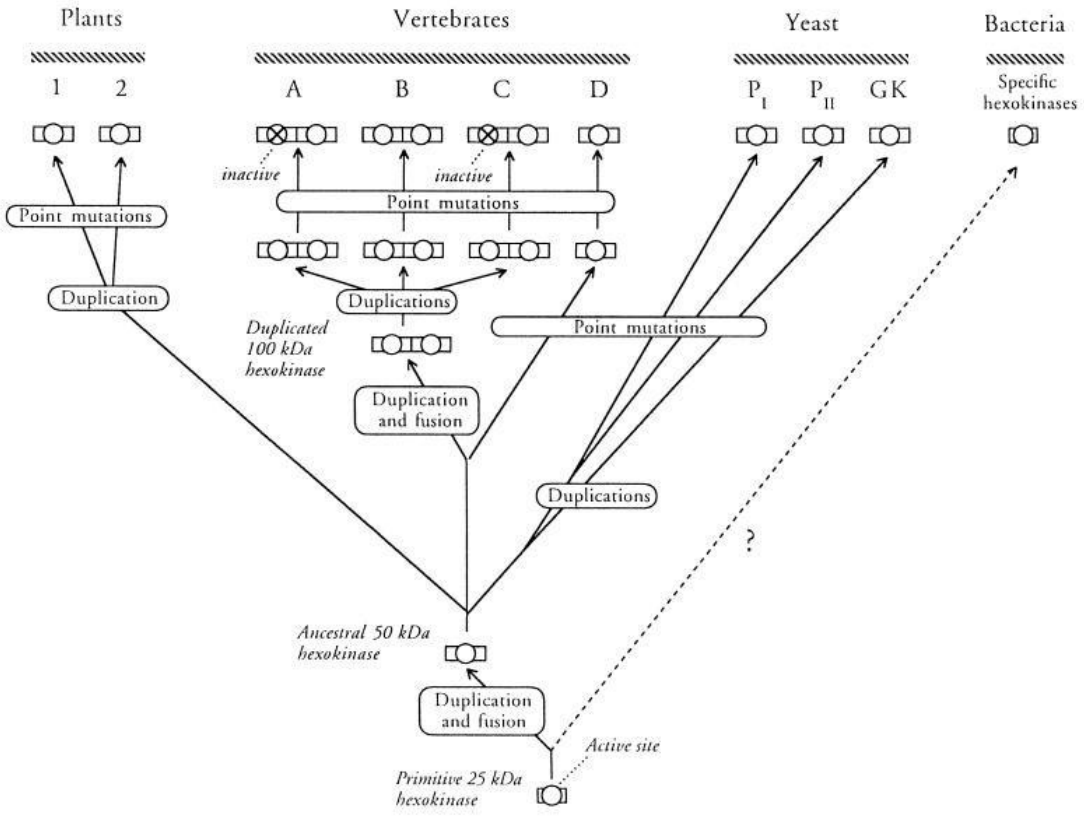


**Fig 1.5: Scheme depicting the hypothesis of hexokinase evolution (Cardenas *et al.*, 1998).** The duplication that produced the 100-kDa animal hexokinases is shown as occurring later than the branch point that separated the 50-kDa hexokinase D from the other isoenzymes. Because of no direct evidence that any of bacterial hexokinases are homologous with the eukaryotic enzymes, the line leading to the bacterial hexokinases is discontinuous.

### 1.2.1.2 Structure of hexokinase

As the pacemaker of glucose metabolism in tissues of human and other species, hexokinase attracted

intensive attention with respect to the analysis of its crystal structure. From the first crystallized hexokinase in yeast (Anderson *et al.*, 1978; Shoham *et al.*, 1980), many hexokinases in different organisms and species, i.e., *Rattus norvegicus*, *Schistosoma mansoni* (Mulichak *et al.*, 1998), and *Homo sapiens* (Liu *et al.*, 2012) have been crystallized and analyzed with different ligands. Via the pioneering crystallographic research of yeast hexokinase, the structures of hexokinases could be divided into large and small lobes, and the active site was found to be located in the pocket embraced by the large and small lobes. With the binding of glucose, relative movements of the large and small lobes induce the conformational change from an open form to a closed form (Anderson *et al.*, 1978). In the closed conformation, the small lobe comes closer to the presumed position of the ATP and makes the interaction possible, which is not possible in the open form (Fig 1.6).

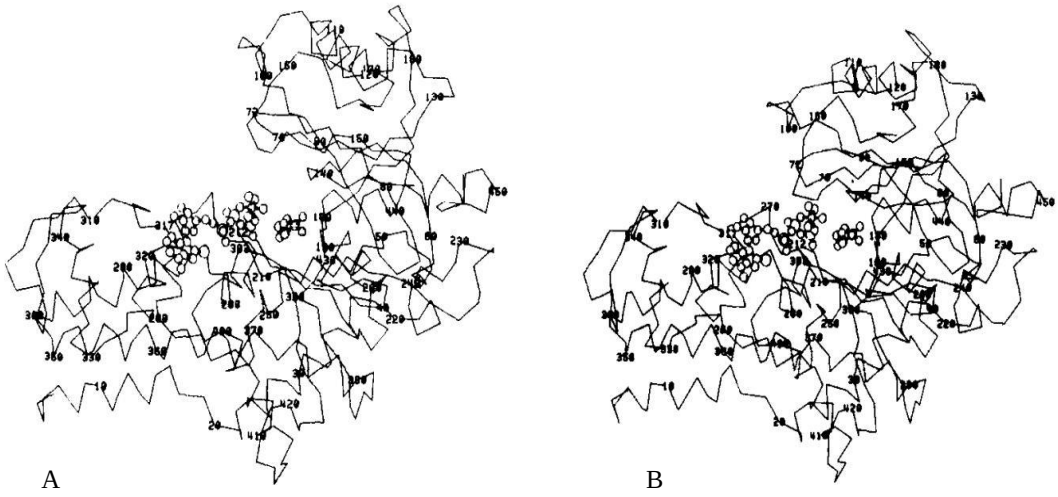


**Fig 1.6: Structure of yeast hexokinase with open (A) and closed (B) conformations (Shoham *et al.*, 1980).**

The crystal structure of human brain HK I or rat HK II revealed that the 100-kDa hexokinase could be organized in two domains linked by a connection helix, which are called the N-terminal and C-terminal halves. These two domains exhibit extensive sequence similarity and are structurally related to yeast hexokinase (Griffin *et al.*, 1991). As shown in the yeast hexokinase structure, the small lobe and the large lobe could be distinguished in the N- and C-terminal halves. In the crystalline state, human and rat HKI were found to be dimerized (Fig 1.7). Within the dimer, two monomers formed a twofold axis in molecular symmetry, in which the N-terminal domain from one subunit is juxtaposed to the

C-terminal domain of another subunit (Rosano *et al.*, 1999).

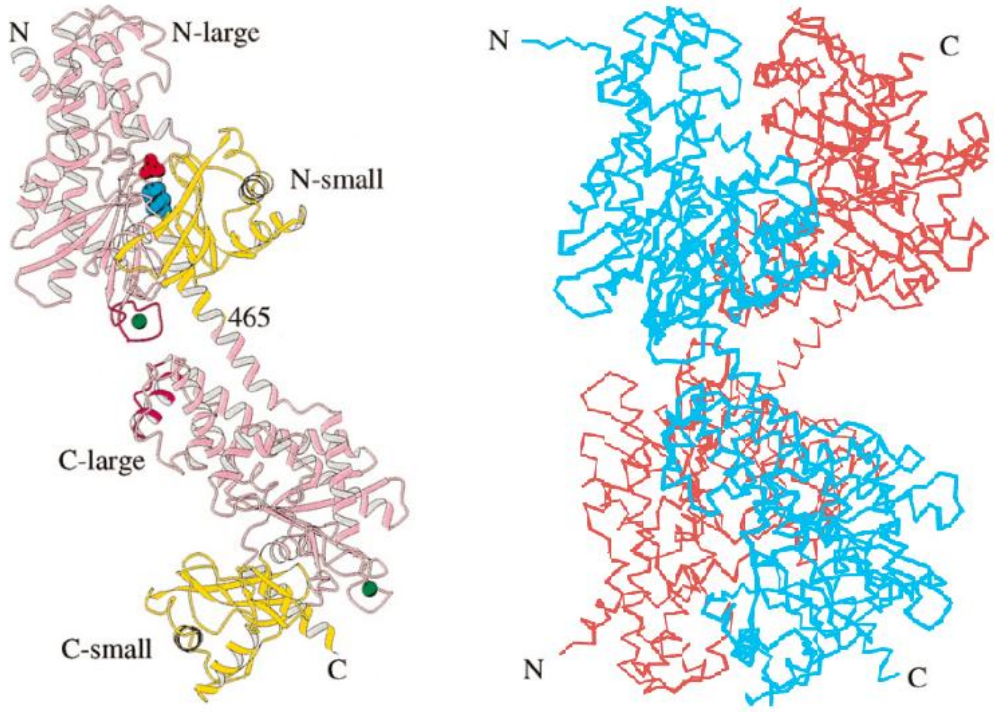


**Fig 1.7: Stereoview of the monomer and dimer of hexokinase I in humans (Aleshin *et al.*, 1998; Rosano *et al.*, 1999).** The chain of the large lobe is in purple; small lobe in yellow; the dimerized hexokinases are in blue and red.

The active conformation of hexokinase was considered to relate to the close form. The conformational transition from open form to close form was supposed to stabilize the binding of ATP (Shoham *et al.*, 1980). The binding sites of glucose and glucose 6-phosphate were clearly exhibited in both 50-kDa and 100-kDa hexokinases by the co-crystallized Glc/G6P complexes of hexokinases (Aleshin *et al.*, 1998). Since the crystal structure of the ATP-hexokinase complex is still not available, the complex of hexokinase with ADP/Glc was used to suggest a $Mg^{2+}$-ATP complex with hexokinase, which was in agreement with proposed metal-ATP complexes of related enzymes (Aleshin *et al.*, 2000). In this model, the binding sites for glucose 6-phophate and ADP overlapped (Fig 1.8), thus evidently demonstrating the structural basis for the direct inhibition of glucose 6-phosphate. Different mutations of hexokinase complexes with glucose and glucose 6-phosphate were obtained and analyzed in order to investigate the mechanisms of catalysis and allosteric regulation. Glucose and glucose 6-phosphate could combine with both N- and C-terminal halves. The binding site of glucose 6-phosphate in the N-terminal half used to be considered to contribute to allosteric inhibition. However, mutations that

eliminate the binding of glucose 6-phosphate in either the N- or C- terminal half had little to no effect on the inhibition (Sebastian *et al.*, 1999; Zeng *et al.*, 1996). Only the mutations at both glucose 6-phosphate binding sites could abolish the product inhibition (Liu *et al.*, 1999). Evidently, the inhibition of glucose 6-phophate consisted of allosteric inhibition (binding at the N-terminal half) and direct inhibition (binding at the C-terminal half).

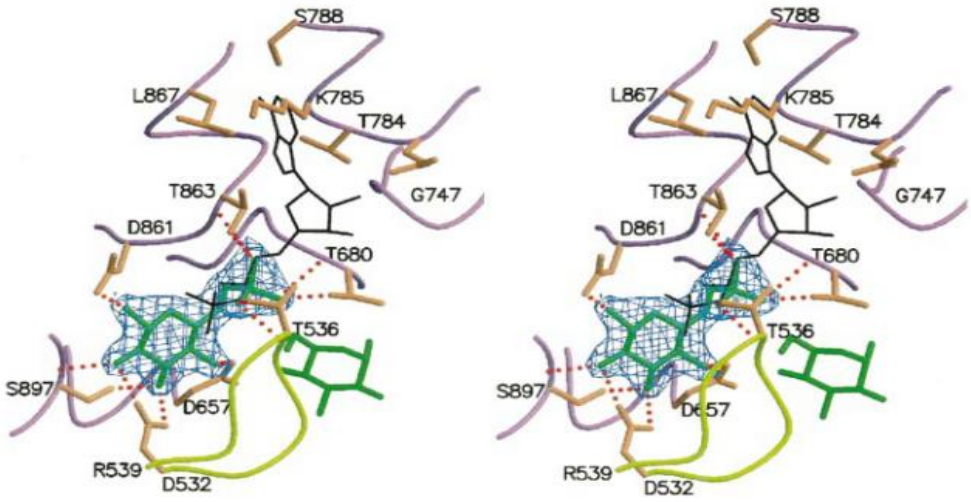


**Fig 1.8: Active site of the C-terminal half of monomeric hexokinase I.** Right: the ADP/Glc-bound active site with ADP and Glc drawn in green, selected side-chains in orange, elements of the small domain in yellow, and segments of the large domain in purple. Dotted red lines designate donor-acceptor interactions. Left: the G6P/Glc-bound active site. ADP in black, taken from the top illustration, represents the overlap with G6P (Aleshin et al., 2000).

Significant inhibition by glucose 6-phosphate was commonly said to be a striking property of the 100-kDa hexokinases in vertebrates in the hypothesis of allosteric conformation. The multiple binding sites of glucose 6-phosphate indicate that product inhibition is not only by allosteric regulation. Some models were constructed to explain the mechanism of glucose 6-phosphate inhibition. White & Wilson (White *et al.*, 1989) proposed that the N-terminal half of 100-kDa hexokinases could block the glucose 6-phosphate binding site of the C-terminal half, and that the binding of glucose 6-phosphate at the N-terminal half might allosterically regulate access to the ATP binding site for the C-terminal half. However, subsequent crystal structures of glucose 6-phosphate complexes of hexokinases revealed product binding. Alshin et al., [2000] improved the model of White & Wilson, while the same shortcoming of anti-cooperative binding of glucose 6-phosphate could not be solved. In this model, two conformational states also exist in the N-terminal half, which differ by a $6^{o}$ rotation about the

N-terminal end of the transition helix. This difference in conformational states relates to the transition from the ATP-compatible to the ATP-antagonistic status of the C-terminal half (Fig 1.9).

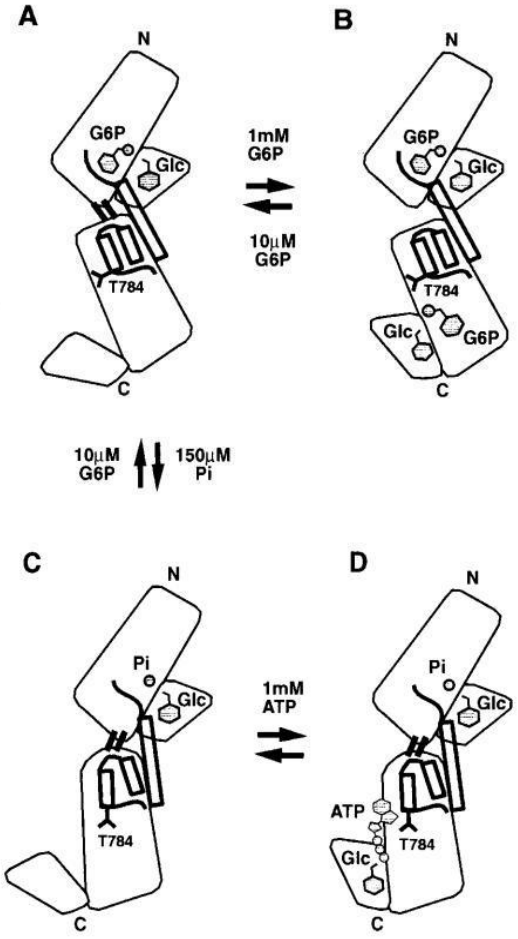


**Figure 1.9: Scheme of the allosteric regulation in hexokinase I monomer.** (a) At low concentrations of glucose 6-phosphate, the allosteric interface between the N- and C-terminal halves maintains the flexible subdomain in an ATP-antagonistic state, in which the Thr784 blocked the binding of ATP. (b) In the presence of elevated concentrations of G6P, the N- and C-terminal halves are decoupled, the ATP binding site was directly overlapped by the binding of glucose 6-phosphate. (c) The competition of Pi promoted the dissociation of glucose 6-phosphate from the N-terminal half and made a rigid-body rotation of that half relative to the C-terminal half. (d) Pi facilitates the binding of ATP (Aleshin et al., 2000).

#### 1.2.1.3 Hexokinase in humans

In mammals there are four different types of hexokinase that have been identified via ion exchange chromatography (González *et al.*, 1964) or electrophoresis (Katzen *et al.*, 1965). The isoforms of hexokinase I, II, and III are all 100 kDa molecules, and type IV is a 50 kDa molecule (Postic *et al.*, 2001). The distributions and localizations of these hexokinase isoforms are quite different in human organs and tissues. Hexokinase I is expressed in the brain at a particularly high level; the tissue relies on the metabolism of glucose to sustain a high rate of energy consumption (Clarke *et al.*, 1999). The expression of type II hexokinase is much more restricted, mainly being found in insulin-sensitive tissues such as adipose tissue and skeletal muscle (Wilson, 1995). Compared to type I, hexokinase II plays a more anabolic role in the process of lipid synthesis in the liver (Sebastian *et al.*, 2000) and

lactating mammary gland (Kaselonis *et al*., 1999), providing NADPH via the pentose phosphate pathway. Type III is in low expression but detectable in lung cells and immunohistochemically found in the perinuclear compartment (Preller *et al*., 1992). As in hexokinase II, the type III hexokinase also was considered to be involved in anabolic pathways (Wilson, 2003). HKIV was found with a low affinity for glucose (5 mM), which plays an important role in glucose homeostasis, and is mainly distributed in the liver and the pancreas (Postic *et al*., 2001).

Due to the N-terminal hydrophobic region, the subcellular localizations of human hexokinase I and II are combined with the outer mitochondrial membrane (Kropp *et al*., 1970; Polakis *et al*., 1985). This combination between hexokinase and mitochondria plays an important role in glucose metabolism and the fate of the cell (BeltrandelRio *et al*., 1992; Pedersen, 2007). The isoform III is also a 100 kDa hexokinase but without the hydrophobic region at the N-terminus and has been found localized both in cytoplasm and the perinuclear compartment, which is supposed to relate to the transport functions in endothelial and epithelial cells (Preller *et al*., 1992). The subcellular localization of hexokinase IV is in cytoplasm, and the function is clear with the hematologic balance of glucose.

Among these four isoforms of hexokinase in human tissues, hexokinase I and II attracted the most concern due to their wide distribution and their relationship with tumor cells. Numerous excellent studies exquisitely elucidate the specific binding of hexokinase I and II with the porin (VDAC: voltage-dependent anion channel) at the outer membrane of mitochondria (Gelb *et al*., 1992; Lindén *et al*., 1982; Sui *et al*., 1997). This combination has been elaborated to fluently utilize the mitochondrial ATPs. Besides this, the more important function of the insert of hexokinase I and II into the porin at the outer membrane of the mitochondrion could prevent cytochrome C release, which regulates cell apoptosis (Arzoine *et al*., 2009; Pastorino *et al*., 2008; Pastorino *et al*., 2002). As described previously, hexokinase I is much more related to energy generation via catabolism, and hexokinase II tends to contribute to anabolism. This difference determines that the expression of hexokinase II is silenced in normal cells except some special cells by the methylation of the transcriptional promoter (Goel *et al*., 2003). However, the demethylation of the promoter can be induced by a term of promiscuous activators, including a mutated p53 gene (Mathupala *et al*., 1997) and hypoxia (Mathupala *et al*., 2001) (Fig 1.10). The overexpression of hexokinase II has been recognized as a hallmark of many cancers, especially the most aggressive, and this phenotype also relates to the shift of glycolysis product from pyruvate to lactate, which is called the ‘Warburg effect’ (Warburg, 1956). In the 1920s, Warburg and his colleagues

(Warburg *et al*., 1930) found cancers frequently rely less on mitochondria, and the metabolism is more like anaerobism; over 50% of their ATP was obtained from metabolizing glucose directly to lactic acid, even in the presence of oxygen. In normal cells, most of the ATP is generated by oxidative respiration in mitochondria composed of the TCA cycle and the respiratory chain. Via the shifted pathway of glcolysis and its off-shoot the pentose phosphate shunt (hexose monophosphate pathway), the rapidly dividing tumor cells are provided with rich sources of carbon precursors, which are essential for the biosynthesis of phospholipids, nucleic acids, fatty acids, porphyrins, and cholesterol (Pedersen, 2007). The consequent research evidently showed that hexokinase II and the VDAC complex play the most pivotal and direct roles in the 'Warburg effect' (Pedersen, 1978; Pedersen *et al*., 2002; Smith, 2000).

In recent years, through the research of subcellular localization of hexokinase II, another key role of hexokinase II is to maintain cancer cell survival by suppressing cell death (Mathupala *et al*., 2006). The N-terminal binding domain of hexokinase II is predominantly essential to anchor to the VDAC protein in this process. Many factors, both metabolic and signal transduction-related, could be implicated in the formation of the HKII/VDAC complex, including ADP concentration, lactate, pH, and the signaling cascades involving protein kinase-B (PKB/Akt) (Gauthier *et al*., 1990; Graham *et al*., 1985; Miccoli *et al*., 1996). The mechanism of preventing apoptosis by the hexokinase II/VDAC complex was concluded to interrupt the formation of the MPTP (mitochondrial permeability transition pore complex). The binding of HKII can reduce the interaction of free VDAC sites with the activated proapoptotic molecules such as Bax and Bad (Capano *et al*., 2002; Pastorino *et al*., 2002). In the process of hexokinase II/VDAC complex formation, Akt, which is known as a potent effector of antiapoptotic stimuli in tumors (Gottlob *et al*., 2001), induces the hexokinase II binding on VDAC and transportation of the antiapoptotic molecule Bcl2 to VDAC on mitochondria (Zhou *et al*., 2005). All these factors finally prevent the proapoptotic molecules from binding to the outer mitochondrial membrane, MPTP, thereby activating and further sealing cytochrome C in the apical surface of the inner mitochondrial membrane (Fig 1.11).

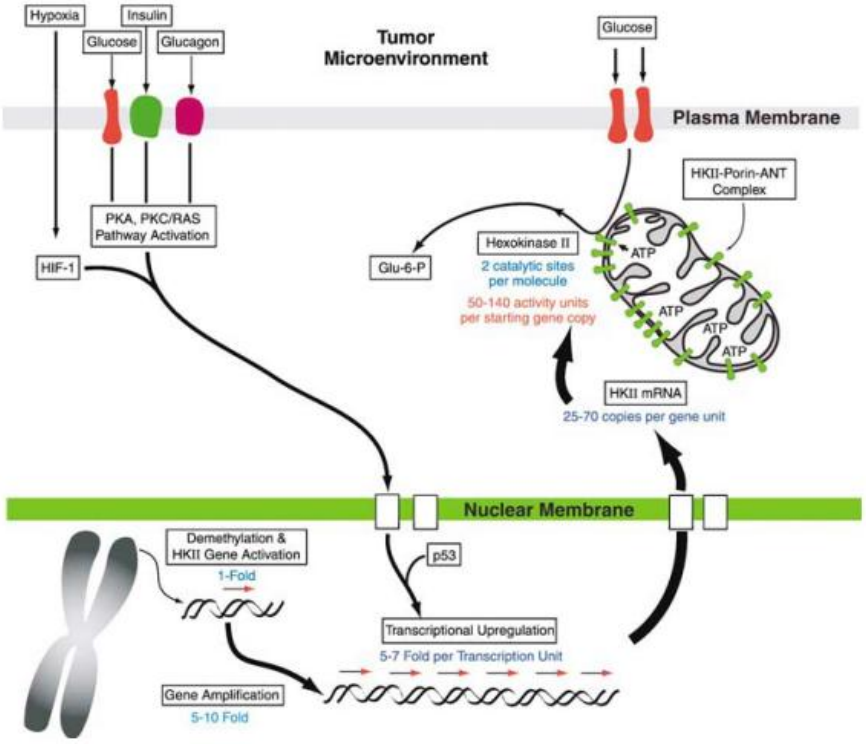


**Figure 1.10: Tumors harness a multitude of genetic, epigenetic, transcriptional and post-translational strategies for enhanced expression and function of hexokinase II.** During tumorigenesis of tissues where the expression of HK II is suppressed, demethylation of the promoter of the gene may be first brought out of its hibernation and then amplified 5-10-fold. There are two active sites obtained in HK II per enzyme moiety. The combination of the mitochondrial voltage-dependent anion channel and HK II further gets rid of the product inhibition by glucose 6-phosphate (Mathupala et al., 2006).

The predilection of hexokinase II in tumor cells can be observed via up-regulation of hexokianse II expression and down-regulation of expression of other isoforms. The phenomenon of the expression of hexokinase IV replaced by hexokinase II in the process of tumors arising in liver and pancreas were observed (Mathupala *et al.*, 2006; Rempel *et al.*, 1994). The shift of hexokinase I to hexokinase II was also found in the malignant gliomas (Wolf *et al.*, 2011). When comparing isoforms of hexokinases in humans, the properties of hexokinase II might be an important factor. Indeed hexokinase II has a much higher affinity for glucose than hexokinase IV, and there are two catalytic sites in hexokinase II that can be equivalent to two hexokinases, I or IV, providing a more efficient phosphorylation of glucose, satisfying the demands of tumor cells (Mathupala *et al.*, 2009). Another reason might be due to the metabolism and expression profiles being altered into something much more like the embryonic/progenitor state in different kinds of tumors (Christofk *et al.*, 2008; Vander *et al.*, 2009). Actually, hexokinase II is essential for the development of embryos. From the embryonic lethality of hexokinase II-deficient mice, the loss of hexokinase II cannot be compensated by other isoforms of

hexokinase during embryonic development (Heikkinen *et al.*, 1999). The essentiality of hexokinase II during the development of embryos and the central nervous system evidently indicates there are some unknown functions.

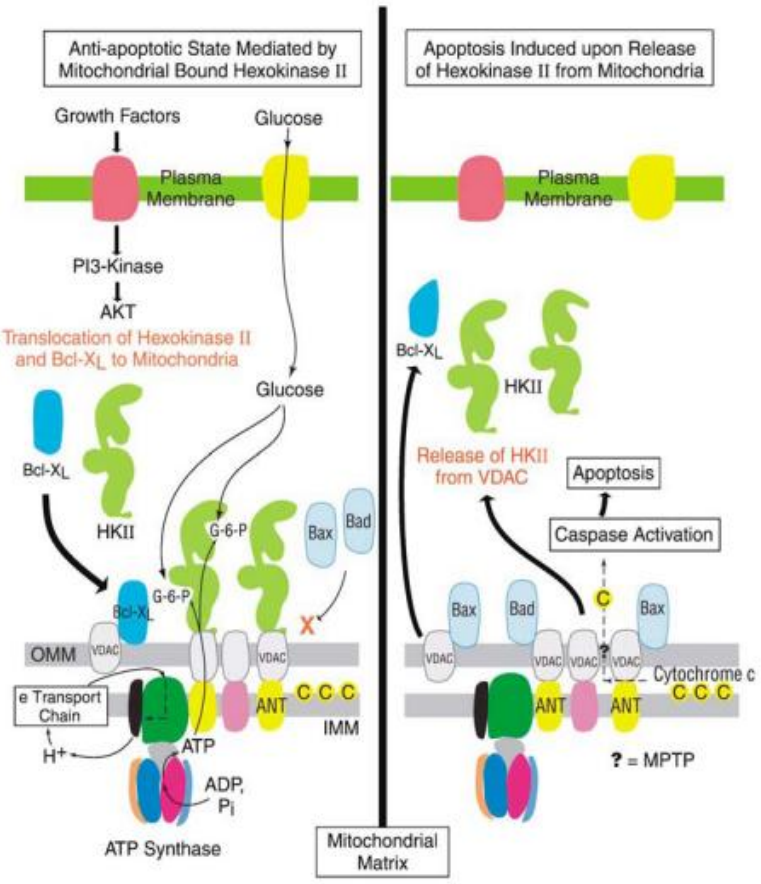


**Figure 1.11: Mitochondrial-bound hexokinase II plays a major role in preventing tumor apoptosis.** Right: without control mechanisms in place to prevent the release of HK II from the mitochondrial membrane, apoptosis would be likely to happen at the particular conditions that exist in a tumor microenvironment. Left: the combination of mitochondrial voltage-dependent anion channels (VDACs) and HK II persist in the channel of adenine nucleotides and inhibit MPTP formation (Mathupala *et al.*, 2006).

### 1.2.1.4 Hexokinase in *Plasmodium falciparum*

As in other species, *P. falciparum* also relies on hexokinase to initially catalyze the phosphorylation of glucose, generating glucose 6-phosphate in the utilization of imported glucose. It has been verified via observation in cultured parasites that the supply of glucose is essential for the survival of *P. falciparum* during the blood stage. A short-term deficit of glucose in the medium leads *Plasmodium* parasites into an abnormal state, and they fail to recover their viability via glucose re-supplementation (Babbitt *et al.*, 2012). The rapacious demand for glucose in *Plasmodium* parasites is represented by the 50-100-fold

enhancement of glucose consumption in red blood cells after becoming parasitized (Roth, 1990). The symptoms of hypoglycemia with fatal consequences are frequently observed in patients with malaria (White *et al*., 1987). As the pacemaker of glucose metabolism, hexokinase is obviously considered essential to *Plasmodium* parasites.

The evidence of hexokinase in *Plasmodium falciparum* was obtained by activity assays in the lysate of parasitized red blood cells (Roth, 1987). The genes of hexokinase in *Plasmodium falciparum* were first cloned and analyzed in the 1990s (Olafsson *et al*., 1992). By genomically sequencing *Plasmodium falciparum* (Gardner *et al*., 2002), there was a single copy of the hexokinase gene found located on chromosome 6 without intron. The deduced primary sequence of hexokinase shows a low identity with human counterparts (only 33%), but the signature of hexokinase is quite conserved, for example multiple glucose binding sites, ATP binding patterns, and multiple glucose 6-phosphate binding sites. Interestingly a similar hydrophobic region was found at the C-terminus of *Pf*HK, which corresponds to the N-terminal mitochondrial binding region in human hexokinase I and II. Subsequently immune electron microscopy also revealed that hexokinase was partially associated with the membrane (Olafsson *et al*., 1992). From research on carbon metabolism in *Plasmodium* parasites, glucose metabolism of *Plasmodium* is somewhat similar to tumor cells in humans: i.e., voracious consumption of glucose, incomplete oxidation to lactic acid and excretion, and an increasing flux of glucose carbon into biosynthesis (glycosylated proteins, nucleic acids, lipids) (Olszewski *et al*., 2011). All these figures of glucose metabolism are in accordance with the demands of proliferating parasites. Beside this, glucose 6-phosphate as the product of hexokinase and the initial substrate of the pentose phosphate pathway, the activity of hexokinase was found to be proportionally related to the rate of oxidized glutathione reduction in the lysates of parasitized red blood cells, and surprisingly hexokinase seemed to be the limiting enzyme in the flux of glucose into the pentose phosphate shunt, not glucose 6-phosphate dehydrogenase (Roth, 1987).

Inhibiting the utilization of glucose by *Plasmodium* parasites has been considered to be a promising approach to eradicate malaria, for example by blocking glucose permeation via inhibition of the glucose transporter (Joet *et al*., 2003), or pentose phosphate pathway block-up via glucose 6-phosphate dehydrogenase inhibition (Beutler *et al*., 2007; Jortzik *et al*., 2011). By catalyzing the first phosphorylation of cellular glucose without other isoenzymes, hexokinase in *Plasmodium* parasites is obviously a promising target of antimalarial medication due to its predominant function in glucose

metabolism and its distinguished protein sequence from the human host.

### 1.2.2 Protein *S*-Glutathionylation

Protein thiols of cysteines represent the important post-translational modification sites in functional regulation and signal transduction, especially during changes in the cellular redox state (Dalle-Donne *et al*., 2009). The modification of thiols can significantly manipulate protein structure, enzyme catalysis, and signaling pathways. Glutathione as the most abundant low-molecular-weight thiol is a major antioxidant and detoxification agent in cells and shows the functions of specific post-translational modification by reacting with the low p$K_a$ cysteinyl residues in proteins, which is called *S*-glutathionlyation (Dalle-Donne *et al*., 2007). *S*-glutathionlyation is promoted not only via oxidative stress but also under physiological conditions. *S*-glutathionlyation can specifically regulate protein activities during redox signaling, which is considered protecting the sensitive protein thiols from irreversible oxidation and simultaneously serves the function of glutathione storage, preventing oxidized glutathione excretion (Adachi *et al*., 2004; Clavreul *et al*., 2006; Qanungo *et al*., 2007). More and more proteins have been identified as potential targets of *S*-glutathionlyation and lead either to inhibition [calcium ATPase (Ying *et al*., 2007), MEKK1 (Cross *et al*., 2004)] or activation [angiotensin II (Adachi *et al*., 2004), SERCA (Adachi *et al*., 2004), and mitochondrial complex II (Chen *et al*., 2007)]. Using the method of biotinylated-GSH labeling, the proteomes of *S*-glutathionlyation have been systematically investigated in some species *in vivo*, i.e., *Arabidopsis* (Dixon *et al*., 2005), *Chlamydomonas reinhardtii* (Michelet *et al*., 2008), human (Fratelli *et al*., 2002; Fratelli *et al*., 2003), *Plasmodium falciparum* (Kehr *et al*., 2011) and yeast (Shenton *et al*., 2003).

The mechanism of protein *S*-glutathionlyation is particularly susceptible to oxidative suppression and is related to a series of redox reactions (Fig 1.12). Protein *S*-glutathionlyation can be directly triggered by a high level of oxidized glutathione with the reaction of thiol-disulfide exchange between oxidized glutathione and the target protein (Wang *et al*., 2001). The exchange of GS moieties between a *S*-glutathionlylated protein (PSSG) and a reduced protein can also serve *S*-glutathionlylation, including the enzymatic monothiol mechanism via glutaredoxin or glutathione transferase (Lind *et al*., 1998; Qanungo *et al*., 2007). In the biochemical studies it was observed that *S*-glutathionlylation can also be mediated by GSNO *in vivo* (Giustarini *et al*., 2005; Martínez-Ruiz *et al*., 2007). To define the function of *S*-glutathionlylation in redox regulation, some criteria were established (Shelton *et al*., 2005): (a) the

reaction is reversible; (b) the site of *S*-glutathionlylation is specific in particular proteins; (c) a physiological stimulus or a physiological response can promote the formation of *S*-glutathionlylation; (d) modification of activity or related cell function can arise from *S*-glutathionlylation. The reverse reaction of *S*-glutathionlylation was convincingly catalyzed by the thiol-disulfide oxidoreductases Grxs (thioltransferases), which is called deglutathionylation (Gallogly *et al*., 2007; Shelton *et al*., 2005). In deglutathionylation, Grx catalyzes the reaction of nucleophilic double displacement. The human sulfiredoxin (Srx1) has been observed in catalyzing the reversal reaction of protein *S*-glutathionlylation induced by NO both *in vitro* and *in vivo* (Findlay *et al*., 2006).

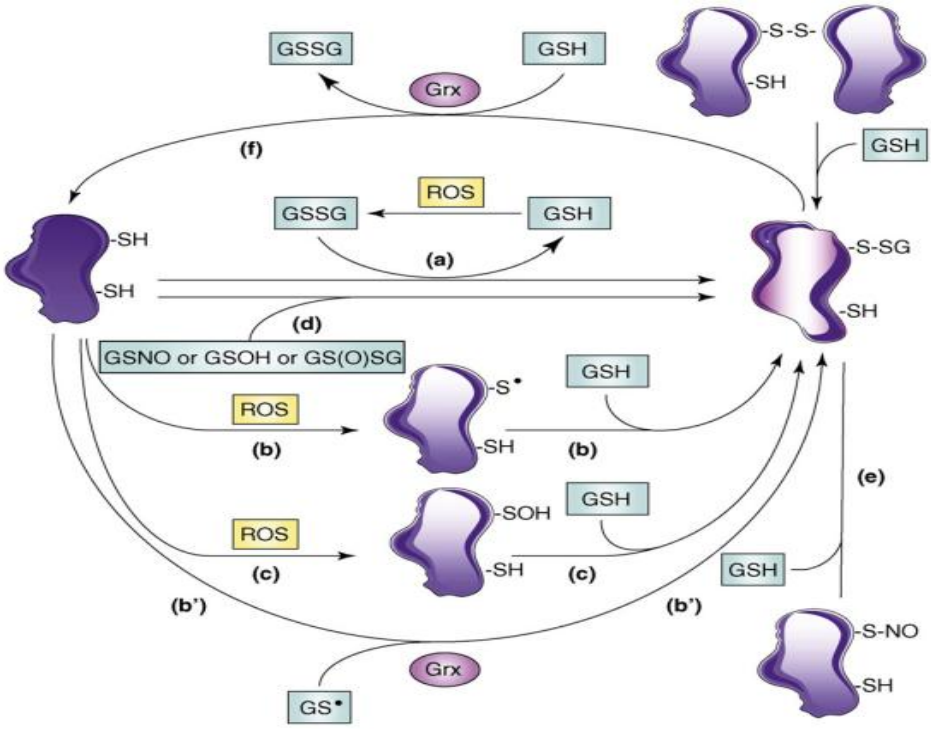


**Figure 1.12: Scheme depicting different pathways leading to the formation of protein S-glutathionylation (Dalle-Donne *et al.*, 2009).**

The oxidation of thiols has been shown to be capable of significantly regulating the activity of hexokinase in humans (Redkar *et al*., 1972). Only the oxidation of a few cysteine residues leads to the loss of activity, and full recovery is related to the addition of excess thiol. The oxidized glutathione was shown to inactive hexokinase (Gilbert, 1984). The thiols of hexokinase seem to be the regulation sites of dithiol-containing redox proteins. Particularly in *Plasmodium falciparum*, hexokinase has been recognized as the target of the thioredoxin superfamily (Sturm *et al*., 2009). The same result was obtained from the identification of glutathionylation in *Plasmodium falciparum* (Kehr *et al*., 2011). All

these studies suggest that the modification of hexokinase thiols in *Plasmodium falciparum* might be an important mechanism of regulation in response to oxidation.

### 1.2.3 Genetic manipulation of *Plasmodium falciparum*

To investigate the functions of specific genes and their encoded proteins, RNA interference (RNAi) and gene knockout are the predominant methods at the RNA and DNA level. Different from the post-modification studies, these methods could help answer the question of whether this protein is essential for survival or some particular response of cells. The mechanism of RNAi is based on the sequence-specific RNA degradation mediated by small, double-stranded, interfering RNAs (siRNA), which have sequence complementary with target message RNA (Du *et al.*, 2003). In this process, the RNA-induced silencing complex (RISC) containing several proteins specifically identifies and cleaves target RNA (Hammond, 2005). This method is considered to be a potent tool to knock down any gene. But whether this RNAi machinery exists in *Plasmodium falciparum* is argued. Two important genes that play key roles in the RNAi pathway could not be found in the genome of *Plasmodium falciparum* (Coulson *et al.*, 2004; Hall *et al.*, 2005), and the functional short RNAs involving RNAi also could not be observed in *Plasmodium falciparum* (Rathjen *et al.*, 2006). However, in other experiments on dsRNA-treated *Plasmodium falciparum,* the inhibition of growth was observed and correlated with a decrease in the level of target mRNA (McRobert *et al.*, 2002). Right now the RNAi technique is mainly used in investigations of the *Anopheles* mosquito, the vector of malaria (Clayton *et al.*, 2013; Thailayil *et al.*, 2011). Different from RNAi, the technique of gene knockout directly manipulates the genes of target proteins. The mechanism of gene knockout makes a deletion (double crossover) or disruption (single crossover) on the *locus* of target genes leading to the elimination or malfunction of target proteins, based on the machinery of homologous gene recombination. This technique has been well used in *Plasmodium* parasites in order to investigate the function of particular proteins (Bissati *et al.*, 2006; Ke *et al.*, 2011; Tarun *et al.*, 2009). The procedures of knockout in *Plasmodium* parasites are similar. The difference is mainly on the different sets of knockout vector constructs, which are designed with different selective markers, including WR92210 (a specific inhibitor of DHFR in *P. falciparum*), blasticidin (BS), and 5-fluorocytosine (5-FC). After electroporation, drug off-and-on cycling is a common strategy to select the parasites that integrate with the knockout plasmids by single or double crossover recombination. The result of the knockout is checked by a diagnostic PCR or southern blot

for the genotype of genomic DNA and northern blot for the transcription.

In the studies of proteins that are supposed to be essential for *Plasmodium* parasites, successful knockout is lethal and not able to distinguish from failure of cell culture. Some special strategies should be applied for this situation. To construct a merodiploid expression system of particular proteins is an option in the blood stage *Plasmodium* parasites, which are haploid. The merodiploid means to insert an additional copy of the target protein into the genome of a haploid organism. In *Plasmodium falciparum*, a rapid and efficient attB X attP recombination system was developed for genetic integration and complementation analyses (Nkrumah *et al*., 2006). In this system the attB site is integrated into the glutaredoxin-like *cg6* gene, the disruption of which is not detrimental for blood stage *Plasmodium falciparum*. The *attP*-containing plasmid constructed with the transgene and the drug resisitance gene is used to transfect *attB*$^{+}$ lines, an additional integrase gene on a separate plasmid is necessary. The result of the episomal expression can be monitored via Western blot. Normally the episomally expressed protein contains a drug-sensitive degradation domain. Without drug protection, this degradation domain can be recognized by ubiquitin, and the ubiquitylased proteins are further digested by the proteosome. Then this transgenetic line of parasites can be used for the knockout step. If the knockout is successful, checked by diagnostic PCR or northern blot, the difference between the parasite cultures with or without protective drugs shows whether the target protein is essential or not.

## 1.3 Objective of the study

*Plasmodium falciparum* is still a life-threatening parasitic disease. Because of the lack of an efficient vaccine and rising drug resistance, controlling the spreading and transmission of malaria is becoming more difficult to achieve. New drug targets must urgently be identified, and novel antimalarials must be designed in this battle. My study aims to evaluate *Pf*HK as a new drug target and to contribute to the further screening of inhibitors.

### 1.3.1 Hexokinase from *P. falciparum*

Due to the reliance of *P. falciparum* on glucose, interrupting the utilization of glucose has been considered a promising approach to combat malaria. Hexokinase, the first rate limiting velocity enzyme in the glucose metabolism pathway, was supposed to be essential for *P. falciparum* survival. However, the difficulties in heterologous overexpression of *Pf*HK restricted the investigation of this enzyme. The

insolubility of recombinant *Pf*HK is the main obstacle to obtaining a high-quality enzyme (Olafsson *et al*., 1994). In this study, we aimed to optimize the conditions of heterologous overexpression and purification in order to obtain purified *Pf*HK and furthermore to determine its biochemical characterization, to screen the conditions of crystallization and to reveal the subcellular localization of this enzyme.

### 1.3.2 *S*-Glutathionylation of *Pf*HK

*Pf*HK was found to be targeted by the thioredoxin superfamily in *P. falciparum* and has been identified as the target of glutathionylation. This enzyme has the potential to be regulated in the response to celluar oxidation. We have attempted to elucidate the redox regulation and the modification of glutathionylation on *Pf*HK.

### 1.3.3 Knockout of *Pf*HK

To evaluate the necessity of *Pf*HK in *P. falciparum*, a strain of *Pf*HK knockout parasites was prepared. Due to the essential role of hexokinase in other species and the fact that no other iosenzymes were found in *P. falciparum*, the *Pf*HK knockout was supposed to be lethal to *P. falciparum*. A merodiploid strain of *P. falciparum* was prepared to express an episomal *Pf*HK in collaboration with Prof. Vaidya's group in the Medicine College of Drexel University, USA. Based on this approach, the necessity of *Pf*HK might be proved or the compensatory pathway of glucose phosphorylation might be found in *P. falciparum*.

# 2. Materials

## 2.1 Chemicals

Most chemicals used in the study were of highest purity available.

| Chemical | Producer |
|---|---|
| Acetic acid | Roth, Karlsruhe |
| Acrylamide and bis-acrylamide solution (30/0.8%) | BioRad, München |
| Adenosine diphosphate (ADP) | Sigma Aldrich, Steinheim |
| Adenosine triphosphate (ATP) | Sigma Aldrich, Steinheim |
| Agarose | PeqLab, Erlangen |
| Albumax | Gibco, Karlsruhe |
| Alkynyl biotin | Invitrogen, USA |
| 6-Aminohexanoic acid | Roth, Karlsruhe |
| Ammonium persulfate (APS) | Sigma Aldrich, Steinheim |
| Ammonium sulfate | Roth, Karlsruhe |
| L-Arabinose | Sigma Aldrich, Steinheim |
| Azido myristic acid | Invitrogen, USA |
| Bradford reagent | BioRad, München |
| Bacto-Agar | Roth, Karlsruhe |
| Boric acid | Roth, Karlsruhe |
| Bovine serum albumin | Roth, Karlsruhe |
| Bromophenol blue | Sigma Aldrich, Steinheim |
| Calcium chloride | Roth, Karlsruhe |
| Carbenicillin | Roth, Karlsruhe |
| Chloramphenicol | Roth, Karlsruhe |
| Coomassie brilliant blue R250 | Sigma Aldrich, Steinheim |
| Coumaric acid | Sigma, Steinheim |
| Cupric sulfate ($CuSO_4$) | Sigma Aldrich, Steinheim |
| Cystatin | Roth, Karlsruhe |
| 1,4-Dithiothreitol (DTT) | Roth, Karlsruhe |
| Dimethyl sulfoxide (DMSO) | Roth, Karlsruhe |
| Dipotassium phosphate ($K_2HPO_4$) | Roth, Karlsruhe |
| Disodium hydrogen phosphate ($Na_2HPO_4$) | Roth, Karlsruhe |
| dNTPs | Fermentas, St. Leon-Rot |
| Ethanol | Roth, Karlsruhe |
| Ethidium bromide | Sigma Aldrich, Steinheim |
| Ethylenediaminetetraacetic acid (EDTA) | Roth, Karlsruhe |
| Ethylene glycol tetraacetic acid (EGTA) | Roth, Karlsruhe |
| Gentamycin | Invitrogen, Karlsruhe |

| | |
|---|---|
| Giemsa (0.4%, w/v) | Sigma Aldrich, Steinheim |
| Glucose | Merck, Darmstadt |
| Glycerol | Roth, Karlsruhe |
| Glycin | Roth, Karlsruhe |
| Hydrochloric acid | Roth, Karlsruhe |
| 4-(2-hydroxyethyl)-1-piperazineethanesulfonic acid (HEPES) | Roth, Karlsruhe |
| Hydrogen peroxide | Sigma Aldrich, Steinheim |
| Imidazole | Roth, Karlsruhe |
| Isopropanol | Roth, Karlsruhe |
| Isopropyl-β-D-thiogalactopyranoside (IPTG) | Roth, Karlsruhe |
| Kanamycin | Roth, Karlsruhe |
| Luminol | Sigma Aldrich, Steinheim |
| Methanol | Roth, Karlsruhe |
| Magnesium chloride | Roth, Karlsruhe |
| β-Mercaptoethanol | Roth, Karlsruhe |
| Milk powder | Roth, Karlsruhe |
| β-Nicotinamide adenine dinucleotide, reduced disodium salt (NADH) | Sigma Aldrich, Steinheim |
| Nickel-nitrilotriacetic acid (Ni-NTA) | Qiagen, Hilden |
| PEG 3350 (Polyethylene glycol) | Roth, Karlsruhe |
| PEG 6000 | Roth, Karlsruhe |
| Pepstatin A | Sigma Aldrich, Steinheim |
| Phenylmethylsulfonylfluoride (PMSF) | Sigma Aldrich, Steinheim |
| Phosphoenolpyruvate (PEP) | Sigma Aldrich, Steinheim |
| Ponceau | Sigma Aldrich, Steinheim |
| Potassium chloride (KCl) | Roth, Karlsruhe |
| Potassium dihydrogen phosphate ($KH_2PO_4$) | Roth, Karlsruhe |
| Potassium hydroxide (KOH) | Roth, Karlsruhe |
| Rhamnose | Sigma Aldrich, Steinheim |
| RPMI 1640 Gibco | Invitrogen, Karlsruhe |
| Saccharose | Roth, Karlsruhe |
| Saponin | Roth, Karlsruhe |
| Sodium acetate | Roth, Karlsruhe |
| Sodium chloride (NaCl) | Roth, Karlsruhe |
| Sodium dihydrogen phosphate ($NaH_2PO_4$) | Roth, Karlsruhe |
| Sodium hydrogen carbonate ( $NaHCO_3$) | Roth, Karlsruhe |
| Sodium dodecyl sulphate (SDS) | Merck, Darmstadt |
| Tetramethylethylenediamine (TEMED) | Sigma Aldrich, Steinheim |
| Triethylamine hydrochloride (TEA-HCl) | Sigma, Steinheim |
| Tris[(1-benzyl-1H-1,2,3-triazol-4-yl)methyl]amine (TBTA) | Sigma Aldrich, Steinheim |
| Tris(2-carboxyethyl)phosphine (TCEP) | Sigma Aldrich, Steinheim |

| | |
|---|---|
| Tetramethylethylenediamine (TEMED) | Sigma Aldrich, Steinheim |
| Tris(hydroxymethyl)aminomethane (Tris) | Roth, Karlsruhe |
| Triton X-100 | Sigma Aldrich, Steinheim |
| Trypton | Roth, Karlsruhe |
| Tween 20 | Merck, Darmstadt |
| Yeast extract | Oxoid LTD, U.K |

## 2.2 Antibodies

| Antibody | Source |
|---|---|
| Mouse anti-histidine$_6$-tag antibody | Dianova, Hamburg |
| HRP Anti-mouse IgG antibody | Pearce, Rockford |
| Anti-GFP antibody | Roche, Mannheim |
| Anti-Exp 1 antibody | Dr. Przyborski, Marburg |
| Anti-Hsp 70 antibody | Dr. Przyborski, Marburg |
| Anti-PfTrxR antibody | Pearce, Rockford |
| Anti-GSH antibody | Virogen, Watertown |

## 2.3 Antibiotics

| Antibiotic | Source | Stock concentration | Working concentration |
|---|---|---|---|
| Carbenicillin | Roth | 50 mg/ml in 50% Ethanol | 100 µg/ml |
| Chloramphenicol | Roth | 25 mg/ml in 100% Ethanol | 25 µg/ml |
| Kanamycin | Roth | 25 mg/ml in water | 50 µg/ml |

## 2.4 Enzymes

### 2.4.1 Restriction Enzymes

| Enzyme | Cleavage sequence | Source |
|---|---|---|
| *AvrII* | 5' C↓CTAGG 3' | Fermentas, St. Leon-Rot |
| *BamHI* | 5' G↓GATCC 3' | Fermentas, St. Leon-Rot |
| *XmaI* | 5' C↓CCGGG 3' | Fermentas, St. Leon-Rot |
| *HindIII* | 5' A↓AGCTT 3' | Fermentas, St. Leon-Rot |
| *NdeI* | 5' CA↓TATG 3' | Fermentas, St. Leon-Rot |
| *XhoI* | 5' C↓TCGAG 3' | Fermentas, St. Leon-Rot |
| *AflII* | 5' C↓TTAAG 3' | New England Biolabs, USA |
| *BsiWI* | 5' C↓GTACG 3' | New England Biolabs, USA |
| *SpeI* | 5' A↓CTAGT 3' | New England Biolabs, USA |
| *SacII* | 5' C CGC↓GG3' | New England Biolabs, USA |
| *BssHII* | 5' G↓CGCGC3' | Fermentas, St. Leon-Rot |
| *XmaI* | 5' C↓CCGGG3' | Fermentas, St. Leon-Rot |

### 2.4.2 DNA Polymerase

| Enzyme | Company |
|---|---|
| AccuPrime™ Taq DNA Polymerase | Invitrogen, Karlsruhe |
| *Pfu* DNA Polymerase | Promega, Mannheim |
| RedTaq® DNA Polymerase | Sigma Aldrich, Steinheim |

### 2.4.3 Other enzymes

| Enzyme | Source | Function |
|---|---|---|
| DNaseI | Roche, Mannheim | DNA digestion |
| DpnI | Fermentas, St. Leon-Rot | Methylated DNA digestion |
| Lysozyme | Sigma Aldrich, Steinheim | Cell lysis |
| Glucose-6-phosphate dehydrogenase | Sigma Aldrich, Steinheim | HK assay |
| T4 Ligase | Fermentas, St. Leon-Rot | Nucleotide fragment ligation |

## 2.5 Biological materials

### 2.5.1 Plasmids

| Plasmids | Antibiotic resistance | Source |
|---|---|---|
| pARL-2+ | Carbenicillin | Prof. Alan F. Cowman, Melbourne University |
| pET30a | Kanamycin | Novagen, Darmstadt |
| pGEM-T Easy | Carbenicillin | Promega, Mannheim |
| pGRO7 | Chloramphenicol | TaKaRa, Göttingen |
| pRAREII | Chloramphenicol | Novagen, Darmstadt |
| pLN | Carbenicillin | Promega, Mannheim |
| pUF-1 | Carbenicillin | Promega, Mannheim |
| pINT | Carbenicillin | Promega, Mannheim |

### 2.5.2 *E. coli* strains

| *E. coli* strain | Usage | Source |
|---|---|---|
| XL-1 Blue | Cloning and plasmid preparation | Stratagene, Amsterdam |
| Top10 | Cloning and plasmid preparation | Invitrogen, USA |
| KRX | Overexpression | Promega, Mannheim |
| BL21 | Overexpression | Invitrogen, Karlsruhe |
| C41 | Overexpression | Avidis, France |

### 2.5.3 *Plasmodium falciparum* strain

| *Plasmodium falciparum* strain | Source |
|---|---|
| 3D7 (Chloroquine-sensitive) | Prof. Lanzer, Heidelberg University |
| Dd2 (Chloroquine-resistant) | Prof. Vaidya, Drexel University |

## 2.6 Kits

| | |
|---|---|
| Bradford kit | Biorad, München |
| HiSpeed® Plasmid Maxi kit | Qiagen, Hilden |
| QIAprep Spin Miniprep Kit | Qiagen, Hilden |
| QIAprep Spin Maxiprep Kit | Qiagen, Hilden |
| QIAquick PCR Purification Kit | Qiagen, Hilden |
| Western lightning chemiluminescence reagent | Perkin Elmer, Boston, U.S.A |

## 2.7 Materials of affinity chromatography

| | |
|---|---|
| Nickel-Nitrilotriacetate-Agarose (Ni-NTA) | Qiagen, Hilden |
| Protino® Ni-TED | Machery-Nagel, Düren |
| Talon | GE Healthcare, Freiburg |

## 2.8 Medium for *E. coli* culture

| | |
|---|---|
| Lysogeny Broth Medium (LB), 1 L | 10 g Tryptone<br>5 g Yeast extract<br>10 g NaCl |
| Terrific Broth Medium (TB), 1 L | 12 g Tryptone<br>24 g Yeast extract<br>9,4 g $K_2HPO_4$<br>2,2 g $KH_2PO_4$<br>4 ml Glycerol |
| 2x YT Medium, 1 L | 16 g Tryptone<br>10 g Yeast extract<br>5 g NaCl |
| Modified LB, 1 L | 12 g Tryptone<br>24 g Yeast extract<br>5 g NaCl<br>5 g $K_2HPO_4$<br>0,142 $Na_2SO_4$<br>40 ml Glycerol |

## 2.9 Instruments

| Instruments | Producer |
|---|---|
| Analytical Balance | Scaltec Instruments, Göttingen |
| Autoclave | Webeco, Bad Schwartau |
| Beckman DU 650 Spectrophotometer | Beckmann, Munich |
| Beckman Optima Max Ultracentrifuge | Beckmann, Munich |
| Bio Photometer | Eppendorf, Hamburg |
| Eppendorf Research® Plus Pipettes | Eppendorf, Hamburg |
| Eppendorf Thermomixer | Eppendorf, Hamburg |
| FPLC-Software Unicorn | Amersham Bioscience, Freiburg |
| FPLC System ÄKTA-FPLC | Amersham Bioscience, Freiburg |
| Fraction Collector Frac-100 | Pharmacia Biotech, Freiburg |
| Freezer -86 °C | Heraeus Instruments, Hanau |
| Gene Pulser Xcell Electroporation | BioRad, Munich |
| GEL DOC 2000 System | BioRad, Munich |
| HeraCell $CO_2$ Incubator for *P. facliparum* Culture | Heraeus Instruments, Hanau |
| Hitachi U-2001 Spectrophotometer | Hitachi, Schwäbisch Gmünd |
| Honeybee 961 Crystallization robot | Zinsser Analytic, Frankfurt |
| Magnetic Stirrers RCT basic | IKA Werke, Staufen |
| Mastercycler® Thermal Cyclers | Eppendorf, Hamburg |
| Megafuge 1.0R Centrifuge | Heraus Instruments, Hanau |
| Mini-PROTEAN 3 cell Electrophoresis Module | BioRad, Munich |
| Minispin® Centrifuge | Eppendorf, Hamburg |
| Mitsubishi P91 Photo Printer | Mitsubishi, Ratingen |
| Neolab Heating Block | NeoLab, Heidelberg |
| Optima™ TLX Ultracentrifuge | Beckmann, Munich |
| OptiMax X-ray Film Processor | Protec, Oberstenfeld |
| QuadroMACS® Magnetic Separator | Miltenyi Biotec GmbH, Bergisch Gladbach |
| Owl EasyCast B1A Mini Gel Electrophoresis Systems (Agraose) | Thermo Scientific, Dreieich |
| pH Meter | Beckman, Munich |
| Pharmacia LKB Multiphor II NovaBlot | Amersham Pharmacia Biotech, Freiburg |
| Rotor Sorvall SLA 3000, SS34 | Thermo Fisher Scientific, Waltham, USA |
| Sonopuls GM 70 Ultrasonicator | Bandelin Electronics, Berlin |
| Sorvall® RC5BPlus Centrifuge | ThermoScientific, Waltham, USA |
| Thermomixer Comfort | Thermo Life Sciences, Egelsbach |
| Ultra Pure Water System | MembraPure, Bodenheim |
| UV/Vis-Spectrophotometer Beckman DU® 650 | Beckmann, Munich |
| Vortex Minishaker MS2 | IKA Werke, Staufen |

## 2.10 Protease inhibitors

| Inhibitor | Stock concentration | Working concentration |
|---|---|---|
| Protease Inhibitor Cocktail Tablets | / | 50 ml solution / one tablet |
| Cystatin | 40 µM in buffer | 80 nM |
| Pepstatin A | 0.3 mM in DMSO | 3 µM |
| PMSF | 100 mM in ethanol | 0.1 mM |

## 2.11 Buffers and solutions

### 2.11.1 Buffer for DNA electrophoresis

| | | |
|---|---|---|
| DNA Sample buffer | 0.1% | Bromophenol blue |
| | 60% | Saccharose |
| | 1 mM | Tris |
| | pH 8.3 | HCl (adjustment) |
| 10 X TBE (electrophoresis buffer) | 1 M | Tris |
| | 1 M | Boric acid |
| | 20 mM | EDTA |
| | pH 8.0 | Acetic acid (adjustment) |

### 2.11.2 Buffer for extraction of *P. falciparum* parasites

| | | |
|---|---|---|
| Saponin lysis buffer | 7 mM | $K_2HPO_4$ |
| | 1 mM | $MgCl_2$ |
| | 1 mM | $NaH_2PO_4$ |
| | 11 mM | $NaHCO_3$ |
| | 58 mM | KCl |
| | 56 mM | NaCl |
| | 14 mM | Glucose |
| | 0.02% | Saponin |
| | pH 7.4 | HCl (adjustment) |
| Cytomix | 12 mM | KCl |
| | 5 mM | $MgCl_2$ |
| | 10 mM | $KH_2PO_4$ |
| | 10 mM | $K_2HPO_4$ |
| | 25 mM | HEPES |
| | 0.15 mM | $CaCl_2$ |
| | 2 mM | EDTA |
| | pH7.6 | KOH (adjustment) |

| | | |
|---|---|---|
| Parasite cell lysis buffer | 137 mM | NaCl |
| | 2.7 mM | KCl |
| | 8 mM | $Na_2HPO_4$ |
| | 1.46 mM | $KH_2PO_4$ |
| | 1% | Triton |
| | pH 7.6 | HCl (adjustment) |

**2.11.3 Buffer for HK assay**

| | | |
|---|---|---|
| HK assay buffer | 7 mM | $MgCl_2$ |
| | 100 mM | Tris |
| | pH 7.0 | HCl (adjustment) |

**2.11.4 Buffer for protein purification**

| | | |
|---|---|---|
| Lysis buffer | 50 mM | Tris |
| | 300 mM | KCl |
| | 10% | Glycerol |
| | pH 7.0 | HCl (adjustment) |
| HK stock buffer | 50 mM | Tris |
| | 300 mM | KCl |
| | 30% | Glycerol |
| | pH 7.0 | HCl (adjustment) |

**2.11.5 Buffer for SDS-PAGE electrophoresis**

| | | |
|---|---|---|
| Electrophoresis buffer | 193 mM | Glycine |
| | 25 mM | Tris |
| | 0.1% (w/v) | SDS |
| | pH 8.3 | HCl (adjustment) |
| SDS Sample buffer (4x) | 240 mM | 1 M Tris-HCl, pH 6.8 |
| | 8% (w/v) | SDS |
| | 40% (v/v) | Glycerol |
| | 5% (v/v) | 14.7 M β-Mercaptoethanol |
| | 0.04% (w/v) | Bromophenol Blue |
| Coomassie staining solution | 0.2% (w/v) | Coomassie brillant blue R250 |
| | 40% (v/v) | 2-Propanol |
| | 10% (v/v) | Acetic acid |
| Coomassie destaining solution | 10% (v/v) | Acetic acid |
| | 40% (v/v) | Methanol |

**2.11.6 Western blot buffer**

| | | |
|---|---|---|
| Anode buffer I | 300 mM | Tris |
| Anode buffer II | 25 mM | Tris |
| Cathode buffer | 40 mM | 6-aminohexanoic acid |
| TBS buffer | 10 mM | Tris |
| | 155 mM | NaCl |
| | pH 8.0 | HCl (adjustment) |
| TBS-Tween (TBST) | 0.05% | Tween 20 (in TBS buffer) |
| Ponceau staining solution | 1% (w/v) | Ponceau S |
| | 5% (v/v) | Acetic acid |
| Ponceau destaining solution | 1% (w/v) | Acetic acid |
| Luminol solution (store in dark | 1.25 mM | Luminol |
| at 4 ℃) | 0.0093% (v/v) | $H_2O_2$ |
| | 0.1 M | Tris-HCl, pH 8.6 |

**2.11.7 Stock solutions**

| Compound | Concentration | Solvent | Storage |
|---|---|---|---|
| APS | 10% (w/v) | $H_2O$ | -20 ℃ |
| L-Arabinose | 20% (w/v) | $H_2O$ | Filter sterilized, -20 ℃ |
| IPTG | 1 M | $H_2O$ | Filter sterilized, -20 ℃ |
| Rhamnose | 20% (w/v) | $H_2O$ | Filter sterilized, -20 ℃ |

# 3. Methods

## 3.1 General methods

### 3.1.1 Preparation of competent cells

Liquid LB medium (3 ml) with an antibiotic was inoculated with *E. coli* cells and grown overnight (~ 15 hours) in a shaking incubator at 37 ℃. The overnight pre-culture was added into 100 ml of LB medium containing the same antibiotic and then was grown in a shaking incubator at 150 rpm at 37 ℃ until the O.D. value reached 0.6-0.8. The *E. coli* cell culture was transferred into Falcon tubes. After 10 minutes placing the cell culture on ice, a pellet was obtained via 10 minutes centrifugation with a speed of 4,000 *g* at 4 ℃. Then the pellet was resuspended in 10 ml ice-cold 0.1 M $CaCl_2$ solution containing 10% glycerol and was left on ice for 15 minutes. A second round centrifugation was performed at 4,000 *g* at 4 ℃ for 10 minutes. This time the pellet was resuspended in 1 ml of ice-cold 0.1 M $CaCl_2$ containing 10% glycerol and aliquoted into labeled Eppendorf tubes and placed into liquid nitrogen for

3 minutes. The frozen competent cells were stored at -80 ℃ and ready to use.

### 3.1.2 Cleavage of double stranded DNA by restriction endonucleases and ligation

The DNA fragment obtained by PCR and the plasmids, which contain the specific nucleotide sequences known as the restriction sites, were cleaved by the restriction endonulease (Roberts, 1976). The digestion procedure was performed at an optimized buffer and temperature for 1 hour according to the restriction endonulease manufacturer's instructions. After digestion the mixture was purified by the QIAquick PCR Purification Kit, and the concentration of DNA was determined via absorption at 260 nm (Sambrook *et al*., 2001). The purity of the DNA sample was examined by the ratio of $A_{260nm}/A_{280nm}$ which ranges from 1.8 to 2.0.

The T4 ligation system was used to connect the PCR product and plasmid, which were digested by the appropriate restriction endonulease. T4 ligase catalyzes the reaction to form a phosphodiester bond between the 5' phosphate group of one fragment and the 3' hydroxyl group of the other. The molar ratio of the vector to the insert can vary from 1:3 to 1:7. The following formula can be used to calculate the amount of insert.

$$\text{insert (ng)} = \frac{\text{vector (ng) x insert (kb)}}{\text{vector (kb)}} \text{ x desired molar ratio of insert : vector}$$

The mixture of ligation left at RT for 1 hour or 4 ℃ overnight (~ 18 h) contained the vector, DNA fragments (insert), and T4 ligase in a proper buffer. After ligation the mixture could be used to transform competent cells.

### 3.1.3 Transformation of competent cells

2 µl of the plasmid or 5 µl ligation product was added into 50 µl of competent cells, mixed thoroughly, and incubated on ice for 30 minutes. The mixture was placed at 42 ℃ for 90 seconds for heat shock and then the cells were put back on ice for 10 minutes. Approximately 400 µl LB medium was added to the cells. After being grown at 37 ℃ for 1 hour, the cells were spread on LB agar plates with the appropriate antibiotic or selection marker. Then plates were placed in an incubator at 37 ℃ overnight, and the colonies were observed the next day.

### 3.1.4 SDS-polyacrylamide gel electrophoresis

The SDS-PAGE is a technique used to separate protein mixtures according to the different molecular

weight under denatured conditions. The detergent SDS can neutralize the negative charge of the polypeptide. The distribution of SDS covered on the protein surface is also related to the molecular weight of the protein. Therefore the proteins can be separated by their different sizes.

SDS-PAGE was performed according to the following steps. Protein samples were mixed with 1x sample buffer and denatured at 95 ℃ for 5 minutes. The denatured proteins were loaded onto the pre-cast discontinuous polyacrylamide gels consisting of 2 parts named stacking gels and resolving gels. The stacking gel contained pockets where the samples were loaded, and the resolving gel on which the proteins were separated by their molecular weight. The gels were run at 200 volts in an electrophoresis tank containing an electrophoresis buffer. After electrophoresis, the gels were stained in Coomassie blue solution and destained with Coomassie destaining solution until protein bands were visible. If Western blot was required, the gels were not stained with Coomasie blue but were directly soaked into the cathode buffer.

| Stacking gels (4%) | |
|---|---|
| 1.5 M Tris pH 6.8 | 1.25 ml |
| SDS (10% in water) | 0.05 ml |
| Acrylamide (Rotiphorese® gel 30)* | 0.65 ml |
| TEMED | 5 µl |
| APS (10%) | 25 µl |
| $H_2O$ | 3.05 ml |
| Resolving gels (12%) | |
| 1.5 M Tris pH 8.8 | 3.75 ml |
| SDS (10% in water) | 0.15 ml |
| Acrylamide (Rotiphorese® gel 30)* | 6 ml |
| TEMED | 7.5 µl |
| APS (10%) | 75 µl |
| $H_2O$ | 5.1 ml |

**Table 3.1: Composition of SDS-PAGE gels.**

### 3.1.5 Western blot

The semi dry Western blot was performed in our experiments (Towbin *et al.*, 1979). The protein was transferred into a polyvinylidene difluoride (PVDF) membrane followed by SDS-PAGE gel separation. The specific antibody was used to detect the target protein through an immunological reaction. The gel was soaked into cathode buffer after the completion of gel electrophoresis. The PVDF membrane was activated by methanol and quickly transferred into anode buffer II solution. Five filter papers that were

pre-soaked in cathode buffer were put onto a cathode graphite plate, and the gel electrogram in cathode buffer was laid onto it. The PVDF membrane in anode buffer II was laid onto the gel electrogram. Then 2 filter papers soaked in anode buffer II and 3 filter papers soaked in anode buffer I were laid onto the PVDF membrane, respectively. The air bubbles among the layers were carefully removed. Finally an anode graphite plate was placed onto it. The transfer process was run at 0.8 mA/cm$^2$ of gel electrogram for 55 minutes.

After the transfer process, the result of the transfer was checked by staining the PVDF membrane in Ponceau staining solution for 1 minute and destaining with 1% acetic acid until protein bands were visible. Then the PVDF membrane was washed with TBST buffer to remove the remaining Ponceau dye and gently shaken in 5% milk powder in TBS buffer for 1 hour in order to block the excess absorption sites and prevent unspecific binding. After that the PVDF membrane was washed 3 times for 10 minutes each in TBST buffer and incubated with the primary antibody for 1 hour at RT. Then the uncombined primary antibody or membrane was rinsed by TBST buffer, and the secondary antibody was added to react with the primary antibody. After 1 hour incubation and 3 times of 10 minutes TBST washing, the membrane was immunostained by exposing it to an enhanced chemiluminescence mixture that contained 1 ml luminal solution and 10 µl coumaric acid for 1 minute. Finally the membrane was wrapped in a transparent foil and exposed to X-ray film. The exposure time was varied between 30 seconds to 10 minutes according to the signal strength.

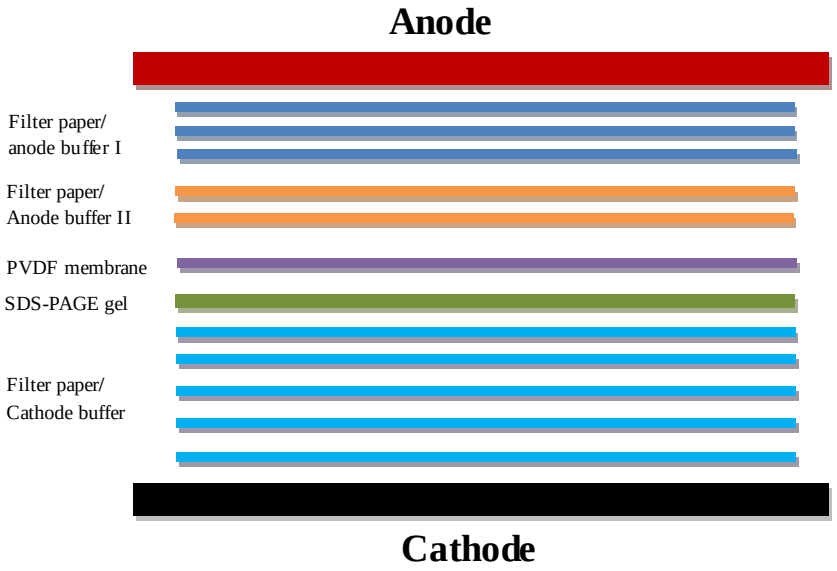


**Figure 3.1: Transfer stack in semi-dry Western blot.** I. Arrangement of the transfer stack from cathode to anode: 5 filter papers in cathode buffer, SDS-PAGE gel in cathode buffer, PVDF membrane in anode buffer II, 2 filter papers in anode buffer II, and 3 filter papers in anode buffer

### 3.1.6 Gel filtration

To further separate the target protein from cell lysate or protein samples, a native gel chromatography on a 16/60 superdex 200 prep grade column was used to determine the molecular mass of the target protein, which was connected to an ÄKTA FPLC system (Amersham Pharmacia Biotech). The gel filtration standard (Amersham Pharmacia Biotech) was used to perform the calibration of the column containing aldolase, albumin, chymotrypsinogen, ferritin, and ovalalbumin as reference proteins. After per-equilibrating with the appropriate buffer, 1 milliliter of a 1 mg/ml protein solution was loaded onto the column. Protein-containing fractions were detected spectrophotometrically at 280 nm and were collected at a flow rate of 1.0 ml/min. The UNICORN 4.11 software was used to evaluate the peak areas and $K_{AV}$ values. The elution fractions containing proteins were further analyzed on SDS-PAGE.

### 3.1.7 Determination of protein concentration

The Bradford method was performed to determine the concentration of proteins. This method is based on the shift of absorbance of maximum of Coomassie Brilliant Blue G-250 dye from 465 nm to 595 nm when the protein-dye complex is formed (Bradford, 1976). The amount of proteins was correlated with increasing absorbance at 595 nm, thereby providing the protein amount measurement.

To determine the protein concentration, a calibration curve with standard concentrations was required. A series of BSA with different concentrations was prepared in order to plot a calibration curve. Each sample contained 5 µl BSA solution and 495 µl dd$H_2O$. 125 µl Bradford reagent was added, vortexed and incubated for 5 minutes at RT. A spectrophotometer was used to determine the absorption in a cuvette at 595 nm. Then, the calibration curve of absorption was plotted, which was correlated with protein concentrations. This calibration curve could be used to calculate the sample concentration by the absorption obtained following the above procedure.

## 3.2 *Pf*HK methods

### 3.2.1 Cloning of *Pf*HK

In order to clone *Pfhk* from a blood stage cDNA library of *P. falciparum* 3D7, two primers (5‘-CGTTCATATGAGTGAGTACGATATTGCAAAAA-3‘, 5‘-CGTTCTCGAGTGGTAATTGAGGA ATGTCCGCAT -3‘) with *NdeI* and *XhoI* restriction sites were used to amplify about 1,482 bp fragments. The PCR procedure was performed according to the following program. Then the PCR

product was checked by agarose gel electrophoresis. After purification with a QIAquick PCR purification kit, both the PCR product and pET 30a vector were digested by *NdeI* and *XhoI* restriction enzymes. The double digestion mixtures were prepared as shown in the table below and incubated at 37 ℃ for 1 hour. When digestion was finished, agarose gel electrophoresis was applied to determine the efficacy of digestion. Furthermore the digestion mixture was purified again and the concentration was measured. A T4 ligation system was applied to connect the fragments and vectors at optimal conditions. Then the ligation mixture was added to *E. coli* XL-1 Blue cells for transformation. After one night of incubation, the colonies were observed on the agar plates with the selection marker (Kanamycin) and were picked up to be cultured in 3 ml LB medium containing Kanamycin (100 μg/ml) overnight (~ 15 hours). The Qiagen Miniprep plasmid kit was used to extract plasmids. The accuracy of colonies was verified by restriction cleavage and sequencing.

| PCR mixture | |
|---|---|
| Component | Volume (μl) |
| 10x buffer | 5 |
| Template (~80 ng) | 1 |
| dNTP (2 mM) | 4 |
| Primer forward (100 μM) | 1 |
| Primer reverse (100 μM) | 1 |
| Polymerase | 0.5 |
| $H_2O_{dd}$ | 37.5 |

| PCR program | |
|---|---|
| Program | Time and Temperature |
| Initialization | 95 ℃ for 3 min |
| Denaturation | 95 ℃ for 30 s |
| Annealing | 55 ℃ for 45 s |
| Elongation | 72 ℃ for 3 min |
| Cycles | 30 cycles |
| Final elongation | 72 ℃ for 10 min |

| Double restriction enzyme digestion | |
|---|---|
| Component | Volume (μl) |
| PCR product | 30 |
| 10 x Tango buffer | 10 |
| *NdeI* (10 U/μl) | 2.5 |
| *XhoI*(10 U/μl) | 2.5 |
| $H_2O_{dd}$ | 5 |

| Ligation mixture | |
|---|---|
| Component | Volume (μl) |
| Insert | 3 |
| Vector | 1 |
| 2 x rapid ligation buffer | 5 |
| T4 ligase | 1 |

### 3.2.2 Heterologous overexpression of *Pf*HK

The plasmid of *PfHK*/pET30a was transformed into *E. coli* C41pGro7 cells. The overnight pre-culture was transferred into 1 liter TB medium containing 50 µg/ml of kanamycin and 25 µg/ml of chloramphenicol antibiotic and 0.8% (w/v) L-arabinose, inducing the pGro7 plasmid. Cell culture was grown in an incubator at 37 ℃. When the optical density (OD 600 nm) reached 0.8, the culture was induced by a final concentration 1mM IPTG and further grown at 18 ℃ for about 48 hours. Cells were harvested as a pellet by centrifugation at 8,000 g for 15 minutes at 4 ℃ and resuspended in 50 mM Tris, 300 mM KCl, 10% Glycerol, pH 7.0. After adding a protease inhibitor cocktail composed of cystatin, pepstatin, and PMSF, cells were stored at -20 ℃.

### 3.2.3 Optimization of the heterologous overexpression of *Pf*HK

Different *E. coli* cell lines were used to optimize the heterologous overexpression of *Pf*HK as well as varying the different expression parameters as summarized in Table 4.2.

### 3.2.4 Purification of *Pf*HK

A small amount of DNase and lysozyme (5 mg/g pellet) was added into the resuspended pellet and stirred on ice for 1 and a half hours. The cells were sonicated 6 times for 30 seconds in the presence of protease inhibitors (100 µM PMSF, 3 µM pepstatin, and 80 nM cystatin) and centrifuged at 18,000 g for 30 minutes. The clear supernatant containing the soluble fraction was exposed to 5 mM imidazole and applied to a Protino® Ni-TED resin column, which was pre-equilibrated with HK purification buffer containing 50 mM Tris, 300 mM KCl, 10% glycerol, 5 mM imidazole, pH 7.0. The column was washed with 10 ml HK purification buffer and twice with elution buffer with 10 mM imidazole, and the recombinant protein was eluted by 500 mM imidazole. All the fractions were checked on SDS-PAGE. The pure fraction was concentrated using a 10 kDa viva spin column and further purified by gel filtration using an ÄKTA FPLC system (Amersham Pharmacia Biotech).

### 3.2.5 Optimization of *Pf*HK purification

The purification procedure was optimized with different columns in combination with gel filtration using an FPLC machine (Table 4.3). Different buffers, pH and salt concentrations were also optimized (Table 4.1).

### 3.2.6 Gel filtration of *Pf*HK

Gel filtration can help separate proteins by their molecular mass. The small proteins are slower than the big ones when passing though the gel filtration medium. *Pf*HK was further purified by gel-filtration chromatography on a HiLoad 16/60 Superdex 200 prep-grade column connected to an ÄKTA FPLC system (Amersham Pharmacia Biotech). After equilibration, the column with 1 column volume of buffer containing 50 mM Tris, 300 mM KCl, 10% glycerol, pH 7.0, sample was loaded onto the column. The elution fraction was collected and detected spectrophotometrically at 280 nm. The protein-containing fractions obtained were analyzed on SDS-PAGE and then concentrated using 3 kDa viva spin columns. The concentration of *Pf*HK was determined using the Bradford protein assay (Bradford, 1976).

### 3.2.7 Western blot using anti-His antibody to identify *Pf*HK

During the purification process, *Pf*HK was identified by the anti-His antibody as the recombinant *Pf*HK containing the 6-His tag as selecting marker. The Western blot was performed as outlined in 3.1.5. The primary antibody was diluted using 3% BSA in TBST (1:1,000). The secondary anti-mouse antibody was diluted using 5% milk powder in TBST (1:5,000). The His-marker was used as positive control.

### 3.2.8 *Pf*HK kinetic assay

#### 3.2.8.1 Determination of $K_m$ values for ATP and glucose

The *Pf*HK assay used in our study was the standard coupled HK assay, which measured the reduction of $NADP^+$ to NADPH at 340 nm and was catalyzed by G6PDH in a coupled assay system at RT (Beulter, 1984). Generally, glucose 6-phosphate produced by HK could be utilized by G6PDH. The generation of NADPH was monitored by the change of absorbance at 340 nm. The reaction mixture for measurement of the $K_m$ for ATP was composed of 0.5 mM glucose, 0.2 mM nicotinamide adenine dinucleotide phosphate (NADP), 0.3 U G6PDH from *Leuconostoc mesenteroides* (Sigma), HK assay buffer (100 mM Tris-Cl, 7 mM $MgCl_2$, pH 7.0), *Pf*HK enzyme, and varying amounts of ATP (50-2,000 µM), which was add to start the reaction. The total reaction volume was 500 µl. Measurement of $K_m$ for glucose on the other hand was performed by varying the concentrations of glucose (20-1,000 µM) and fixing the concentration of ATP at 2 mM.

$$\text{Glucose} + \text{ATP} \xrightarrow{\text{Hexokinase}} \text{glucose 6-phosphate} + \text{ADP}$$

$$\text{Glucose 6-phosphate} + \text{NADP} \xrightarrow{\text{G6PDH}} \text{glucosamine 6-phosphate} + \text{NADPH}$$

| | | | |
|---|---|---|---|
| HK assay buffer | : | 500 – x µl | |
| Hexokinase | : | x µl | |
| Glucose (50 mM) | : | 5 µl | 0.5 mM |
| $NADP^+$ (10 mM) | : | 10 µl | 0.2 mM |
| G6PDH (0.1 U/µl) | : | 3 µl | 0.3 U/mL |
| ----------Baseline---------- | | | |
| ATP (200 mM) | : | 5 µl | 2 mM |

$\varepsilon_{NADPH} = 6.22\ mM^{-1}cm^{-1}$

$$VA = \frac{\Delta A/min * V_0}{6.22 * v_i}[U/ml]$$

$V_0$ is the total volume of assay, and $v_i$ is volume of enzyme used.

The stability of the baseline was determined before the assays were carried out in order to prevent the background reactions that would affect the integrity of assays. Such background reaction could be from contamination or the *E. coli* proteins co-purified with *Pf*HK. A standard reaction mixture for the HK assay was prepared as outlined above in the presence of all substrates and G6PDH, but the reaction was started by adding ATP. In a similar set up, expression was performed using C41 pGro7 cell without *Pf*HK and purified as outlined for *Pf*HK. The fractions that normally contain positive bands of *Pf*HK were then used to check the stability of the baseline as outlined.

#### 3.2.8.2 *Pf*HK's pH and buffers profile

To determine the optimum buffer and pH conditions for *Pf*HK activity, three buffers as outlined below were tested. Because $Mg^{2+}$ is necessary for the *Pf*HK activity, 7 mM $MgCl_2$ was added to all buffers.

| Buffer | pH range |
|---|---|
| Tris buffer (100 mM) | 6.5-8.1 |
| Hepes buffer (50 mM) | 6.5-8.1 |
| MOPS buffer | 6.5-7.9 |

#### 3.2.8.3 Feedback inhibition with ADP and G6P

In product inhibition studies, ADP as the product of the reaction was added to the assay mixture. The initial rates were measured for a series of ADP concentrations (0-1.5 mM) at a fixed glucose concentration (0.3 mM) while varying the concentrations of ATP (0-3 mM) using the assay described in 3.8.2.1; the total volume of the reaction mixtures was adapted to 200 µl. A similar measurement was carried out by fixing the ATP concentration (1 mM) and varying glucose concentrations (0-1 mM). For the G6P feedback inhibition test, the ADP assay was applied to measure the decrease of NADH at 340 nm, at which point the production of ADP was catalyzed by a coupled reaction of pyruvate kinase and lactate dehydrogenase. The reaction mixture was composed of 0.5 mM glucose, 2 mM ATP, 5 mM PEP, 0.2 mM NADH, 5 U PK, 5 U LDH, *Pf*HK enzyme and buffer (100 mM Tris-HCl, 7 mM Mg $Cl_2$, pH 7.4). A series of G6P concentrations (0-0.5 mM) were measured by the same procedure as in the ADP feedback inhibition assay. The data were automatically read by an Infinite M 200 multiwell reader (TECAN. Inc) and analyzed by the GraphPad Prism 5 software (GraphPad Software, Inc).

#### 3.2.8.4 Test for HK activity in full blood and *P. falciparum*-infected RBC

In order to determine whether the *P. falciparum* infection has an impact on the host HK activity, the HK activities in infected RBC and uninfected RBC were determined. After synchronization and continuous culture, the parasitized erythrocytes with *P. falciparum* at the trophozoite stage (IRBC) were separated from uninfected erythrocytes (UIRBC) by LD-columns (MACS, Miltenyi Biotec). A plate of non-parasitized erythrocytes was cultured under the same conditions as control. The erythrocytes were washed three times by PBS pH 7.4 and lysed in 0.02% saponine PBS buffer. The RBC lysates were centrifuged at 1,000 g for 10 minutes at 4 °C. Then supernatants were transferred into new tubes and protein concentration was determined using the Bradford method. The assay of HK activity was performed as described in 3.2.8.1. To avoid the background of hemoglobin, the assay was changed to fluorescence spectrometry. The NADPH generation was monitored at 340 nm and 460 nm. The data

were automatically read by an Infinite M 200 multiwell reader (TECAN. Inc) and analyzed by the GraphPad Prism 5 software (GraphPad Software, Inc).

A possible contamination of IRBC lysate with parasites was checked by Western blot using *P. falciparum*-specific antibodies (*Pf*TrxR and *Pf*GluPho). The ratio of contamination was also determined by measuring the activity of GluDH in buffer C (100 mM potassium phosphate, 1 mM EDTA; pH 8.0) (Zocher *et al.*, 2012), which only exists in *P. falciparum* (see below) and not in hRBC.

$$\text{Glutamate} + \text{NADP}^+ \xrightarrow{\text{GDH}} \text{2-oxoglutarate} + \text{NADPH}$$

| | | | |
|---|---|---|---|
| Assay buffer (pH8.0) | : | 180 – x µl | |
| $NADP^+$ (1 mM) | : | 10 µl | (0.05 mM) |
| GDH (RBC lysates) | : | x µl | |
| ----------Baseline---------- | | | |
| Glutamate (100 mM) | : | 10 µl | (5 mM) |

### 3.2.9 *Pf*HK regulation by *P. falciparum* redox proteins

The recombinant *P. falciparum* redox proteins (*Pf*Trx1, *Pf*Grx, *Pf*Plrx) were prepared according to the procedures in our lab (Becker *et al.*, 2003; Kanzok *et al.*, 2000; Rahlfs *et al.*, 2001). The concentrations of these proteins were adjusted to 5 mg/ml. After pre-reducing these proteins with 4 mM DTT for 1 hour at 4 °C, the excess DTT was removed via gel filtration chromatography (Zeba™, Thermo Scientific). The protein concentration was measured via the Bradford method. *Pf*HK was diluted to the normal stock solution which was used for the standard HK assay outlined in 3.2.8.1, and mixed with reduced *Pf*Trx, *Pf*Grx, *Pf*Plrx (0-20 µM), or DTT (5 mM), respectively. The mixtures were incubated for 15 minutes at RT. Then the standard HK assay was performed to determine the activity of each treatment.

### 3.2.10 *S*-Glutathionylation of *Pf*HK

The recombinant *Pf*HK was diluted to 400 µg/ml and incubated with different concentrations of both reduced and oxidized glutathione (0.001-10 mM) for 30 minutes at RT and overnight at 4 °C,

respectively. The glutathionylated *Pf*HK was detected by semi-dry Western blots under non-reducing conditions, using a monoclonal anti-GSH antibody (Virogen, diluted 1:500 in 5% non-fat milk with TBST) and a phosphatase-conjugated anti-mouse antibody (Dianova, 1:5,000 in 5% non-fat milk with TBST). A control was applied using *Pf*HK incubated under the same conditions but without glutathione. To monitor the influence of glutathionylation on the enzymatic activity of *Pf*HK, enzymes were incubated with different concentrations of oxidized glutathione (1-10 mM) for 1 hour at RT. Aliquots were taken every two minutes and assayed for activity. The deglutathionylation was performed with the incubation of glutathionylated *Pf*HK with the reducing compound (DTT) and the pre-reduced members of the thioredoxin superfamily. Western blot and activity assays were used to determine this reversible glutathionylation.

### 3.2.11 Deletion mutant of *Pf*HK

To verify the function of the hydrophobic region at the C-teminus of *Pf*HK, a truncated mutant of *Pf*HK was designed. After analyzing the alignment of HKs in different species, the last 15 amino acid residues were deleted, which were supposed to contribute to the membrane association of the protein.

#### 3.2.11.1 Mutagenesis PCR

In order to heterologously overexpress the truncated *Pf*HK, a pET30a plasmid containing the C-terminus of deleted *Pf*HK was constructed. An efficient, one-step, site-directed plasmid mutagenesis protocol was performed (Liu *et al.*, 2008), using the *PfHK/pET30a* as a template. This method allowed facile, large, single insertions, deletions, and multiple mutations within a single PCR reaction. Two primers (5‘-AGGGAGCAGCCATCCTCGAGCACCACCACCACCAC-3‘, 5‘- GTGCTCGAGGA TGGCTGCTCCCTTTCCTGAACCATC -3‘) were designed following the protocol.

The following PCR program was performed, and the PCR product was purified by the Qiaquick PCR purification kit. The template plasmid was digested for 2 hours at 37 °C using 5 units of *Dpn*I restriction enzyme. Then 10 µl of the product was analyzed by agarose gel electrophoresis. Then the amplified plasmid was transferred into XL-1 Blue *E. coli* cells. A positive colony was picked and sent to sequencing for verification.

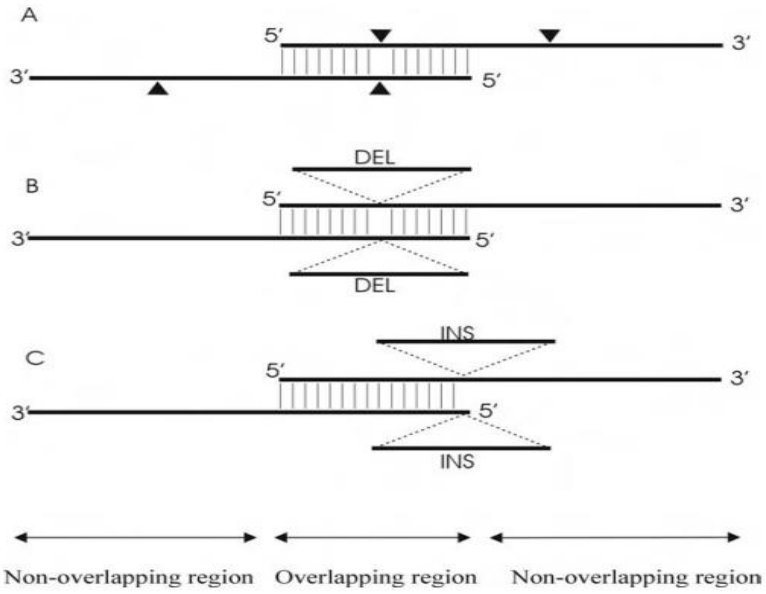


**Figure 3.2: Schematic diagram of the primer design for site-directed mutagenesis.** Primer designs are shown for site-directed mutation (A), deletion (B), and insertion (C). Triangles, DEL, and INS indicate the locations of the mutations, deletion, and insertion, respectively, in the primer sequences (Liu *et al*., 2008).

| PCR mixture | |
|---|---|
| Component | Volume (µl) |
| 10x buffer | 5 |
| Template (~10 ng) | 1 |
| dNTP (2 mM) | 5 |
| Primer forward (100 µM) | 0.5 |
| Primer reverse (100 µM) | 0.5 |
| Pfu polymerase (3U) | 1 |
| $H_2O_{dd}$ | 37 |

| PCR program | |
|---|---|
| Program | Time and Temperature |
| Initialization | 95 ℃ for 5 min |
| Denaturation | 95 ℃ for 1 min |
| Annealing | 60 ℃ for 1 min |
| Elongation | 72 ℃ for 15 min |
| Cycles | 12 cycles |
| Annealing | 35 ℃ for 1 min |
| Final elongation | 72 ℃ for 30 min |

| *DpnI* digestion | |
|---|---|
| Component | Volume (µl) |
| PCR product | 30 |
| 10 x Tango buffer | 5 |
| *DpnI* (10 U/µl) | 0.5 |
| $H_2O_{dd}$ | 14.5 |

#### 3.2.11.2 Heterologous overexpression of truncated *Pf*HK

The plasmid of truncated *PfHK*/pET30a was transformed into *E. coli* BL21 cells. The overexpression and purification procedures were similar to the full-length *Pf*HK described in 3.2.2.

### 3.2.12 GFP construction of full-length and truncated *Pf*HK

Green fluorescent protein (GFP) is widely used to investigate proteins' subcellular localization, which is originally 238 amino acids in length and can emit green fluorescence at 509 nm under the exciting light (Shimomura *et al*., 1962; Tsien, 1998). After transfection with the vector containing target protein and GFP, the GFP-fused target protein can be overexpressed and examined. Because GFP is co-localized with the target protein, the immunofluorescence from GFP could be detected under a fluorescent microscope and reveals the compartment localization of the target protein. In *P. falciparum*, this method could be used to examine compartment-specific proteins in living parasites.

To determine the localization and the function of the C-terminal hydrophobic region of HK in *P. falciparum*, the *PfHK* gene must be integrated downstream of the GFP gene in the vector. The *pARL-2a+* vector was chosen to carry *PfHK* fused with N-terminal GFP. Two pairs of primers (Table 3.3) with *BssHII* and *XmaI* restriction sites were designed to clone the full-length and truncated *PfHK* from the *PfHK/pET30a* plasmid.

| | | |
|---|---|---|
| ***PfHK*** | **Full-length** | atatGCGCGCAGTGAGTACGATATTGCAAAAAATG<br>atatCCCGGGTTATGGTAATTGTGGAATGTCCGC |
| | **Truncated** | atatGCGCGCAGTGAGTACGATATTGCAAAAAATG<br>atatCCCGGGTTAGATGGCTGCTCCCTTTCCTG |

**Table 3.2: Primers for HK-GFP constructs.** The *BssHII* and *XmaI* restriction sites are underlined.


**Figure 3.3: Structure of GFP fusion construction of the *PfHK* gene in *pARL-2a+***

After the PCR program, a QIAquick PCR purification kit was used to clean the PCR product. Because the restriction enzymes BssHII and XmaI work in different buffers, a two-step digestion (see below) was applied to digest insertions and vector. After analysis by agarose gel electrophoresis, the T4 ligation system was applied to connect the fragment and vector. The *PfHK/ pARL-2a+* vectors containing the fusion constructs were verified by sequencing. To prepare the plasmid for transfection,

the Qiagen Maxi Kit was used to extract and purify plasmid from XL-1 blue cells. Then a future precipitation step was required to obtain the sterile DNA with high purity and concentration.

| Two-step digestion | |
|---|---|
| Component | Volume (µl) |
| PCR product or vector | 30 |
| 10 x Tango buffer | 5 |
| *XmaI* (10 U/µl) | 2.5 |
| $H_2O_{dd}$ | 12.5 |
| 37 °C 2 Hours | |
| *BssHII* (10 U/µl) | 3 |
| 10 x Tango buffer | 7 |
| 37 °C 2 Hours | |

#### 3.2.12.1 *P. falciparum* cell culture

The 3D7 strains of *P. falciparum* in intraerythrocytic stages were cultured in our lab (Trager *et al.*, 1976). The strains were propagated in RBC ($A^+$) and cultured in RPMI 1640 medium plus 9 mM glucose, 0.2 mM hypoxanthine, 0.5% Albumax, 2.1 mM L-glutamine, and 22 µg/ml gentamycin. The culture was maintained in an incubator containing 3% $CO_2$, 3% $O_2$, and 94% $N_2$ at 37 °C. On a daily basis, the parasite growth was monitored by using Giemsa stained blood smears (10% Giemsa, 20 minutes). Normally every 48 hours parasites propagate 3 to 8-fold.

#### 3.2.12.2 Synchronization

Synchronization of parasites was performed with 5% (w/v) sorbitol as described (Lambros *et al.*, 1979). The cell culture (5% hematocrit, 10 ml) with predominantly ring stages was centrifuged (2,100 rpm, 3 minutes). A pellet of 500 µl of parasitized RBC was obtained. The pellet was resuspended in 5 ml of 5% (w/v) sterile sorbitol and incubated for 10 minutes at RT. After incubation, the parasites were centrifuged (2,100 rpm, 3 minutes) again to spin down the parasitized RBC. The supernatant was aspirated, and the pellet was washed twice by resuspending it in complete medium. The result of synchronization was checked by Giemsa-stained thin blood films (10% Giemsa, 20 min).

**3.2.12.3 Parasite transfection**

The electroporation method (Crabb *et al*., 2004) was used to carry out the transfection with the *P. falciparum* 3D7 strain. A 5 ml parasite culture at ring stage (8-10 hours) with 5-8% parasitemia was centrifuged at 1,500 g for 5 minutes. Cytomix buffer was mixed with 150 micrograms of plasmid (GFP-HK fusion gene in pARL-2a+) in a total volume of 400 µl. 400 µl plasmid Cytomix solution was used to resuspend the parasite pellet, and the suspension was transferred into a sterile electroporation cuvette. Then the parasites were electroporated at 310 V, 950 µF (Gene pulser, Bio-Rad) as described (Crabb *et al*., 2004). The resulting time constant was about 13 milliseconds. The transfected parasites were quickly transferred into 15 ml fresh complete medium (pre-warmed to 37 ℃) with 3.5% hematocrit. After 6 hours, the selection marker (2 nM WR99210) was added for selection after transfection. The concentration of WR 99210 was increased to 5 nM after 3-4 weeks. The RPMI medium with WR99210 was changed daily, and 100 µl of fresh erythrocytes was added weekly.

**3.2.12.4 Immunofluorescence imaging**

Immunofluorescence imaging was carried out in collaboration with Dr. Jude Przyborski's group at Philipps University in Marburg. The cells were fixed in 4% paraformaldehyde/0.0075% glutaraldehyde in PBS pH 7.4 for 30 minutes at 37 ℃ (Tonkin *et al.*, 2004). The fluorescence quenching was achieved by adding 100 mM glycine/PBS. To label the nucleus, Hoechst DNA binding dye (50 ng/ml) was used to reveal the nucleus. The images were obtained on a Zeiss Axio Observer inverted epifluorescence microscope system.

**3.2.12.5 Western blot analysis**

The transgenic parasites were cultured as described in 3.2.12.3. LD-columns (MACS, Miltenyi Biotec) were used to enrich the parasitized red blood cells with trophozoite stage *P. falciparum*. After washing, the IRBCs were centrifuged at 300 g for 3 min at room temperature and ruptured by 0.1% saponine for 45-60 seconds. Parasites were resuspended in 10 mM Tris pH 7.4 buffer, which contains a complete cocktail of protease inhibitors from Roche, and lysed by three freezing-thawing cycles by liquid nitrogen. The lysates were centrifuged at 50,000 g for 30 minutes at 4 ℃. The supernatants of parasite cytosol were transferred into another new tube, and the pellets of the membrane fraction of the parasite were washed with 1 ml of PBS buffer. All the cytosol fractions and membrane fractions were

centrifuged again at 50,000g for 30 minutes at 4 ℃. After the second centrifugation, the membrane pellets were resuspended in PBS buffer according to the initial volume of lysates.

The proteins in membrane pellets and cytosol fractions were separated by 10% SDS-PAGE gel and then transferred to a PVDF membrane. The membranes were probed with anti-GFP (1:1,000, Roche), anti-Hsp70 (1:1,000, T. Blisnick, Paris), or anti-Exp1 (1:500, Jude Przyborski) antibodies, respectively, followed by HRP-conjugated secondary anti-mouse and anti-rabbit antibodies (1:10,000, Jackson Immuno Research). All antibodies were diluted in 5% non-fat milk in TBST buffer. The membrane was then incubated with enhanced chemiluminescence agents for detection and exposed to an X-ray film for a proper time starting from 30 seconds to 10 minutes. The film was developed by using an OptiMax X-ray film processor, and the signal was detected.

### 3.2.13 *Pf*HK knockout

Previous studies demonstrated that glucose is essential for *P. falciparum*, and hexokinase is the key enzyme catalyzing the first intercellular reaction of imported glucose. Glucose 6-phosphate, the product of hexokinase, is the initial substrate of glycolysis and the pentose phosphate pathway, which supply most of the energy, reducing power, and intermediate products for other metabolic processes. There is evidence that without glucose, malaria parasites appear as shrunken, rounded bodies with pyknotic nuclei and fail to recover viability by glucose re-supplementation. To verify whether there is another compensation approach when the activity of hexokinase is blocked, the knockout of *Pf*HK can give solid proof. Because in other species, the homozygous deficiency of HK cannot survive (Wu *et al*., 2012), and *P. falciparum* only has a single copy of hexokinase in the genome, the strategy of hexokinase knockout preparation in *P. falciparum* is to construct a merodiploid strain of the parasite. A merodiploid is an essentially haploid organism that carries a second copy of a part of its genome. The knockout preparation was carried out in collaboration with Prof. Vaidya's group at the College of Medicine of Drexel University in Philadelphia, USA.

#### 3.2.13.1 Construction of the merodiploid strain

Two pLN vectors with *attP* site were chosen to carry *PfHK* fused with an N-terminal GFP-DHFR-HA tag and a DHFR-HA tag, respectively. Two pairs of primers with *BsiWI* and *AflII* restriction sites (5'-atatCTTAAGAGTGAGTACGATATTGCAAAAAATG-3', 5'-atatCGTACGTTATGGTAATTGT

GGAATGTCCGC -3‘ ) were designed to clone the full-length *PfHK* from the *PfHK/pET30a* plasmid.

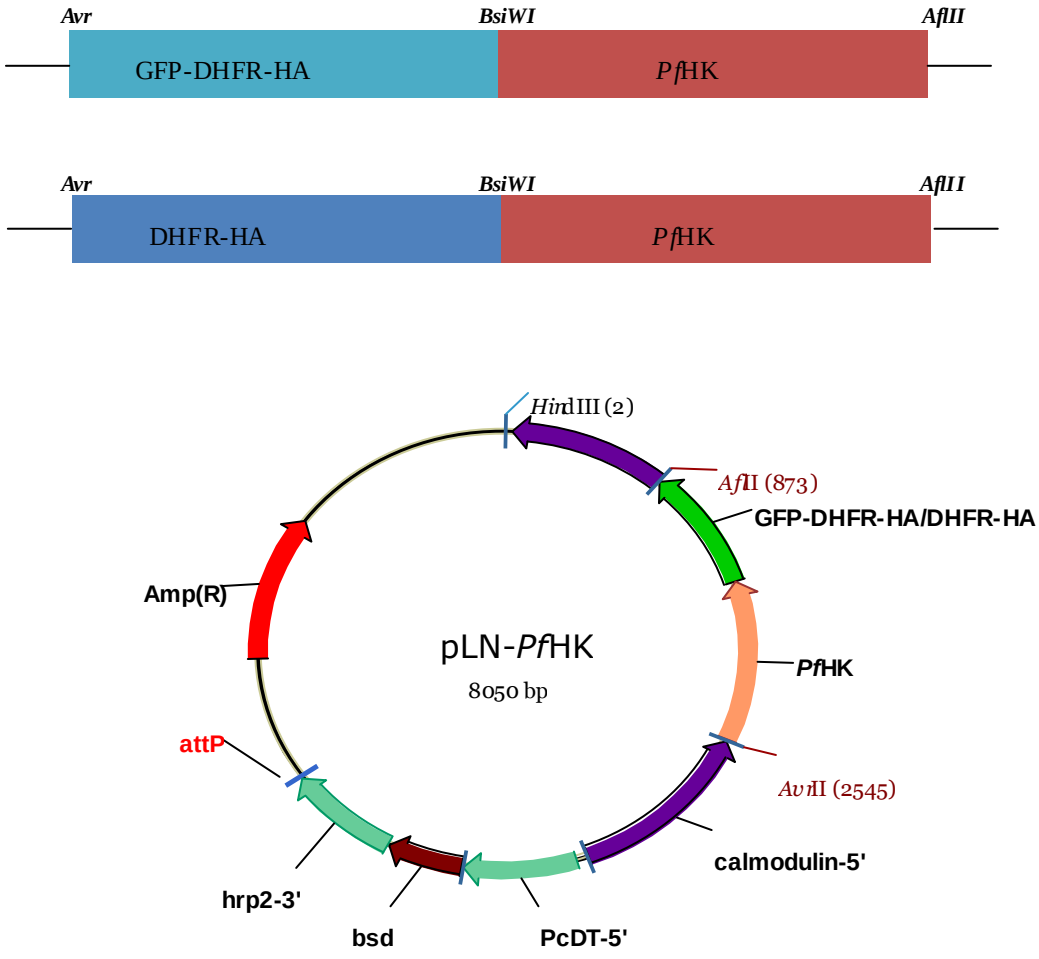


**Figure 3.4: The *PfHK* gene in the *pLN* vector.**

After PCR the QIAquick PCR purification kit was used to clean the PCR product. Because the restriction enzymes BssHII and XmaI work at different temperatures, a two-step digestion (see below) was applied to digest insertions and vector. After analysis by agarose gel electrophoresis, the T4 ligation system was applied to connect the fragment and vector. The *PfHK/ pLN* vectors containing the fusion constructs were verified by sequencing. To prepare the plasmid for transfection, the Qiagen Maxi Kit was used to extract and purify plasmid from the cells. Then a furture precipitation step was required to obtain the sterile DNA with high purity and concentration.

| Two-step digestion | |
|---|---|
| Component | Volume (µl) |
| PCR product or vector | 4 (500 ng DNA) |
| Buffer 2 | 1 |
| 10xBSA | 1 |
| *AflII* (10 U/µl) | 1 |
| $H_2O_{dd}$ | 3 |
| 37 ℃ 1 Hour | |
| *BsiWI* (10 U/µl) | 1 |
| Buffer 2 | 1.5 |
| 10xBSA | 1.5 |
| $H_2O_{dd}$ | 6 |
| 55 ℃ 1 Hour | |

The procedure of parasite transfection was applied as described in 3.2.12.3. The transgenic Dd2attB parasites, which integrated a 44-bp *attB* fragment into the nonessential *cg6* gene encoding a glutaredoxin-like protein, were used to carry the merodiploid plasmid. The Bxb1 integrase expressed in *trans* from the pINT plasmid facilitated the integration of the pLN±GFP-DHFR-HA-*Pf*HK plasmid into the *cg6-attB* site by single-crossover recombination. The attB×attP recombination generates two sites, *attL (left)* and *attR (right)*. After transfection and several weeks' continuous culture with drug selection, the transgenic parasites were obtained, and Western blot was applied to check the expression of integrated *Pf*HK, using anti-GFP antibody.

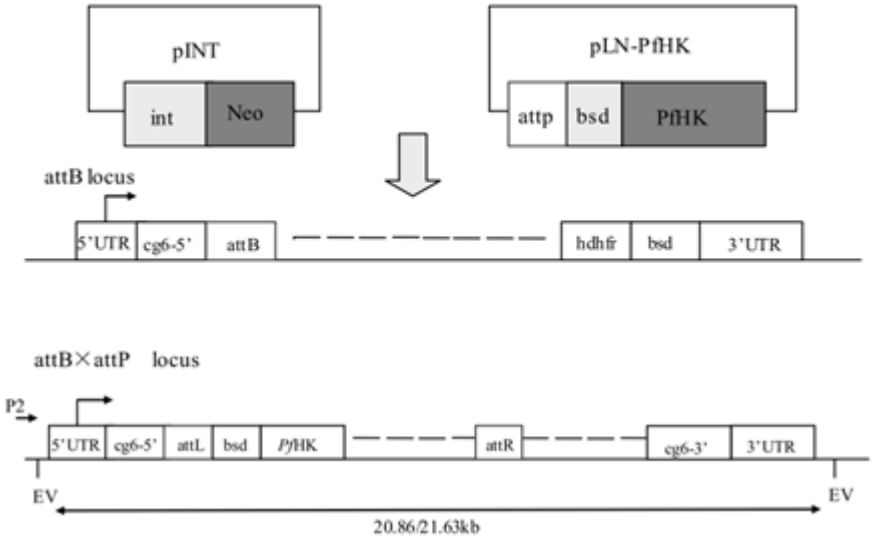


**Figure 3.5: Scheme of the dual-plasmid attB×attP recombination approach according to the method reported by Nkrumah et al., 2006.**

To knock out the endogenous hexokinase, we used the double crossover recombination method. The pUF-1 vector was chosen to construct the knockout plasmid. Two fragments in the 5'UTR and 3'UTR of hexokinase on Chromosome 6 were amplified by two pairs of primers (Table.3.3). The 569 bp fragment of 5'UTR was designed with *NcoI* and *EcoRI* restriction sites. The 854 bp fragment of 3'UTR was designed with *SpeI* and *SacII* restriction sites.

| | |
|---|---|
| **5'-UTR** | CTCCATGGGATTAAAAATTTTCACATTAAGGAATAA<br>TAGAATTCCAGAAAAGTATATGGTAAATAATTACTC |
| **3'-UTR** | GAACTAGTGTCTGTATGTGAGTGTGTGA<br>ATCCGCGGATTTCTGATGCCATGTTAGTAATTTC |

**Table 3.3: Primers for knockout constructs**. The *NcoI* , *EcoRI* , *SpeI*, and *SacII* restriction sites are underlined.

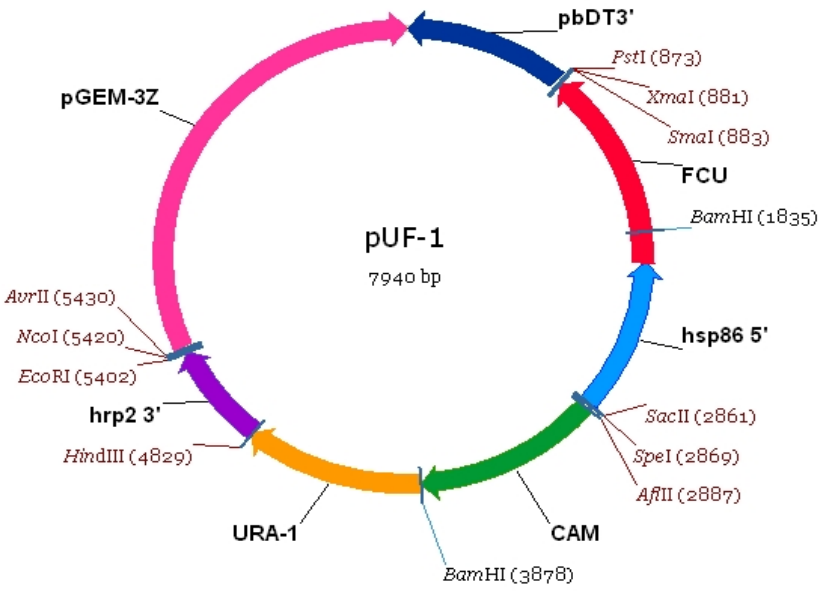


**Figure 3.6: Structure of the pUF-1 vector**

After sequencing, two fragments were integrated into pUF vectors and transferred into Top 10 competent cells. The Qiagen Maxi Kit was used to prepare large amount of plasmid. The transfection method was applied as described in 3.2.12.3. The parasites were continuously cultured under drug pressure of DSM1, which is a specific inhibitor of *Plasmodium* dihydroorotate dehydrogenase

(DHODH). The same drug on-and-off cycle was performed to obtain the recombinant parasites. Then 5-fluorocytosine (5-FC) was used for the negative selection. Theoretically, only the knockout parasites would exhibit resistance to the toxic precursor compound 5-FC. A significant portion of the *Pf*HK gene with bsd cassette was removed by the double crossover recombination in the strain of knockout and lost the remnant plasmid containing the yFCU negative selection gene cassette. Southern and northern blots were used to analyze the efficiency of knockout.

### 3.2.14 *Pf*HK crystal screening

In order to study the structure of *Pf*HK in atomic detail, it is essential to obtain the crystals of this protein. A protein crystal can be used for X-ray diffraction, and then the data of X-ray diffraction can be used for structure solution and structure refinement. The protein structure can be revealed by computer calculations. We used both hanging drop and sitting drop methods to try to produce *Pf*HK crystals, which were based on the principle of water vaporization or certain volatile agents between the droplet containing protein and the reservoir solution. Along with water vaporization from the droplet, the concentration of precipitant in the droplet gradually increases until a crystal forms. If the conditions are optimal, the crystal could grow large (McRee, 1993; Rhodes, 1993).

Initially, the crystal screening was performed with the JCSG Core Suite kit from Qiagen by using the Honeybee 961 robot (Zinsser Analytic Inc), which allows a minimum volume of 1 nanoliter of protein solution for screening and fast plate preparation. The full set of the JCSG Core Suite kit is composed of four screens of 384 unique conditions that have three types of precipitants, salt, organic, and polymers, on the basis of analyzing over 500,000 crystallization experiments. After the preliminary screening, several promising solutions were selected for further testing using a manual hanging drop method. Each droplet was a mixture of 2 µl *Pf*HK solution and 2 µl reservoir solution on the cover slips. These cover slips were placed over small wells containing 800 µl of the reservoir solution. The wells were sealed by silicon oil and placed at RT. The droplets were checked by microscopy.

# 4. Results

## 4.1 *Pf*HK characterization

In this study, a putative hexokinase in *P. falciparum* has been identified, cloned, and heterologously overexpressed. The kinetic profile and post-translational modification were also described. These findings provide further information of glucose phosphorylation by hexokinase in *P. falciparum* and on the suitability of the enzyme as drug target.

### 4.1.1 Sequence alignment and phylogenetic tree

The hexokinase gene in *P. falciparum* was identified several years ago (Olafsson *et al.*, 1994; Olafsson *et al.*, 1992). When searching PlasmoDB, there is a single gene of hexokinase in *P. falciparum* 3D7 (PF3D7_0624000) located on chromosome 6 from position 981,066 to 982,547. The nucleotide sequence of *Pf*HK is 1482 bp without intron. This gene is expressed in both sexual and intraerythrocytic stages. The molecular mass of the predicted amino acid sequence is 55,262 Da and the isoelectric point is 7.1. The homolog searching in the Protein Data Bank (PDB) shows the highest similarity with human hexokinase I (33% identity). The amino acid sequence alignment of the *P. falciparum* putative hexokinase, together with those of five hexokinases from other species, is shown in Fig. 4.1. The deduced protein sequence of *Pf*HK has a hexokinase signature, as do those of other species. The consensus regions in hexokinase were found in *P. falciparum* putative hexokinase such as multiple glucose-binding sites, binding sites of the sugar moiety of glucose 6-phosphate, multiple binding sites of the phosphate moiety of glucose 6-phosphate, and multiple ATP binding patterns. The strictly conserved sequence, LGGTN, which moves forward to embrace the binding sites and is supposed to be functionally important for contributing to the formation of the glucose-binding site, is substituted in *Pf*HK to FGGTN. In the putative hexokinase sequence of *P. falciparum*, no unique insertion or deletion was found.

The C-terminal hydrophobicity profile, mentioned in previous reports (Olafsson *et al.*, 1994), was checked via hydrophobic cluster analysis (www.ExPASy.org/tools). Although there was no significant hydrophobic cluster region found, the last 20 amino acids seemed to have the potential to be a binding region to the parasite membrane.

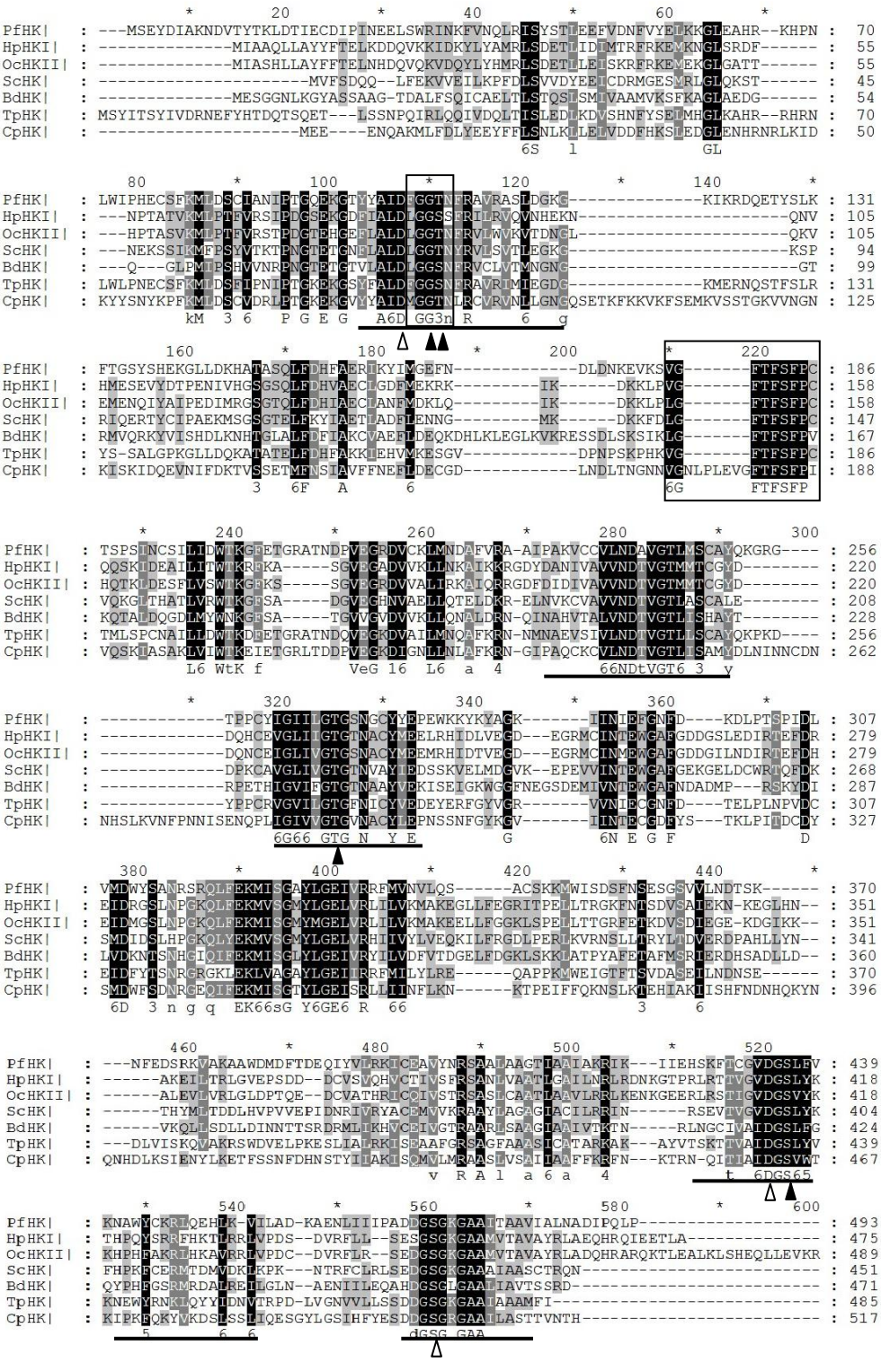

**Figure 4.1: Multiple sequence alignment of *Pf*HK with six hexokinases from other species.** *Pf*HK (XP_966222.1), *Hp*HKI N-terminal (NP_001096656.1), *Oc*HKII N-terminal (XP_002709755.1), *Sc*HK (NP_013551.1), *Bd*HK (EGF82377.1), *Tp*HK (XP_765570.1), and *Cp*HK (XP_667007.1)**.** The box indicates the signature sequence. Underlined residues indicate the adenosine triphosphate-binding pattern. Black arrows indicate binding sites of the phosphate moiety of G6P. White arrows indicate the binding sites of the sugar moiety of G6P.

Based on the multiple alignment of highly similar HK sequences, a phylogenetic tree was constructed (Figure 4.2). The hexokinase in *P. falciparum* was catalogued in the cluster of apicomplexans. It revealed the homologous evolution of hexokinase in apicomplexans.

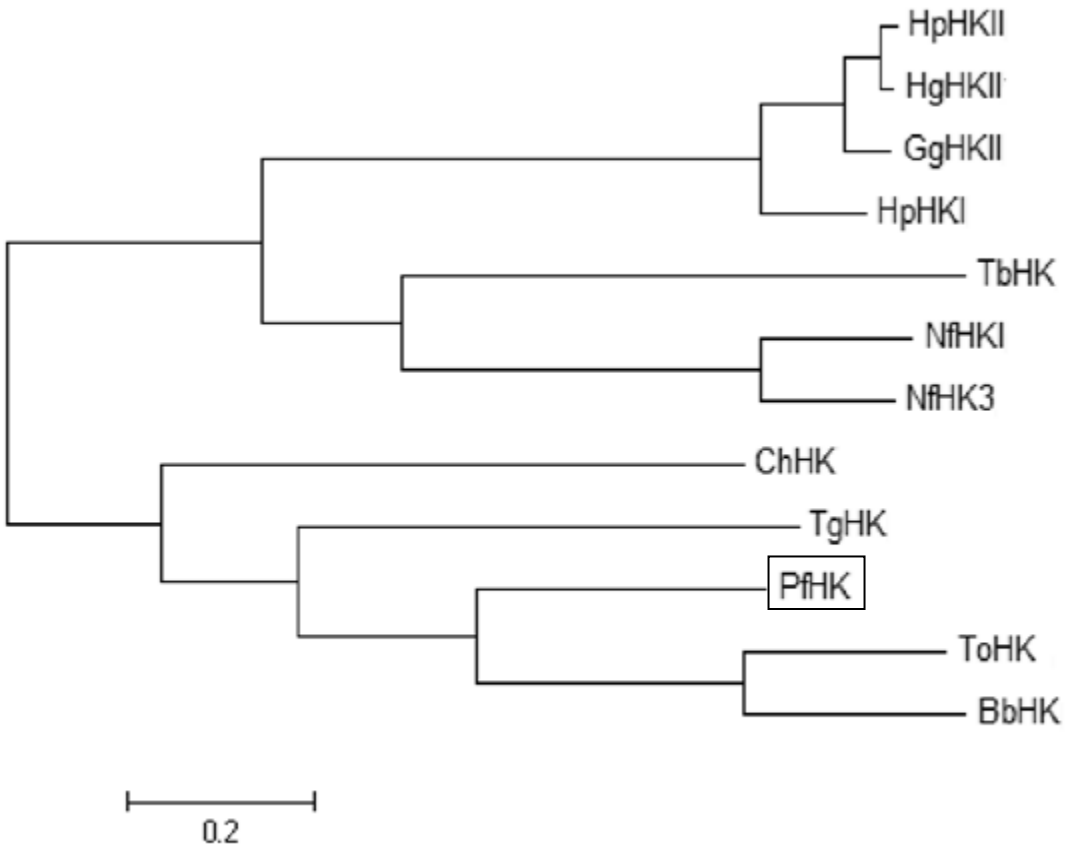


**Figure 4.2: Radial phylogenetic tree generated by using the neighbour-joining method based on the results of multiple sequence alignments of HKs from various species.** Tg, *Toxoplasma gondii*, XP_002368674.1; To, *Theileria orientalis*, BAM38568.1; Ch, *Cryptosporidium hominis*, XP_667007.1; Hp, *Homo sapiens*, CAA86476.2; Tb, *Trypanosoma brucei*, CAC69958.1; Nf, *Neocallimastix frontalis*, AFJ73476; Hg, *Heterocephalus glaber*, EHB01702.1; Gg, *Gallus gallus*, NP_989543.1; Bb, *Babesia bovis*, XP_001608748.1. Scale bar, evolutionarily indicated 0.2 substitutions per site.

### 4.1.3 Cloning, heterologous overexpression and purification of recombinant *Pf*HK

To clone the *HK* gene from *P. falciparum*, a gametocytic cDNA library of the *P. falciparum* 3D7 strain was used. The specific primers were designed as described in Methods. After the PCR, a 1482 bp fragment was obtained and cloned into the pET30a vector, which attached a 6-His tag to the C-terminus of the protein. The sequencing result guaranteed accuracy.

To obtain the active *Pf*HK, there were several barriers to overcome. The main problem of heterologous overexpression was the insolubility of the recombinant proteins (Olafsson *et al.*, 1992). In our study, we successfully overexpressed and purified the recombinant *Pf*HK in *E. coli*, and yielded nearly 0.5 mg/l recombinant *Pf*HK from *E. coli* culture after purification. The molecular mass of purified recombinant of *Pf*HK was 55 kDa. The heterologous overexpression and purification of recombinant *Pf*HK was optimized as summarized in Tables 4.1, 4.2, and 4.3.

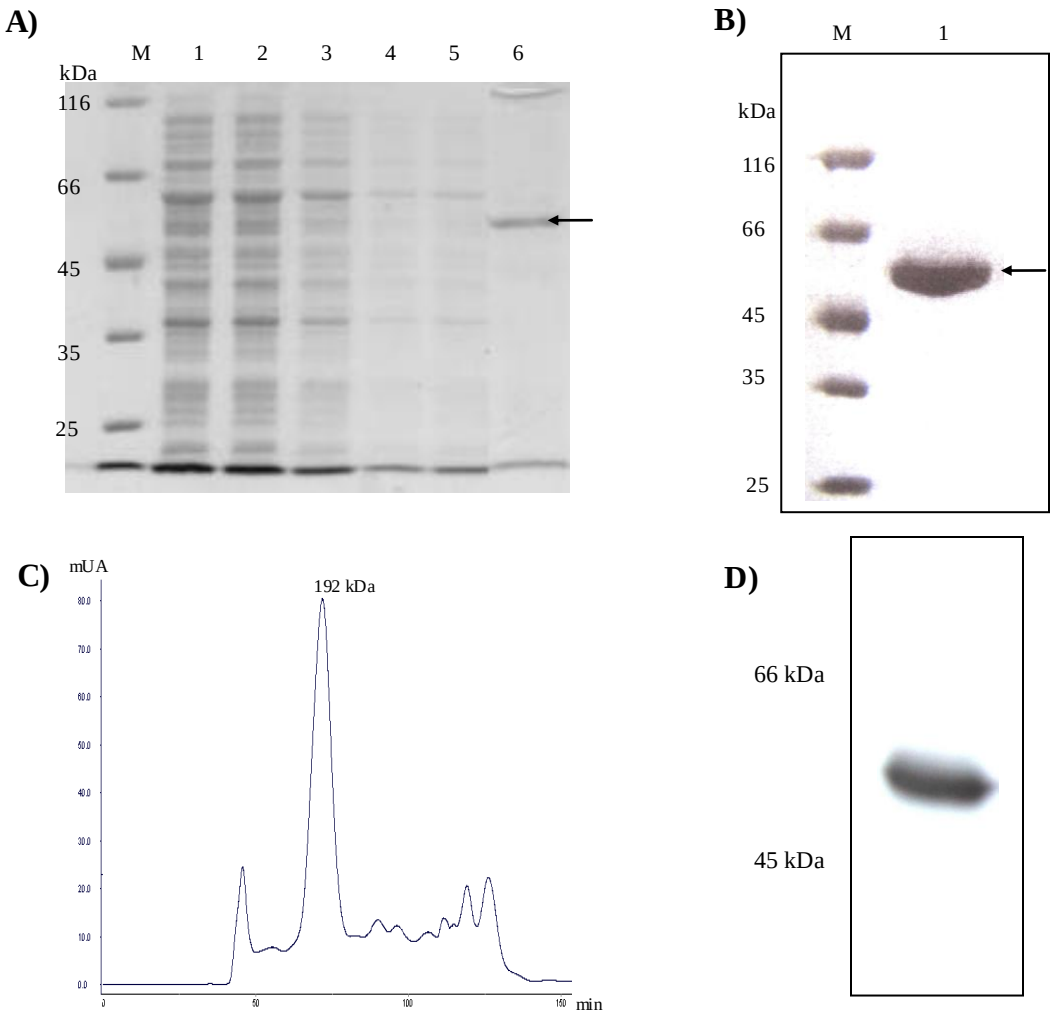


**Figure 4.3: Purification and gel filtration result of recombinant *Pf*HK. A)** 12% SDS-PAGE gel of *Pf*HK after Protino Ni-TED purification. M, unstained molecular weight marker; 1: supernatant; 2: flow through; 3: wash fraction; 4-6 elution with 10 mM, 20 mM, 500 mM imidazole, respectively. **B)** 12% SDS-PAGE gel of *Pf*HK containing fraction after gel filtration. **C)** Gel filtration chromatogram after Protino Ni-TED, an elution time of 69.8 corresponds to 192 kDa. **D)** Western blot of recombinant *Pf*HK using an anti-His antibody.

### 4.1.4 *Pf*HK oligomerization studies

Apart from the bacterial 35 kDa hexokinase, most of the hexokinases are 100 kDa enzymes in

vertebrates and 50 kDa enzymes in invertebrates (Ureta *et al.*, 1987). There is a hypothesis that 100 kDa vertebrates' enzymes evolved from the 50 kDa invertebrates' enzymes. In reports, vertebrate hexokinases exist as monomers of 100 kDa with the exception of hexokinase D, a monomer of about 50 kDa without dimerization (Cárdenas *et al.*, 1978; Holroyde *et al.*, 1976). In the fungal and invertebrate group, the enzymes exist as monomers, but in a few cases they readily dimerize (Ureta *et al.*, 1987). Although the subunit molecular weight of *Pf*HK was 55 kDa and belongs to the invertebrate group, *Pf*HK was found to be a tetramer in our studies. From the results of native gel filtration chromatography, using different salt concentrations (KCl 500 mM and 150 mM) and pH (7.0 and 7.4), *Pf*HK remained a tetramer structure both in the presence and absence of its substrate. To avoid the possible interference of intermolecular disulfide bridges, the protein sample was incubated with excess DTT (4 mM) at 4 ℃ for 1 hour before gel filtration chromatography. There was no observable change in the tetramer structure of *Pf*HK (Fig. 4.4)

| **Buffer** | **Results** |
|---|---|
| US buffer | This buffer was not suitable for resuspension and purification |
| HEPES, 300 mM KCl, pH 7.0 | This buffer was better than US buffer, but still a large part of *Pf*HK was in the pellet |
| 100 mM Tris, 300 mM NaCl, pH7.4, 10% glycerol | This buffer was good for resuspension and purification. |
| 100 mM Tris, 300 mM KCl, pH 7.0,10% glycerol | This buffer was the best for resuspension and purification. |

**Table 4.1: Optimization of the buffers used for heterologous overexpression of *Pf*HK**

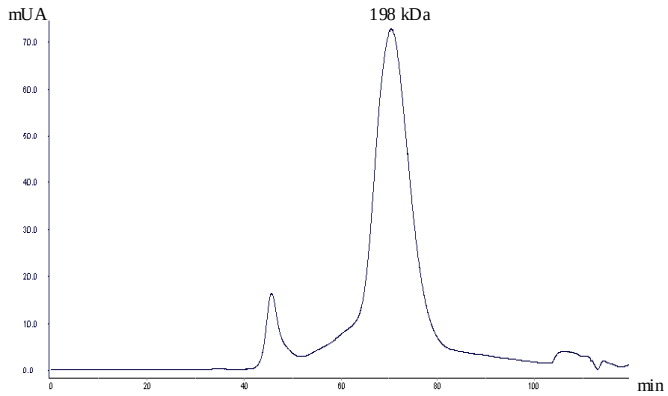


**Figure 4.4: *Pf*HK tetramer structure in the presence of 4 mM DTT.** In the gel filtration chromatogram, the elution time of 69.6 corresponds to a molecular mass of 196 kDa

| ***E.coli* strain** | **Medium** | **Temperature** | **Time** | **Inductor and concentration** | **Western blot** | **Inference** |
|---|---|---|---|---|---|---|
| BL 21 | LB 2xYT TB | 37 °C, RT | 4 hours overnight | IPTG (0.1, 0.3, 1 mM) | Tested Positive | Medium: no significant difference<br>Temperature: better at RT for overnight<br>IPTG: no significant difference<br>Final yield very low |
| C41 | LB 2xYT TB | 37 °C, 18 °C RT | 4 hours overnight | IPTG (0.1, 0.3, 1 mM) | Tested Positive | Medium: TB is the best<br>Temperature: better at RT for overnight<br>IPTG: 1 mM IPTG was the best<br>Final yield very low |
| KRX | LB 2xYT TB | 37 °C RT | 4 hours overnight | Rhamnose: 0.05 and 0.1 % | Tested Positive | Medium: no significant difference<br>Temperature: no significant difference<br>IPTG: no significant difference<br>Final yield very low |
| BL pRAREII | LB 2xYT TB | 37 °C, 18 °C RT | 4 hours overnight | IPTG (0.1, 0.3, 1 mM) | Tested Positive | Medium: no significant difference<br>Temperature: better at RT for overnight<br>IPTG: no significant difference<br>Even worse with pRAREII |
| C41 pRAREII | LB 2xYT TB | 37 °C RT | 4 hours overnight | IPTG (0.1, 0.3, 1 mM) | Tested Positive | Medium: no significant difference<br>Temperature: better at RT for overnight<br>IPTG: 1 mM IPTG was the best<br>No improvement |
| C41 pGro7 | LB 2xYT TB | 37 °C, 18 °C RT | 24 hours 48 hours | IPTG (0.1, 0.3, 1 mM) | Tested Positive | Medium: TB is the best<br>Temperature: at 18 °C for 48 hours was the best<br>IPTG: 1 mM IPTG was the best<br>The best and applied as the standard method |

**Table 4.2: Optimization of the heterologous overexpression of *Pf*HK.** Western blot was performed using anti-His antibody and all samples tested positive for *Pf*HK

| Material | Condition used | Inference |
|---|---|---|
| Ni-NTA | Equilibrated the column material with buffer of pellet resuspended and eluted with an imidazole concentration gradient. | The protein binds well, but the unspecific binding cannot be removed in further gel filtration. |
| | Before the washing step, upload 5% ethanol in pellet resuspended buffer and eluted with an imidazole concentration gradient. | The protein binds well, but the unspecific binding cannot be removed in further gel filtration. |
| | Equilibrated the column material with buffer containing 5 mM imidazole then loaded the lysate and eluted with an imidazole concentration gradient. | The protein binds weakly but purity improved. |
| Protino Ni-TED | Equilibrated the column material with buffer of pellet resuspended and eluted with an imidazole concentration gradient. | The protein binds well, but the unspecific binding cannot be removed in further gel filtration. |
| | Before the washing step, upload 5% ethanol in pellet resuspended buffer and eluted with an imidazole concentration gradient. | The protein binds well, but the unspecific binding cannot be removed in further gel filtration. |
| | Equilibrated the column material with buffer containing 5 mM imidazole then loaded the lysate and eluted with an imidazole concentration gradient. | The protein binds well, the unspecific binding improved much. The main contamination with Hsp 60 is reduced. |
| TALON | Equilibrated the column material with buffer of pellet resuspended and eluted with an imidazole concentration gradient. | The protein binds weakly and unspecific binding cannot be removed. |
| | Equilibrated the column material with buffer containing 5 mM imidazole then loaded the lysate and eluted with an imidazole concentration gradient. | No improvement but protein binding became even worse. |

**Table 4.3: Optimization of the purification of heterologously overexpressed *Pf*HK**

### 4.1.4 Test of buffers, pH and salt for *Pf*HK

Different buffers were tested to determine the optimal *Pf*HK buffer. The Tris-HCl, HEPES-NaOH, and MOPS buffers were tested with a concentration of 100 mM and pH set at the buffering range of each buffer. *Pf*HK recorded the best activity in Tris-HCl buffer pH 7.0 and Hepes-NaOH buffer pH 7.4 (Fig. 4.5). No acitivity was found in MOPS buffer.

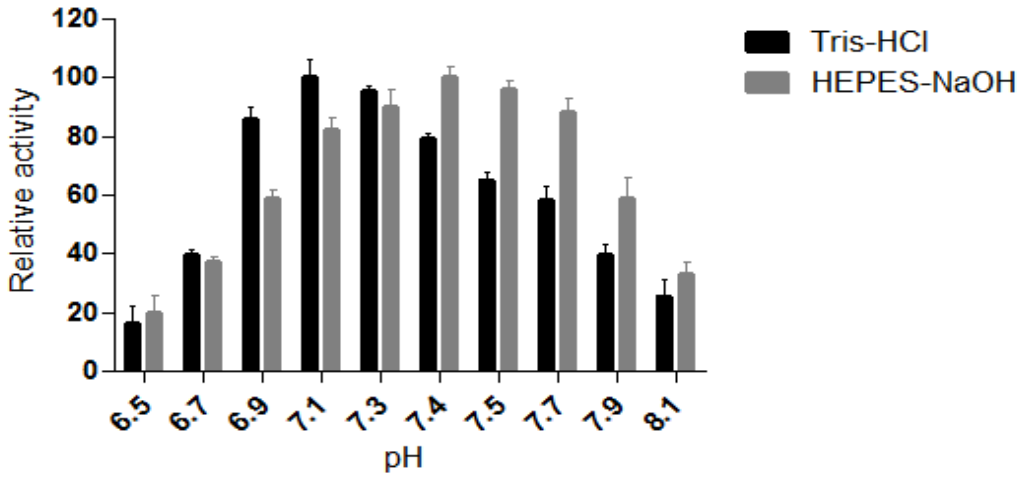


**Figure 4.5: *Pf*HK pH profile in Tris-HCl and Hepes-NaOH buffers; the highest activity was set to 100%**

### 4.1.5 *Pf*HK kinetic studies

The kinetics figures of hexokinase in *P. falciparum* were mainly determined using the recombinant protein with a C-terminal His-tag. The glucose 6-phosphate dehydrogenase-coupled assay was applied as the standard assay. Determining NADPH generation corresponds to the rate of G6P generation. The $K_m$ values for each substrate were calculated from the measurments of varying the substrate concentrations over a specific range relative to each $K_m$ value. The maximum of velocity was also concluded. The methods of Lineweaver-Burk, Eadie-Hofstee, and Hanes were used to process the primary data of absorbance (Figure 4.6). *Pf*HK was found to exhibit high affinity and therefore a low $K_m$ value for glucose and exhibited relatively low affinity and therefore a high $K_m$ value for ATP. The $K_m$ for ATP and glucose of *Pf*HK in parasites lysate were also determined (Table 3.4).

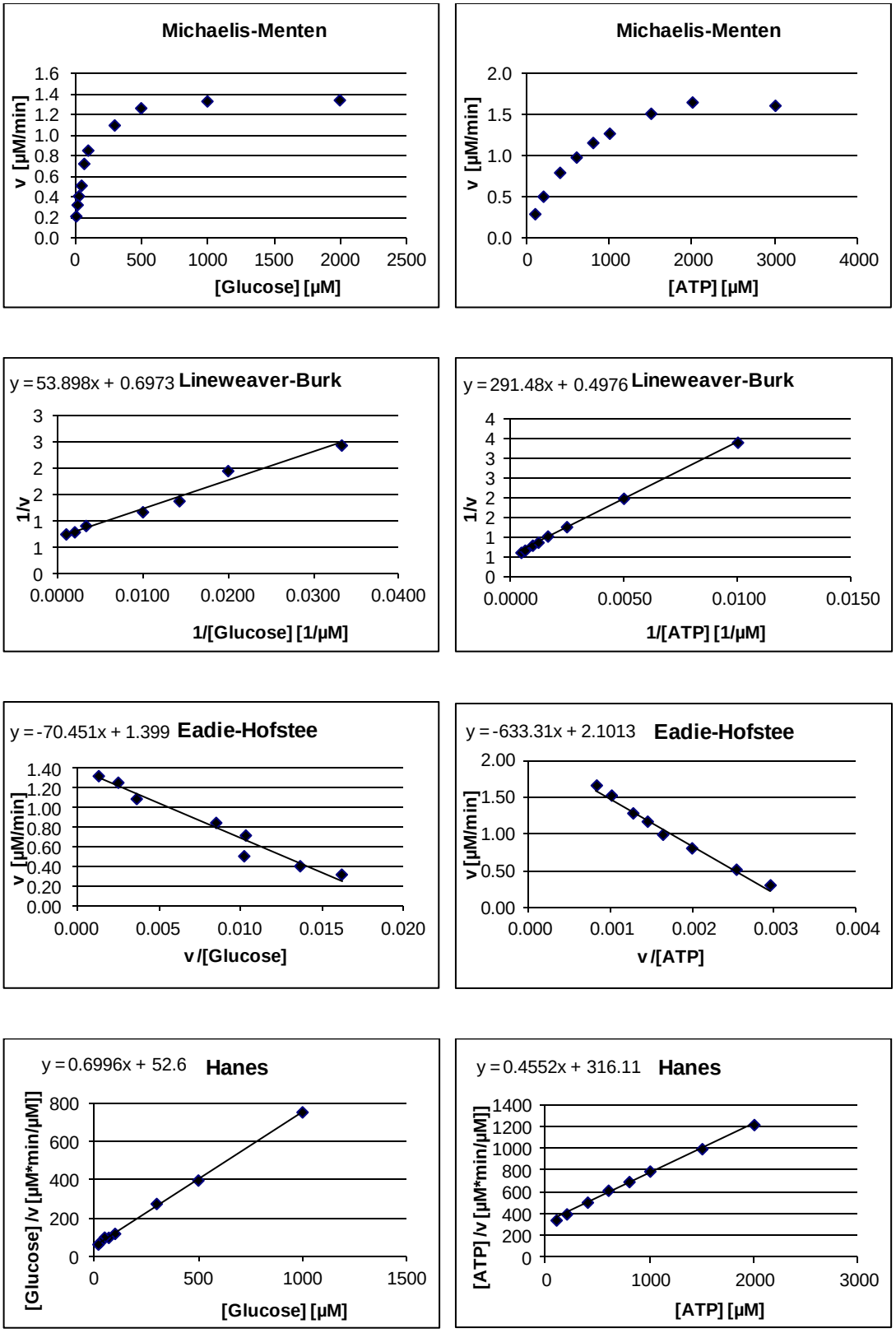


**Figure 4.6: Michaelis-Menten, Lineweaver-Burk, Eadie-Hofstee, and Hanes graphs of *Pf*HK with glucose and ATP.**

The initial-velocity studies of *Pf*HK using different combinations of ATP and glucose yielded linear converging double reciprocal plots (Fig. 4.7 A and D). An intersecting pattern was also observed when the results were replotted with ATP as the independent variable (Fig. 4.7 D). Straight linear plots were yielded by the secondary plots of the slopes and intercepts against the reciprocal of the substrates (Fig. 4.7 B, C, E, and F). An internal check was performed by comparing the plotting sequence with kinetic parameters.

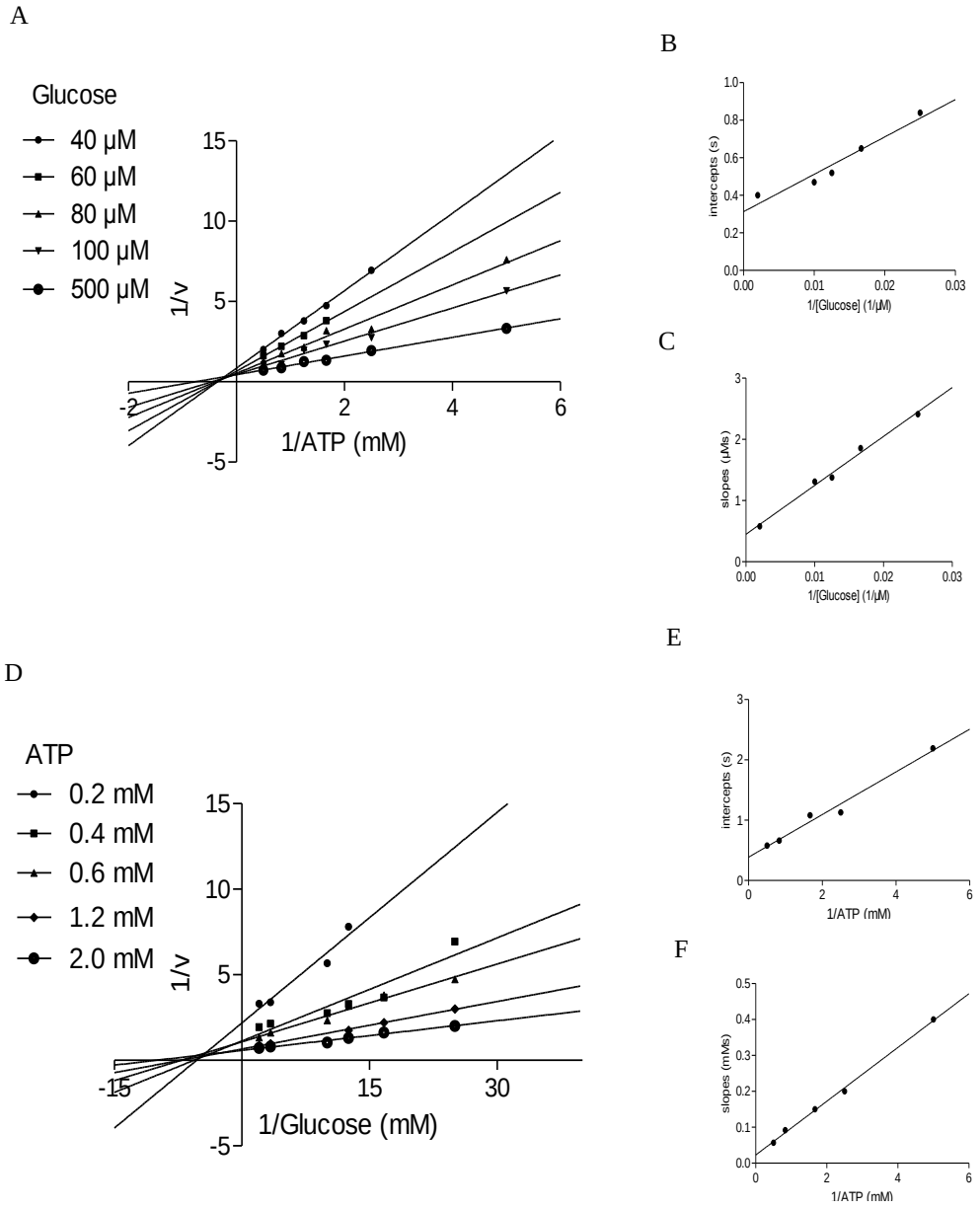


**Figure 4.7: The double reciprocal plots of *Pf*HK for the reaction with ATP and glucose as substrates. A)** Primary plots of 1/v against 1/ [ATP] at various concentrations of glucose. **B)** Secondary plots of intercepts of primary plots against 1/ [Glucose]. **C)** Secondary plots of slopes of primary plots against 1/ [Glucose]. **D)** Primary plots of 1/v against 1/ [Glucose] at various concentrations of ATP. **E)** Secondary plots of intercepts of primary plots against 1/ [ATP]. **F)** Secondary plots of slopes of primary plots against 1/ [ATP].

| **Recombinant *Pf*HK** | **$K_m$ (µM)** | **$V_{max}$ (U/mg)** | **$k_{cat}$ ($s^{-1}$)** |
|---|---|---|---|
| **ATP** | **709.4 ± 89.4** | **31.47 ± 4.69** | **31.13 ± 1.64** |
| **Glucose** | **72.45 ± 7.83** | **33.29 ± 3.08** | **31.38 ± 2.9** |
| ***Pf*HK in *P.falciparum* lysate** | **$K_m$ (µM)** | **$V_{max}$ (U/mg)** | **$k_{cat}$ ($s^{-1}$)** |
| **ATP** | **427 ± 52.77** | **0.06 ± 0.008** | **0.057 ± 0.07** |
| **Glucose** | **87.19 ± 10.85** | **0.051 ± 0.07** | **0.049 ± 0.08** |

**Table 4.4: Kinetic parameters of *Pf*HK.**

### 4.1.6 *Pf*HK product inhibition

Many products of enzymatic reactions do inhibit the enzymes' activity. The patterns of product inhibition can provide useful information to understand the enzyme reaction mechanisms. In this study, the effect of ADP on the *Pf*HK reaction was measured by the glucose 6-phosphate dehydrogenase coupled assay, and the effect of G6P was measured by the pyruvate kinase and lactate dehydrogenase coupled assays because G6P is the substrate of glucose 6-phosphate dehydrogenase. G6P was found to be a competitive inhibitor with respect to ATP, as indicated by the intersection on the x-axis in Figure 4.8 and the increasing $K_m$ values with increasing inhibitor concentration. A mixed-type inhibition of G6P was found towards glucose. ADP showed a mixed type inhibition with respect to ATP and glucose (Fig 4.9). The $IC_{50}$s of ADP and G6P were also determined, which were 2.19 mM for ADP, and 0.32 mM for G6P, respectively (Fig. 4.10).

### 4.1.7 Redox regulation of *Pf*HK

As the target protein of members of the thioredoxin superfamily (*Pf*Grx, *Pf*Trx, and *Pf*Plrx) in *P. falciparum*, *Pf*HK was able to be recognized by the conserved Cys-X-X-Cys motif of the active site and suspected to be regulated by these proteins (Sturm *et al.*, 2009). In the present study, the recombinant *P. falciparum* redox proteins (*Pf*Grx, *Pf*Trx, and *Pf*Plrx) and DTT were incubated with *Pf*HK for 30 minutes at room temperature. The activity of *Pf*HK was 10-20 % up-regulated by these redox proteins and DTT (Fig. 4.11).

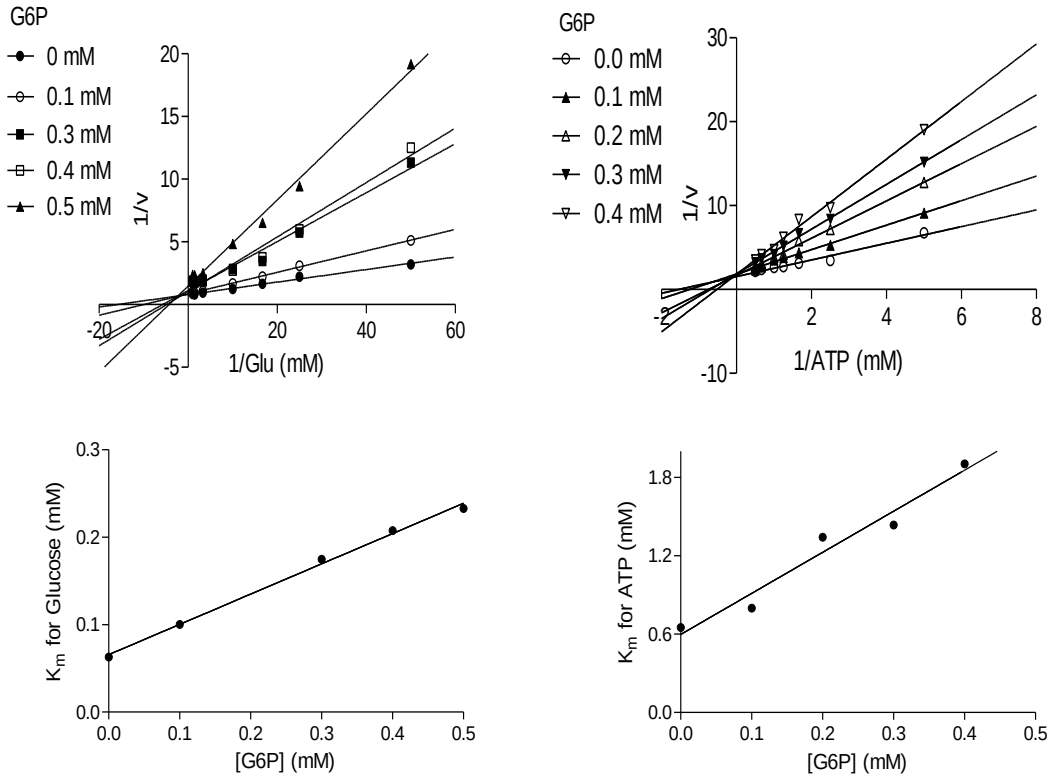


**Fig 4.8: Inhibition of *Pf*HK by G6P.**

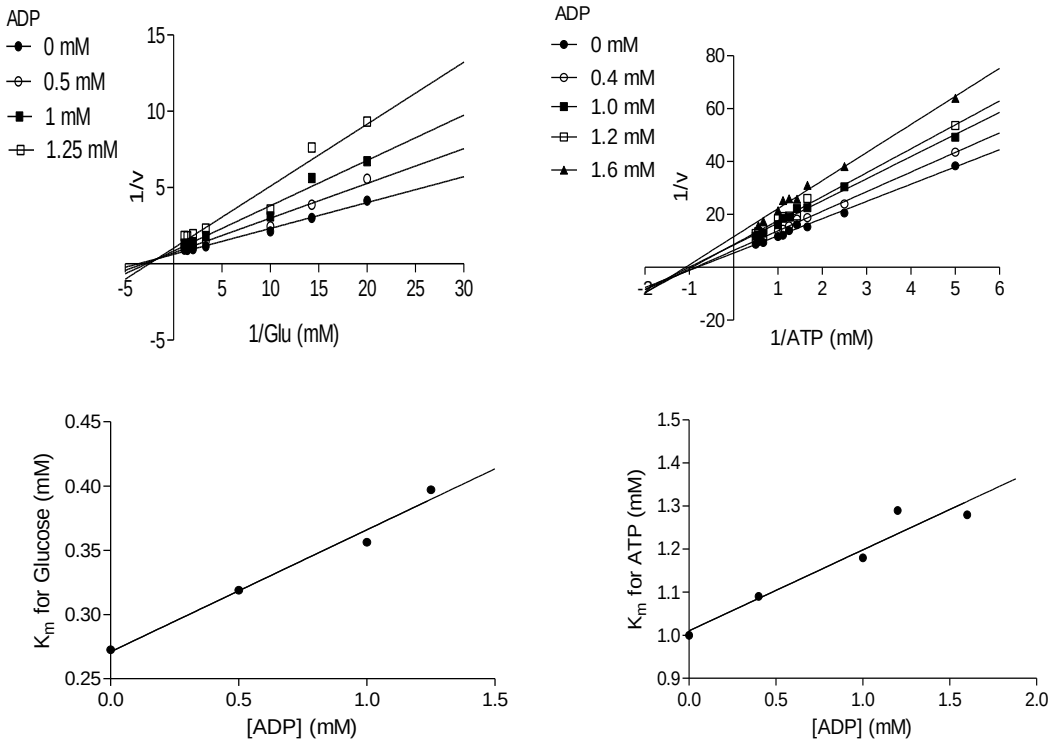


**Fig 4.9: Inhibition of *Pf*HK by ADP.**

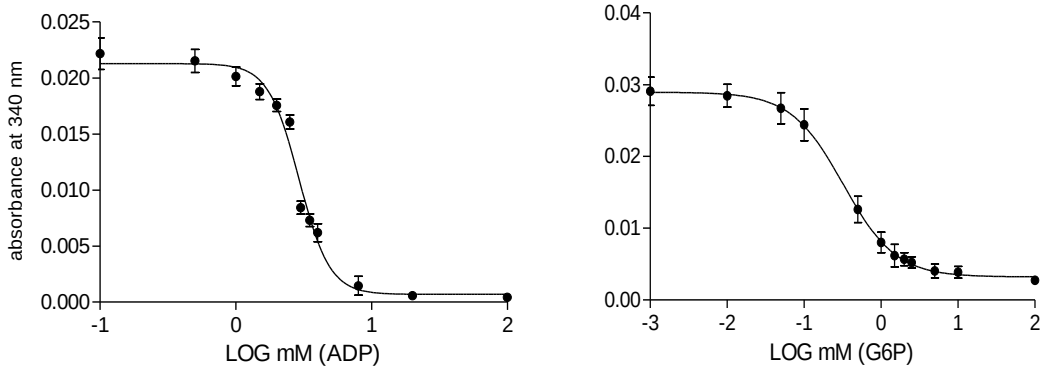


**Fig 4.10: $IC_{50}$s of ADP and G6P on *Pf*HK.**

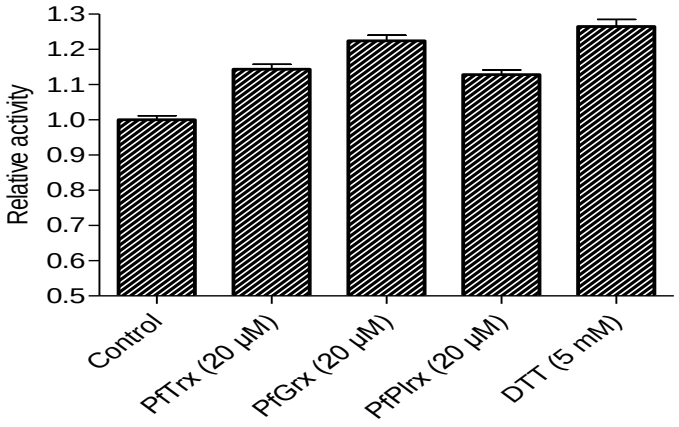


**Figure 4.11: Activity of *Pf*HK after incubation with redox proteins and DTT.**

### 4.1.8 *S*-Glutathionylation of *Pf*HK

Cysteine residues in proteins have the potential to form disulfides with glutathione, which can regulate activities or structures of these proteins. *Pf*HK was one of the proteins identified to be *S*-glutathionylated in *P. falciparum* (Kehr *et al.*, 2011). The anti-GSH-antibody was applied to determine the glutathionylation of recombinant *Pf*HK. As shown in Fig. 4.12A, the recombinant *Pf*HK was probed by the anti-GSH antibody. Both reduced and oxidized glutathione were incubated with recombinant *Pf*HK. The positive signal only existed in the sample incubated with 10 mM oxidized glutathione; DTT in the loading buffer can remove the signal. Western blots showed that the level of glutathionylation was increased with increasing concentrations of oxidized glutathione (Fig. 4.12B).

Mass-spectrometry was also applied to analyze the glutathionylation of *Pf*HK; different concentrations of oxidized glutathione were incubated with *Pf*HK. Then after digestion by trypsin, MALDI-TOF was employed to monitor the peptides of *Pf*HK. The glutathionylation was confirmed by the result of

mass-spectrography, but not all the cysteines were detected (Fig. 4.13).

A

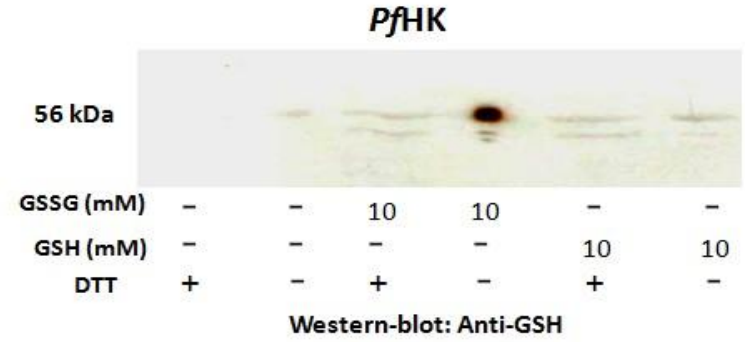


B

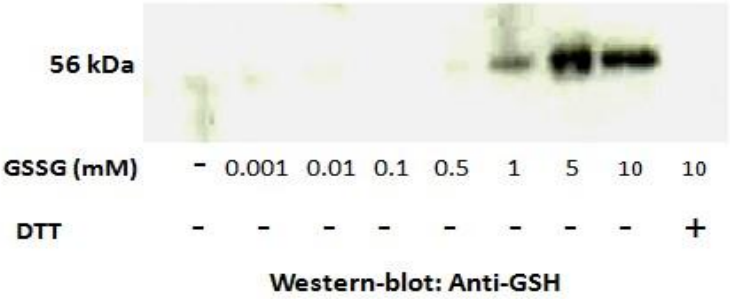


**Figure 4.12: Western blot of glutathionylation of *Pf*HK. A)** Both oxidized and reduced glutathione were incubated with *Pf*HK, using loading buffer with or without DTT. **B)** Different concentrations of oxidized glutathione were incubated with *Pf*HK.

To determine the influence of glutathionylation on the activity of *Pf*HK, the recombinant *Pf*HK was incubated with different concentrations of oxidized glutathione at room temperature and 4 ℃ (Fig. 4.14 and 4.15). The activity of *Pf*HK was significantly inhibited by the glutathionylation. This inhibition of glutathionylation was related to incubation conditions, indicating that the glutathionylation process could be enhanced by higher temperature and concentration of oxidized glutathione and prolonged incubation time.

The deglutathionylation experiment was performed with the pre-reduced protein of the thioredoxin superfamily and DTT. Different concentrations of the members of thioredoxin superfamily (*Pf*Trx1, *Pf*Grx and *Pf*Plrx) (5-20 μM) and conditions (RT and 37 ℃) were tested, but the activity of glutathionylated *Pf*HK could only be partially recovered by DTT (Fig. 4.16). After incubation with oxidized glutathione, the stability of recombinant *Pf*HK was changed to be weak. In the desalting step

to remove the excess oxidized glutathione, some precipitation occoured after centrifugation. Buffer with glycerin could attenuate the precipitation. It seems the covalent modification of glutathionylation could influence or regulate the conformational stability of *Pf*HK.

MSEYDIAKNDVTYTKLDTIECDIPINEELSWRINKFVNQLRISYSTLEEFVDNFVYELKK
GLEAHRKHPNLWIPHECSFKMLDSCIANIPTGQEKGTYYAIDFGGTNFRAVRASLDGKGK
IKRDQETYSLKFTGSYSHEKGLLDKHATASQLFDHFAERIKYIMGEFNDLDNKEVKSVGF
TFSFPCTSPSINCSILIDWTKGFETGRATNDPVEGRDVCKLMNDAFVRAAIPAKVCCVLN
DAVGTLMSCAYQKGRGTPPCYIGIILGTGSNGCYYEPEWKKYKYAGKIINIEFGNFDKDL
PTSPIDLVMDWYSANRSRQLFEKMISGAYLGEIVRRFMVNVLQSACSKKMWISDSFNSES
GSVVLNDTSKNFEDSRKVAKAAWDMDFTDEQIYVLRKICEAVYNRSAALAAGTIAAIAKR
IKIIEHSKFTCGVDGSLFVKNAWYCKRLQEHLKVILADKAENLIIIPADDGSGKGAAITA
AVIALNADIPQLP

**Figure 4.13: Glutathionylated cysteins in *Pf*HK as detected by mass spectrometric analysis.** Red indicates the cysteine residues that were not detected; grey indicates the cysteine residues that were not glutathionylated in all the samples; green indicates the cysteine residues that were glutathionylated in part of the samples; yellow indicates the cysteine residue that was glutathionylated in all the samples.

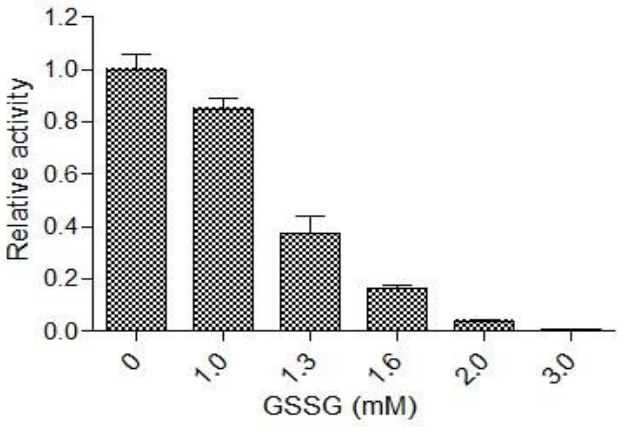


**Figure 4.14: *Pf*HK incubated with different concentrations of oxidized glutathione at 4 ℃ overnight.**

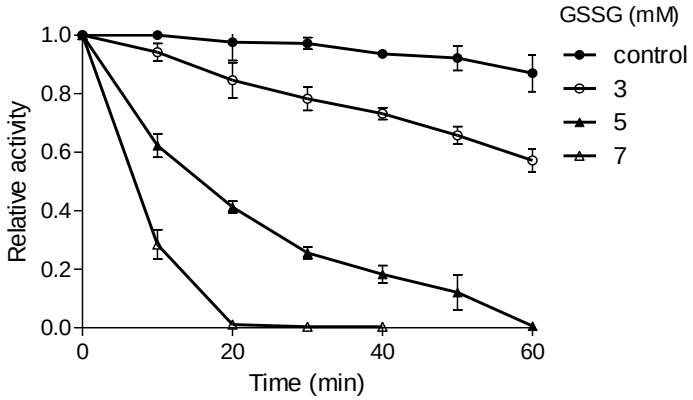


**Figure 4.15: *Pf*HK incubated with different concentrations of oxidized glutathione at room temperature.**

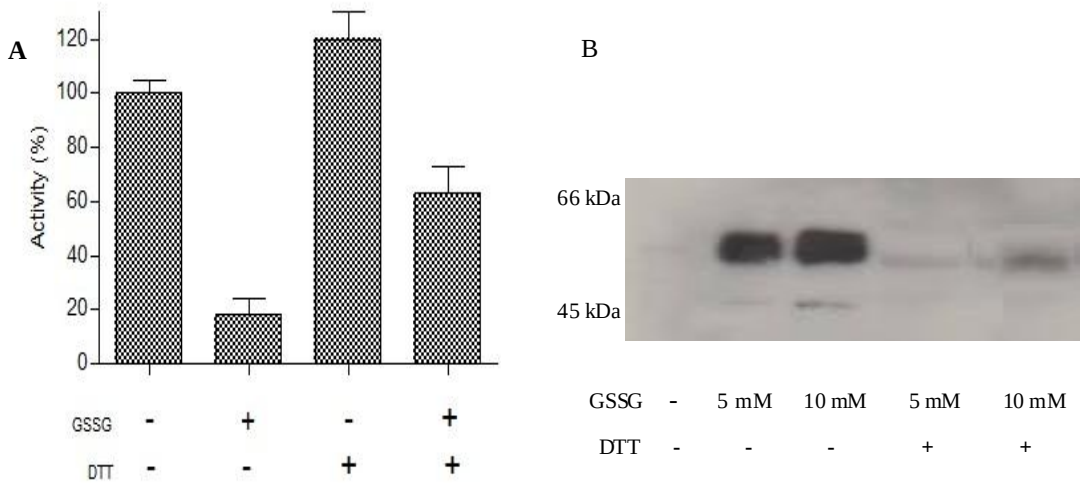


**Figure 4.16: Reversibility of the glutathionylation of *Pf*HK. A)** Enzyme activity; **B)** Western blot.

### 4.1.9 Inhibition of *Pf*HK by compounds with antimalarial activity

To verify whether the current effective antimalarials can influence the activity of hexokinase in *P. falciparum*, the antimalarials (artemisinins, quinolines, anifolates, methylene blue, and their derivatives) were added to the standard assays of hexokinase. No inhibitory effect was found at drug concentrations of up to 100 µM. This result indicated that *Pf*HK is not a major target of these antimalarials.

## 4.2 *Pf*HK localization

After successfully transfecting the parasites with the vector fusing GFP to full-length and truncated *Pf*HKs, the subcellular localizations of *Pf*HK were studied by examining transgenic parasites via immune fluorescence microscopy. Both the full-length and truncated *Pf*HK were located in the parasite cytosol (Figures 4.17 A and C). There was no detectable difference between the full-length and truncated *Pf*HKs, and there was no membrane association tendency of the full-length *Pf*HK. To further determine whether there was membrane association, Western blots using anti-GFP antibodies confirmed that *Pf*HK only existed in the cytosol of parasites. To control the separation of membrane and cytosolic fraction of the parasites, the antibodies of membrane protein Exp1 and the cytosolic protein Hsp70 were probed in the samples after ultra-centrifugation. The inevitable contamination by the Exp-1 and Hsp70 were observed in both membrane and cytosolic fractions. But the GFP-*Pf*HK was only detected in the cytosolic fraction of the parasite lysates by the anti-GFP antibody (Fig. 4.17 B and D).

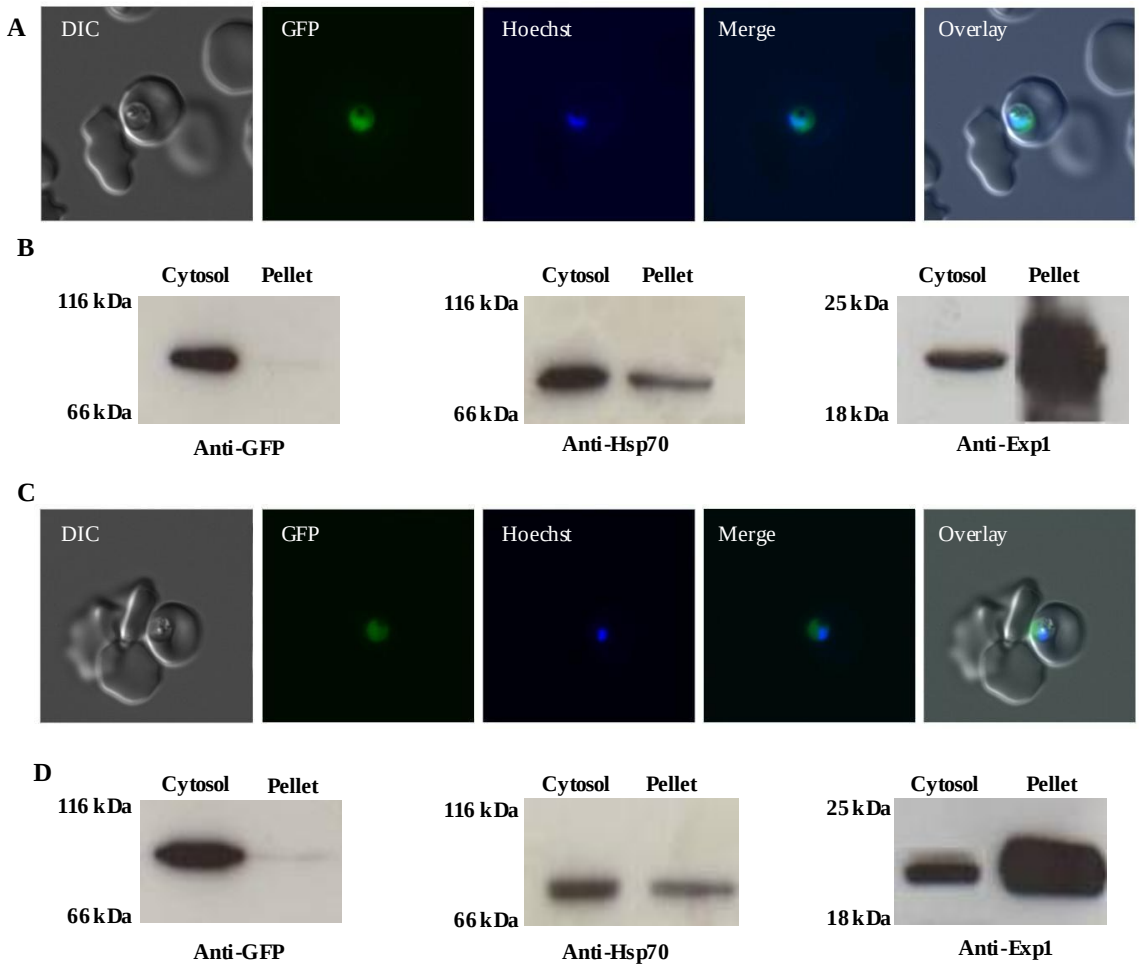


**Figure 4.17: The images of subcellular localization of *Pf*HK. A)** Localization of full-length *Pf*HK in the cytosol. **B)** Western blot of the lysates of parasites transfected with full-length *Pf*HK, using anti-Hsp70 as the marker for the cytosolic fraction, anti-Exp1 as the marker for the membrane fraction, and anti-GFP antibodies. **C)** Localization of truncated *Pf*HK in the cytosol. **D)** Western blot of the lysates of parasites transfected with truncated *Pf*HK.

## 4.3 Activity of HKs in *P. falciparum*-infected erythrocytes

The continuously cultured, parasitized erythrocytes were harvested by the magnetic columns. After harvest the parasitemia reached over 98%. In order to avoid interference of hemoglobin, the activities of HK in the lysates were monitored by a fluorescence spectrometer. The G6PDH-coupled assay was applied to determine the NADPH generation at 340 nm (ex) and 460 nm (em). There was a significant difference between the HK activity in parasitized erythrocytes and the uninfected erythrocytes. The enhancement was approximately 10-fold. The activity of HK in uninfected erythrocytes was similar to the one that was cultured without parasites (Fig. 4.18). After measuring the protein concentrations, the standardized activities in the parasitized erythrocytes, uninfected erythrocytes and control group were 2.86, 0.25, and 0.26 RFU/min per µg of protein in lysates, respectively. Different amounts of lysates

were applied to determine the activities of HKs (Fig. 4.18).

In the process of erythrocyte rupture, there is the possibility of contamination from parasites. Because the activity of *Pf*HK in *P. falciparum* was pretty high, approximately 65.99 RFU/min/µg, the contamination of *Pf*HK can possibly significantly influence the test. To check for a possible contamination by parasite lysates, Western blot was employed by using the antibodies that selectively react with proteins (*Pf*TrxR and *Pf*GluPho) that only exist in parasites. By the Western blot results, a contamination of erythrocyte samples by parasite lysates became evident (Fig. 4.19).

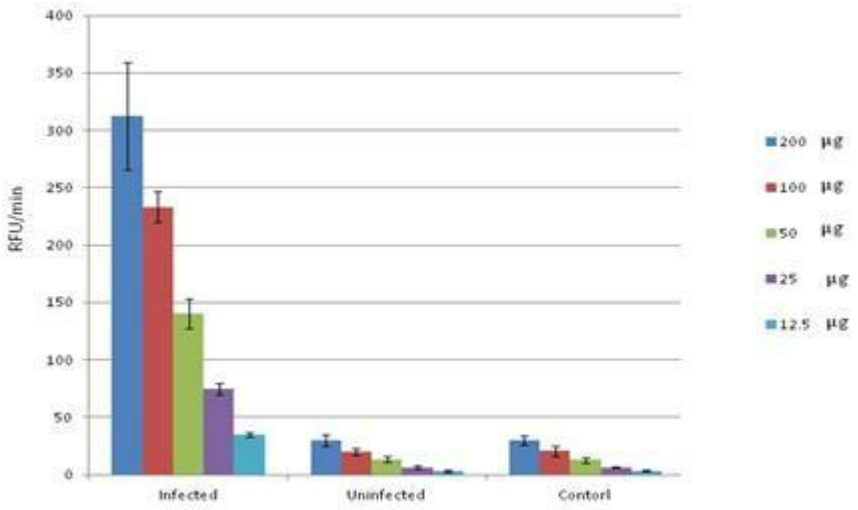


**Figure 4.18: Activities of HKs in RBC lysates.**

In order to determine and evaluate the contamination of parasite lysates further, the activity of GDH, which is not present in human erythrocytes but only in *P. falciparum*, was employed. In the PBS buffer with pH 8.0, the NADPH generation could be monitored at 340 nm (ex) and 460 nm (em). The activity of GDH was only found in the infected RBC sample, not in uninfected and control samples. The activity of GDH in the infected RBC sample was 0.155 RFU/min/µg, which all came from the contaminated parasite lysate. At the same conditions, the activity of GDH in parasite lysate was 10.93 RFU/min/µg. Combined with the HK assay, the ratio between the enzyme activities (EA) of *Pf*HK and *Pf*GDH was 6.038 ($[EA]_{PfHK}/[EA]_{PfGDH}$ = 65.99/10.93). That means if there is 1 RFU/min/µg GDH activity found in IRBC lysate, approximately 6 RFU/min/µg HK activity would come from the contamination of parasite lysate. Based on this ratio we can estimate the activity of HK that was contributed by *Pf*HK in the parasitized erythrocyte sample. After calculation, 0.94 RFU/min/µg (6*0.155 RFU/min/µg) of HK activity was contributed by *Pf*HK, and the remaining activity of HK (1.92 RFU/min/µg) was still much higher than in the uninfected and control samples (0.26

RFU/min/µg). This indicates that HK activity in IRBCs is upregulated by a factor of approximately 8. However, these results need to be comfirmed by replicates.

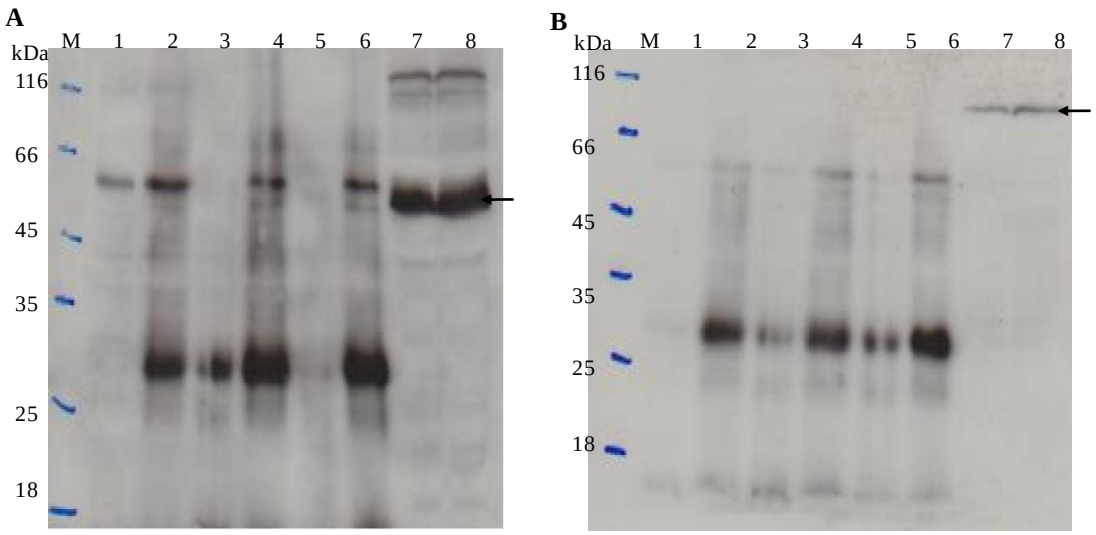


**Figure 4.19: Western blots of infected and uninfected RBC using antibodies against *Pf*TrxR (A) and *Pf*GluPho (B).** 1: 100 µg of infected RBC lysate; 2: 200 µg of infected RBC lysate; 3: 100 µg of uninfected RBC lysate; 4: 200 µg of uninfected RBC lysate; 5: 100 µg of control sample; 6: 200 µg of control sample; 7: 100 µg of parasite lysate; 8: 200 µg parasite lysate. From the films, clear bands of TrxR and GluPho were probed (arrows). Some unspecific bands were also detected in the RBC lysates.

## 4.4 Crystallization and structure prediction of *Pf*HK

The crystal screening of recombinant *Pf*HK was initially performed using the sitting drop method, and a JSCG Core Suite kit was chosen. In the first round of screening, 480 different formulas of salt, pH, and precipitator were automatically prepared and tested by the crystal screening robot. The concentration of recombinant *Pf*HK was 7.8 mg/ml and was stored in the buffer containing 100 mM Tris and 300 mM KCl with pH 7.0. The concentration of recombinant *Pf*HK could not be raised further because of precipitation. The proteins were found to precipitate very fast in the crystal screening buffers. However, after 2 months there was a litter of crystals forming in two screening buffers. The crystals demonstrated different colors from the background with a polarizing filter (Fig. 4.20 A), and there was no crystal found in the control wells, which only contained buffers (Fig. 4.20 B).

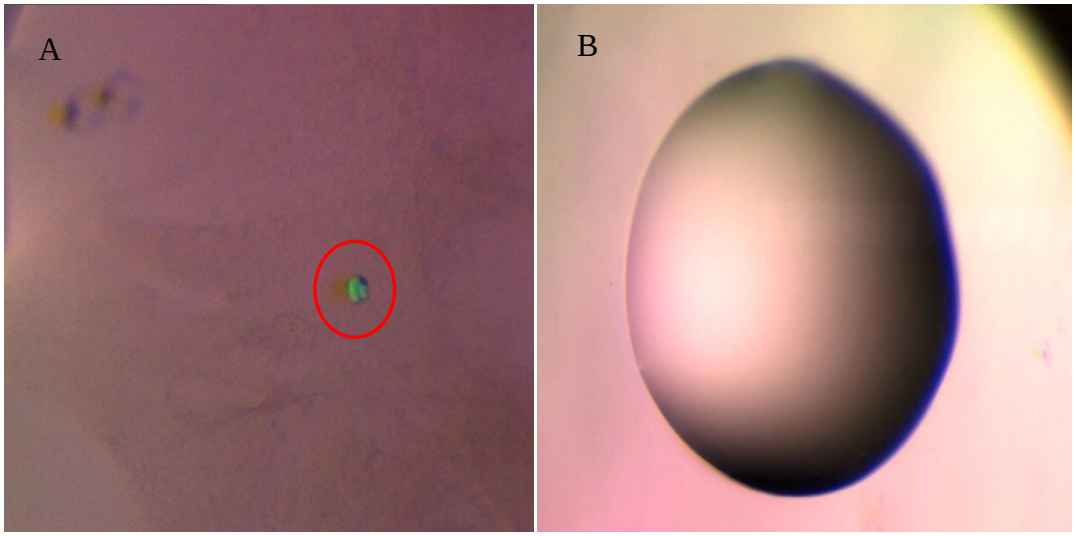


**Figure 4.20: Image of the crystal screening. A)** The crystal in the mixture of buffer and protein. **B)** The control sample only with buffer.

From the result of the preliminary trials, three conditions seemed promising to further optimization (Table 4.5). The hanging drop method was used to perform the second round of screening. By slightly varying the concentration of components and pH value, a series of buffers that were similar to the promising buffers in preliminary trials were tested manually. To stabilize the enzyme in screening buffer, the substrate of *Pf*HK ATP (2 mM) was also added, but there seemed to be no difference. After a week's storage at room temperature, all the tests were precipitated, and two months later no crystal existed in these trials.

| **Drop 1** | **Drop 2** | **Drop 3** |
|---|---|---|
| 0.2 M $MgCl_2$, 0.1 M imidazole, pH 8.0, 40% MPD | 0.2 M $MgCl_2$, 0.1 M Tris, 10% glycerin, pH 8.5, 25% 1,2-propaediol | 0.2 M $MgCl_2$, 0.1 M Tris, pH 8.5, 30% PEG 4000 |

**Table4.5: Promising conditions for crystallization screening.**

Due to the absence of hexokinase crystal structures in *Plasmodium* parasites, the secondary and tertiary structures of *Pf*HK were predicted by the homologous hexokinases in the PDB database. Although the alignment shows low identities with other hexokinases, the binding sites are quite conserved with some substitutions. Based on the N- and C-terminal halves of human crystal structures (1DGK), two structure models were constructed (Fig. 4.22 A and B). Two ADP binding site are observed in these two models. One is on the surface and another is at the binding site of ATP. The binding site of G6P overlappes with the ADP binding site, which is the same as in human hexokinase I. Three insertions belong to the undefined part of the model. The insertion (63~76 residues) contains a couple of positively charged

residues; a neighboring region of human hexokinase interacts with the second half of the dimer. Another two insertions at the surface, 133-143 and 206-213, which are missing in humans, are near each other. The residues contributing to the binding of glucose and ADP at the active site are illustrated in Figure 4.22 C. Based on the models, Cys77, Cys85, Cys193, Cys236, and Cys445 are at the surface of *Pf*HK; Cys186, Cys249, Cys260, Cys273, and Cys399 are conserved in human hexokinase and internally located in *Pf*HK.

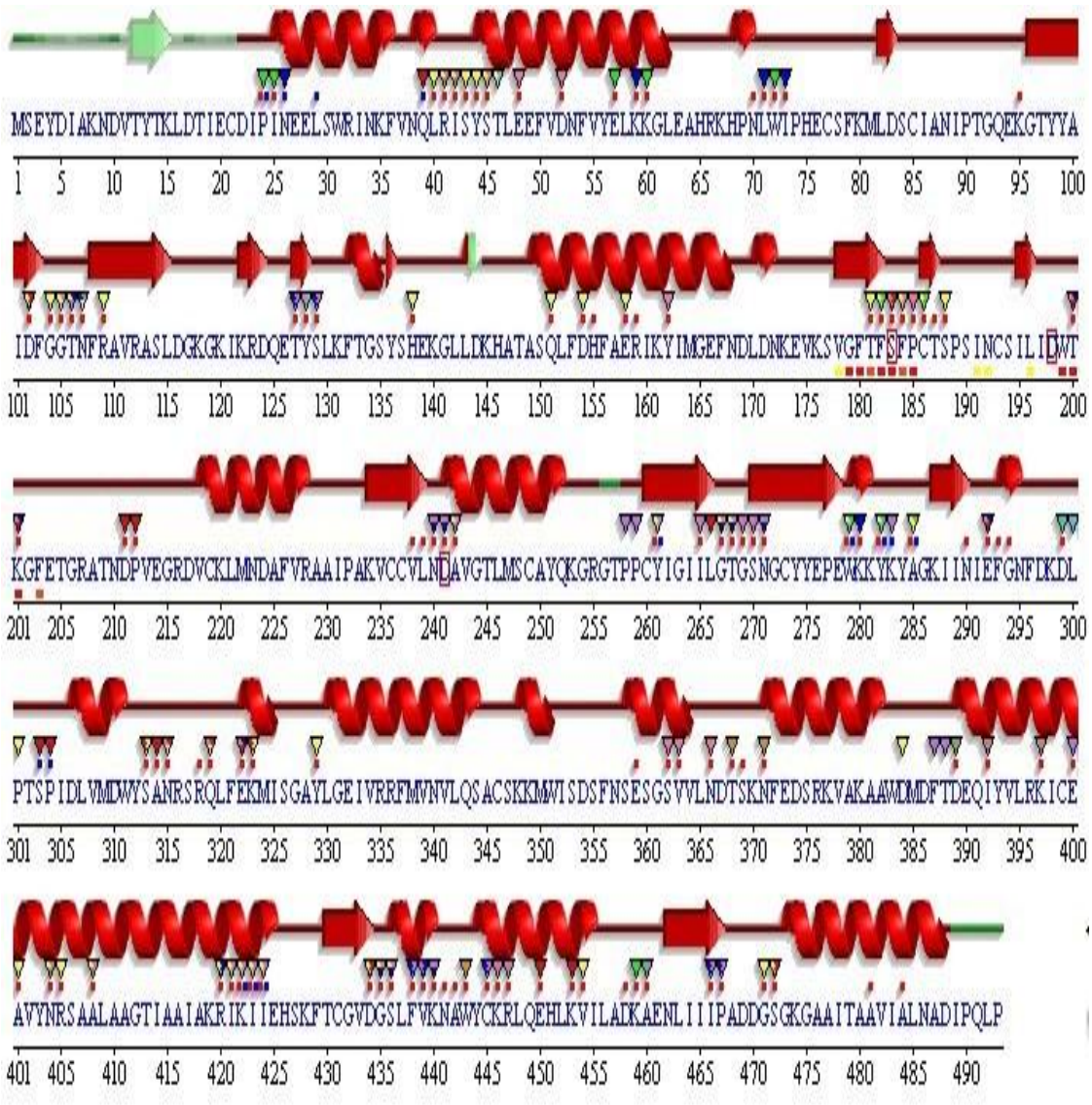


**Figure 4.21: The predicted secondary structure of *Pf*HK.** helix, strand; the image was created by the PDBsum online server.

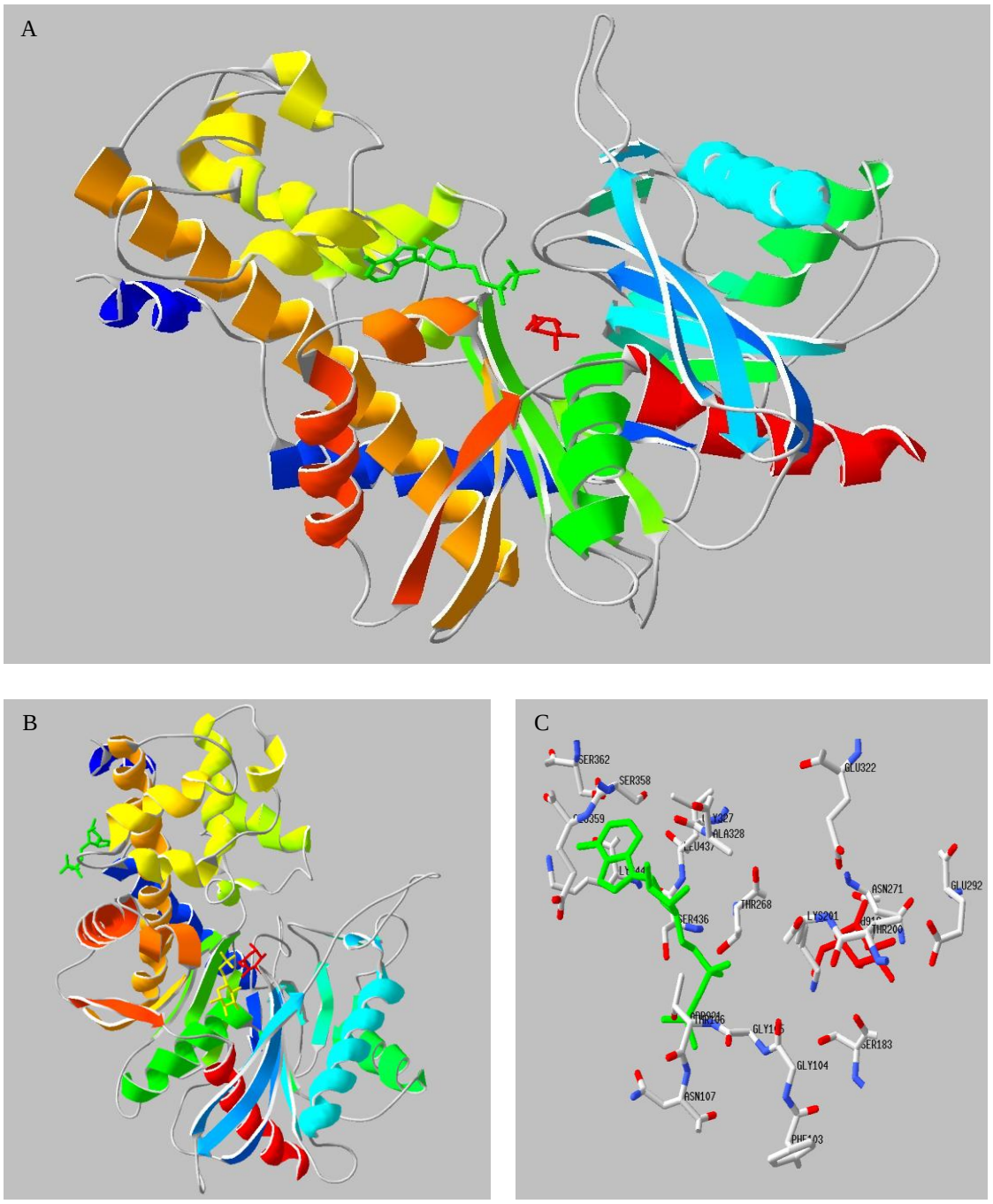


**Figure 4.22: The *Pf*HK models and details of substrate binding sites. A)** The predicted model I of *Pf*HK based on the C-terminal half-structure of human hexokinase I (Access number: 1DGK) by the Swiss-Model Server. The green molecule is ADP, showing the ATP binding site. The red molecule is glucose. **B)** The predicted model II of PfHK based on the N-teminal half-structure of human hexokinase I, showing the surface binding site of ADP. The yellow molecule is G6P, which overlappes with the binding site of ATP compared to model I. **C)** Amino acids in the peptide binding pocket of the model of PfHK on the ternary complex with glucose, ADP, and the pentapeptide of FGGTN, which embraces the binding sites of glucose and ATP.

## 4.5 *Pf*HK knockout

### 4.4.1 Generation of a *Pf*HK merodiploid strain

The *Plasmodium falciparum* hexokinase genes, with DNA encoding DHFR-HA and GFP-DHFR-HA added to the 5' end (designated ±GFP-DHFR-HA-*Pf*HK), were cloned into the pLN plasmid, which contains *attP* sites, and cotransfected into Dd2attB strains along with the pINT vector, which carries a gene encoding the Bxb1 integrase from mycobacteriophage. After two to three weeks continuous culture, the integration of the target gene was checked via diagnostic PCR in the parasites observed after transfection. Subsequently, the episomal plasmids were eliminated by removing the selective drug G418 and blasticidin for at least one month. Western blot was applied to check the episomally overexpressed *Pf*HK in the transgenic parasite lysates using anti-GFP antibodies. From the Western blot results, the clear bands of episomally overexpressed *Pf*HK were observed in the films (Fig. 4.23). In the cell culture with blasticidin, both episomal *Pf*HKs expressed well. Unfortunately, the episomal *Pf*HKs were not degraded without TMP. That means that the conditional knockout down could not be realized. After knocking out the endogenous *Pf*HK, the parasites will only rely on the episomally expressed *Pf*HK. To show the status of *Pf*HK eliminated in parasites, a control of wild type strain was added to the next knockout step.

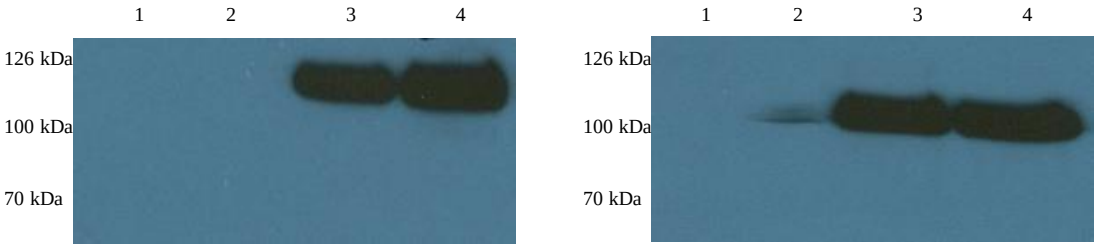


**Figure 4.23: Western blot of the episomal *Pf*HK. A)** GFP-DHFR-HA-*Pf*HK. **B)** DHFR-HA-*Pf*HK. 1: blasticidin and G418; 2: blasticidin, G418 and TMP; 3: G418; 4: G418 and TMP.

### 4.4.2 Knockout of *Pf*HK in both wild type and merodiploid Dd2 strains

Due to this step of the experiment being time-consuming, the parasites transfected with knockout vectors are still in cell cultures. This part of the work is in progress, and it will take a few more months to obtain the results.

# 5 Discussion

## 5.1 Hexokinase in *Plasmodium falciparum*

To investigate the kinetics of *P. falciparum* hexokinase, the heterologous overexpression of *Pf*HK in high purity is necessary in order to exclude the interference of contamination. In this thesis, we have successfully obtained homogeneous *Pf*HK from heterologous overexpression and purification via our optimized methods. Different from the heterologous overexpression of hexokinase in *Toxoplasma gondii* (Saito *et al.*, 2002) and *Schistosoma mansoni* (Armstrong *et al.*, 1996), we did not choose the strategy of an N-terminal fusion partner protein (glutathione S-transferase) to increase the solubility. To overcome the insolubility of heterologously overexpressed *Pf*HK (Olafsson *et al.*, 1994), chaperones (hot shock proteins) coexpression and low temperature incubation of cell culture were applied to reduce the misfolding of recombinant protein and make it soluble. After harvesting, glycerol in resuspension buffer can stabilize the heterologously overexpressed *Pf*HK and increase the yield. Because of the C-terminal His-tag, the recombinant protein can be purified by the Protino Ni-TED column. The coexpressed chaperones need to be removed by adding 5% imidazole to cell lysates during column elution, otherwise chaperones will combine with the recombinant *Pf*HK by intermolecular disulfide bonds and can not be removed via additional gel filtration (FPLC). The productivity of heterologous overexpression of *Pf*HK in *E. coli* was 0.5 mg of purified enzyme from 1 liter of cell culture. This enzyme from *P. falciparum* has for the first time been successfully heterologously overexpressed and purified.

The oligomeric structure of *Pf*HK in our study is a tetramer from the result of gel filtration chromatography. The molecular mass of native *Pf*HK should be around 55 kDa as calculated from the encoded amino acid sequence. The SDS gel electrophoresis shows a similar molecular mass (55 kDa). The elution peaks of *Pf*HK in gel filtration chromatography are stable at 69.6 minutes (approximately correlated with 200 kDa) from different tests with different salt concentrations. The test with DTT in the elution buffer shows no difference, excluding the intermolecular disulfide bonds. These data clearly indicate that the *Pf*HK is a tetramer, which is quite different from the hexokinases from the human host. Whereas the hexokinases in most species characterized show normally as monomers or dimers, only in the high concentration or in the complex associated with mitochondria hexokinase can form a tetramer complex (Aleshin *et al.*, 1998). Additionally, a study of *Trypanosoma cruzi* reveals that hexokinases in

this parasite also exist as tetramers under native conditions (Cáceres *et al.*, 2003).

Hexokinase from *P. falciparum* turned out to be a 50-kDa type enzyme similar to invertebrate hexokinases and vertebrate hexokinase IV. *Pf*HK shows a similarity of 44% with *T. gondii* HK and of 33% compared to human hexokinases. Hexokinase of *P. falciparum* clustered with other apicomplexan HKs in the phylogenetic tree (Fig 4.2), elucidating the evolutionary origin of *Plasmodium*.

The kinetic studies reveald that the $K_m$ values of *Pf*HK are similar to the enzyme of *S. mansoni* and show higher affinity to glucose and a similar affinity to ATP as human hexokinase II (Table 5.1). When compared to the $K_m$ values tested by Eugene and Roth [1987] in the lysates of infected red blood cells, the affinities to both glucose and ATP were much higher in our tests. The discrepancy between the $K_m$ values of *Pf*HK from our tests and those from earlier studies might be due to the presence of other factors in cell lysates. In human red blood cells, the dominant HK is hexokinase I, which shows lower $K_m$ values for glucose and ATP than *Pf*HK. It therefore cannot be excluded that *P. falciparum* has to compete with the red blood cell for glucose. The demands of glucose consumption in *P. falciparum* may mainly be met by the high activity of *Pf*HK and the enhancement of glucose permeability. The transport of glucose into red blood cells and parasites is mediated by the specific glucose transporter (GLUT) and *Plasmodium falciparum* hexose transporter (*Pf*HT) respectively. *Pf*HT ($K_m = 1.3 \pm 0.3$ mM) glucose transport is accommodated significantly better than human GLUT1 ($K_m > 30$ mM). It was suggested much more glucose is transported into IRBC and further into parasites (Woodrow *et al.*, 2000; Woodrow *et al.*, 1999). And there is evidence that *Plasmodium falciparum* exports proteins to the surface of red blood cells and changes the permeability of the RBC membrane for glucose (Ginsburg *et al.*, 1983; Marti *et al.*, 2004).

The initial velocity studies with glucose and ATP shows that the Michaelis-Menten equation is obeyed by *Pf*HK. The double reciprocal plots obtained from the initial rate studies illustrate that the kinetic mechanism of *Pf*HK is a sequential (ternary complex) mechanism, in which the binding of substrates to the enzyme must occur before the formation of products. The same conclusions were also exhibited in tests of other 50-kDa hexokinases in both invertebrate and vertebrate species (Danenberg *et al.*, 1975; Gregoriou *et al.*, 1981). To differentiate between random and ordered sequential mechanisms, product inhibition study was applied to elucidate the order of substrate binding and the release of products.

| | $K_m$ (mM) | | |
|---|---|---|---|
| **Organism** | **ATP** | **Glucose** | **Reference** |
| *Homo Sapiens* Type I | 0.5 | 0.03 | John E. Wilson, 2003 |
| *Homo Sapiens* Type II | 0.7 | 0.3 | |
| *Homo Sapiens* Type III | 1.0 | 0.003 | |
| *Schistosoma mansoni* | 0.92 | 0.128 | Robert L. Armstrong *et al.*, 1996 |
| *Toxoplasma gondii* | 1.05 | 0.008 | Tomoya Saito *et al.*, 2002 |
| *Plasmodium falciparum* | 3.1 | 0.43 | Eugene F. Roth, 1987 |
| *Plasmodium falciparum* | 0.7 | 0.07 | Present study |

**Table 5.1: Summary of kinetic parameters of hexokinase**

Due to the fact that individual binding sites of G6P existed and overlapped with ATP binding sites in *Pf*HK, G6P was found to be a mixed type inhibitor with respect to glucose, and a competitive inhibitor with respect to ATP. Surprisingly, the feedback inhibition of ADP was found to be a mixed type with respect to both glucose and ATP. That means ADP was observed binding with the binary complexes of enzyme-glucose and enzyme-ATP, whereas G6P was observed binding only with the binary complex of enzyme-glucose and not enzyme-ATP. To explain this outcome, the plausible explanation is that these inhibition patterns indicate a random Bi Bi mechanism without a leading substrate binding first to the enzyme (Fig 5.1), because in an ordered mechanism the product of the first substrate should be a competitive inhibitor with respect to that substrate (Alberty, 1958). A mixed type inhibition of ADP with respect to both ATP and glucose has been also observed in rat brain hexokinase (Grossbard *et al.*, 1966) and bovine brain hexokinase (Ning *et al.*, 1969). One explanation for this observation is that ADP can bind at both substrate sites, whose ribose-5-P portion of the nucleotide had affinity for the sugar site. However, another explanation is more attractive: ADP interaction with enzymes is not merely to act at a product site but also a separate inhibitory nucleotide binding site (Purich *et al.*, 1971). Danial *et al.* [1971] proved this hypothesis via mixed type inhibition of ADP with respect to ATP, even at the saturating levels of glucose, and the same was true when the ATP site was nearly saturated. In our studies, the same result was observed. The competitive inhibition of G6P with respect to ATP means that G6P cannot bind to the sugar binding site of the binary complex of enzyme-ATP formed. This could be explained by the instability of the binary complex of enzyme-ATP and by the fact that the binding of glucose can form the close conformation of the enzyme to stabilize the binding of ATP. The absence of a crystal structure in the binary complex of hexokinase-ATP proves this possibility from

another perspective.

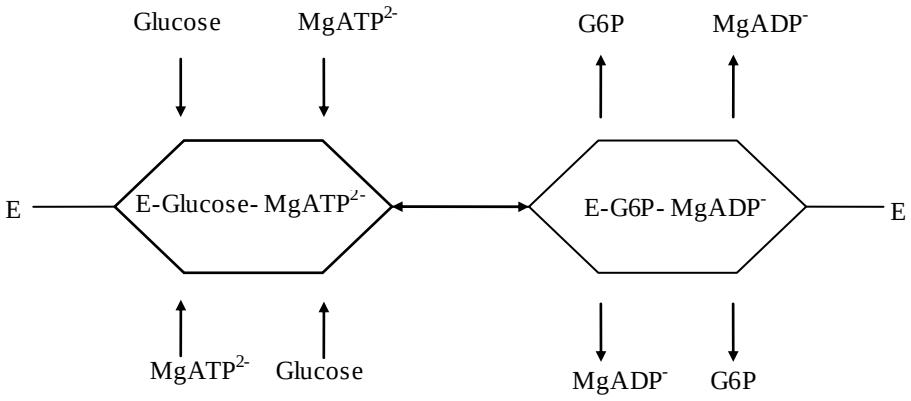


**Figure 5.1: Schematic representation of a random mechanism of *Pf*HK where E is the enzyme.**

Interestingly, in contrast to other invertebrate 50-kDa hexokinases, *Pf*HK shows the sensibility to G6P inhibition ($IC_{50}$: 0.32 mM), and the predicted structure of *Pf*HK also revealed the conserved binding motif of G6P; however, the inhibition of *Pf*HK by G6P is not as strong as in the vertebrate 100-kDa hexokinases. For example human hexokinase I is significantly inhibited by G6P at the physiological concentrations. Along with the observation that G6P inhibition was found in the 50-kDa hexokinase in starfish (Mochizuki, 1981) and the C-terminal fragment of 51 kDa from human hexokinase I, the hypothesis of N-terminal allosteric regulation of G6P was doubted. A new view of the evolutionary relationship between the hexokinases suggested that G6P sensitivity arose before the gene duplication and fusion from 50-kDa to 100-kDa (Colowick, 1973; White *et al.*, 1989). According to this view, the ancestral 50-kDa ancestor of the 100-kDa human hexokinases resembled the *Plasmodium* hexokinase more closely than the yeast enzyme.

The feedback inhibition of G6P for hexokinases was considered to prevent excessive phosphorylation, which leads to ATP depletion and controls the flux of glucose utilization, avoiding the excessive production of lactate. In vertebrates, hexokinase I and II show high affinities to the substrates and wide distribution in brain and other tissues, demonstrating the overall rate of glucose phosphorylation commensurate with cellular energy demands. In hepatic cells, the function of glycogen storage relies the glucokinase, which acquires the relatively low affinity of glucose, but an absence of G6P inhibition facilitates the transformation of plasma glucose into glycogen via the activation of insulin. In the other tissues this unrestricted accumulation of G6P is dangerous, for ATP is invested before its net production. The transfer of high-energy phosphoryl from ATP to glucose actually makes the first reaction

irreversible and thereby the regulations in the rest of the pathway become insignificant. Therefore, it is vital to rigorously regulate the first reaction. In previous studies, it has been observed that the energy demands of *Plasmodium falciparum* rely on anaerobic glycolysis, with regeneration of $NAD^+$ by conversion of pyruvate to lactate, which is further excreted into host blood cells (Sherman, 1998). Although *Plasmodium* parasites do not have the burden of harmful lactate, which is the result of anaerobic glycolysis, to maintain blood cell integrity, it is also important for the development of the intraerythrocytic stage. Similar patterns of reduced sensitivity of inhibition by G6P were also observed in the parasite *Schistosoma mansoni* and some cells exhibiting high anaerobic glycolytic activity (Tielens *et al*., 1994). The hypothesis for this reduced sensitivity to inhibition by G6P was related to ATP demand. Due to the absence of increased ATP demand in the cells of anaerobic glycolysis with a low rate of respiration, large amounts of pyruvate formed cannot be degraded to carbon dioxide via the TCA cycle and result in the production of lactate. The altered regulation of hexokinases would be a factor contributing to this high anaerobic glycolyisis. Despite the hexokinases in *Trypanosomes*, which are also a 50-kDa parasitic hexokinase and exhibit insensitivity to inhibition by G6P, excessive investment of ATP is also dangerous. Via the special compartmentation of hexokinases, which is called glycosome, *trypanosomes* are protected from the dangerous design of glycolysis (Bakker *et al*., 2000). In glycosomes, the ratio of ATP/ADP regulates the activity of hexokinase in order to prevent the accumulation of intermediates. The observation of G6P inhibition in *Plasmodium falciparum* and the relatively high $IC_{50}$ compared to the micromolar range of physiological G6P concentration in humans indicate a plausible mechanism of a modest regulation of hexokinase activity. Considering that the substrate affinities of *Pf*HK are also intervenient to the values of human HK I and glucokinase, this might be a parasitic strategy of *Plasmodium falciparum*.

The hypothesis of membrane association came from a cluster of hydrophobic peptides at the C-terminal of *Pf*HK, which is similar to the N-terminal hydrophobic region in human hexokinase I. The N-terminal 21 amino acid residues of human hexokinase I are essential for binding with the outer membrane of mitochondria, and mutants are only observed in the cytosol (Polakis *et al*., 1985; Schwab *et al*., 1989). In humans the combination of hexokinase I and II with the outer membrane of mitochondria are considered to be close to ATP generation. However, further research shows that this anchor plays more important functions besides glucose phosphorylation. Extensive evidence indicates that the dissociation of hexokinase from mitochondria leads to the dysfunction of mitochondria and cell apoptosis, which is

related to the release of cytochrome C (Kelley *et al.*, 2002; Majewski *et al.*, 2004; Pastorino *et al.*, 2002). The function of the hydrophobic peptide at the C-terminus of *Pf*HK is therefore interesting to explore.

By analyzing the hydrophobic residues online, the last 15 residues of *Pf*HK could form an α-helix showing moderate hydrophobic properties. A truncated *Pf*HK was constructed to delete the last 15 residues. Due to the adenine nucleotide translocator being in proximity to this region, no activity was detected in the truncated *Pf*HK. Surprisingly, GFP fluorescence microscopy illustrated that the sub-cellular localization of *Pf*HK was cytosolic. No conspicuous difference was found between the full-length and the C-terminally truncated *Pf*HK. The results of our studies are quite disparate from the compartmentation of immune electron microscopy by Olafssen [1994]. They found that a statistically significant amount (65.7%) of *Pf*HK was associated with the parasite membrane structure (Olafsson *et al.*, 1994). Western blot also confirmed the cytosolic compartmentation of *Pf*HK in our studies, which was indicated by the antibodies of *Pf*Hsp70 existing mainly in parasite cytosol and *Pf*Exp1 combining with the parasite membrane, and the signal of anti-GFP only existed in the cytosol fraction. The same observation from Western blot was also mentioned by Olafssen [1994], despite the fact that detergent was used to dissolve the membrane fraction. In the view of facilitating glucose phosphorylation, Olafssen supposed the membrane association made *Pf*HK close to the site of glucose uptake. However, it seems that proximity to the ATP generation site is more attractive for hexokinases in humans and other species. For *Plasmodium* parasites, in which the ATP supplement relies on cytosolic anaerobic glycolysis, it can be deduced that *Pf*HK exists in the cytosol where ATP generation is more reasonable. The discrepancy between our studies and Olafssen's cannot be explained by the diversity of methods. Since the resolution of the graph of immune electron microscopy is low by Olafssen, a much clearer picture with high resolution is necessary to settle this argument.

## 5.2 Structure analysis of *Pf*HK for estimating the potency as antimalarial drug target

So far more than 50 crystal structures of hexokinases in different species have been investigated and refined, including *Homo sapiens*, *Saccharomyces cerevisiae*, *Rattus norvegicus*, *Schistosoma mansoni*, and others. Most of the crystal structures were obtained from humans and yeast in order to reveal the substrate binding and catalytic mechanism, especially concerning the allosteric regulation of G6P in 100-kDa human hexokinases and the activation in glucokinase (Bebernitz *et al.*, 2009; Liu *et al.*, 2012;

Rosano *et al.*, 1999). Indeed the high-resolution structure and details of the binding sites from enzyme crystals could also facilitate inhibitor screening. Due to a lack of heterologous overexpression of *Pf*HK, the crystal structure of *Pf*HK has not been investigated yet. In our study, hundreds of conditions were tested for crystal screening via a high-throughput method by a robot. Some conditions showed promising signs of crystal formation, but we have not obtained a crystal big enough for X-ray diffraction analysis because of the instability of *Pf*HK at room temperature. Although obtaining a crystal of *Pf*HK is still a challenge, it is worthwhile to screen for specific inhibitors. Based on the conserved motifs of hexokinases, a model of *Pf*HK was constructed via homolog modeling with human hexokinase I.

In the predicted model of *Pf*HK, approximately 33% of the amino acid residues are conserved in all the hexokinase members from the alignment of different species, and 13% are perfect matches. When superposing the structures of hexokinases, it is easy to find that these conserved residues form quite similar binding site motifs and structures between enzymes. A large number of glycine residues are conserved ($Gly^{61}$, $Gly^{96}$, $Gly^{165}$, $Gly^{215}$, $Gly^{254}$, $Gly^{267}$, $Gly^{269}$, $Gly^{286}$, $Gly^{331}$, and $Gly^{435}$), which are located at the beginnings or ends of α-helices and β-strands, changing the direction of the chain. The conservation of these glycine residues might provide the necessary flexibility to hexokinase molecules for the conformation change when binding glucose and ATP. As low identities, most of the discrepancies in structures exist in the flexible regions between different hexokinases. In order to analyze its potency as a drug target, the predicted model of *Pf*HK was superimposed with the crystal structure of human hexokinase I (PDB ID: 1DGK). Most of the α-helices and β-strands overlapped well in these two enzymes. Three significant insertions (63~76, 133~143 and 206~213 residues) were recognized from the superposition (Fig. 5.2). All these insertions are located at the surface, which does not seem to contribute to the substrate binding and catalysis. However at the insertion between amino acid 63 and 76, a series of positively charged residues form a loop that could be accessed by the nucleophilic perssad. At the same position in human hexokinase I, it is overlapped by the second half of the molecule. The differences in both regions might form the basis of selective inhibition and further inhibitor screening.

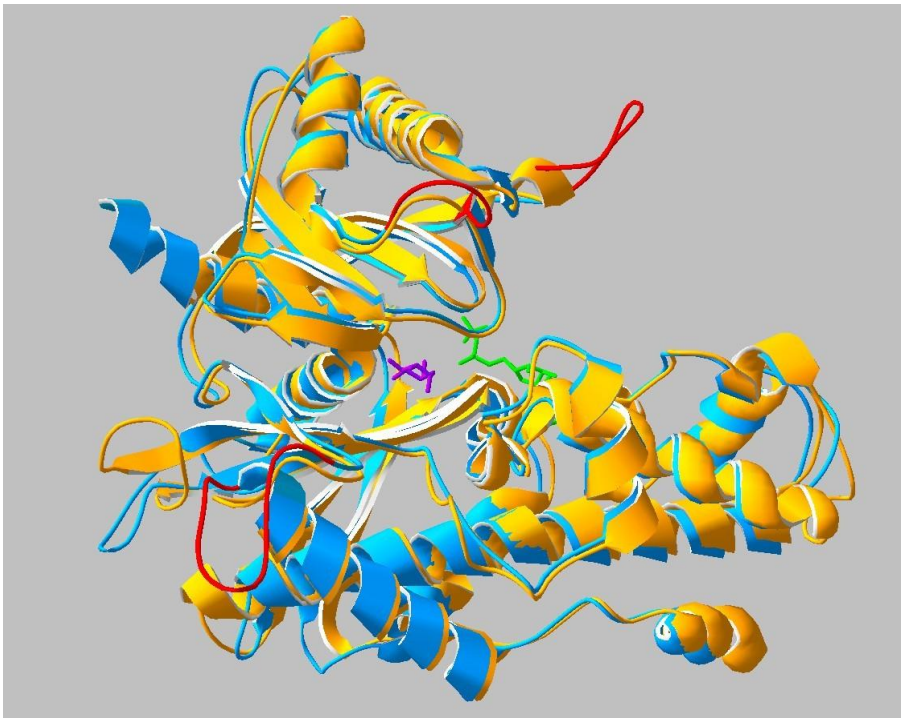

**Figure 5.2: Comparison of human hexokinase type I (yellow) (amino acids 16 to 459) and a model of *Pf*HK (blue) (amino acids 29 to 488)**. Glucose (purple) and ADP (green). The insertions in PfHK are labeled in red. Image created by PDB Viewer 4.1.0.

Even though the substrate binding motifs are conserved among hexokinases, specific inhibitors for *Pf*HK are still possible to obtain. The high throughput screening of hexokinase inhibitors in another parasitic protozoon, *Trypanosome brucei*, yielded ten small molecules that were promising and were further characterized from 220,000 unique compounds (Sharlow *et al.*, 2010). One compound (ebselen) showed the specific inhibition of *Tb*HK in the nanomolar range ($IC_{50}$: 50 nM), serving as leads for the development of therapeutics. In humans, the inhibition of hexokinase was well studied in tumor cells, where the activity of this enzyme is extremely enhanced and vital for survival. A few compounds were identified as inhibitors of human hexokinase II, which is predominant in various tumor cells, including chloromethyl ketone (Johnson *et al.*, 1982), lonidamine (Gatto *et al.*, 2002), and 3-bromopyruvate (Kim *et al.*, 2007). Particularly, 3-bromopyruvate (3-BrPA) has shown remarkable efficacy in preventing tumor growth and eradicating existing tumors in animal models. The mechanism of 3-BrPA inhibition might be due to the covalent modification of HK-II, probably at cysteine residues.

## 5.3 Cysteine residues of *Pf*HK as the target of redox regulation and *S*-glutathionylation.

As shown in the structure analysis, there are 15 cysteine residues distributed in the sequence of *Pf*HK. In previous studies, these cysteine residues, which have the potential to be regulated by proteins of the

thioredoxin superfamily, were first observed by Sturm *et al.*, [2009]. In this work we found that the thioredoxin superfamily in *Plasmodium falciparum* could slightly enhance the activity of *Pf*HK, and a similar result was observed for DTT treatment. The reason might be that most cysteine residues at the surface of hexokinase were in a reduced status under native conditions that has been observed in bovine (Redkar *et al.*, 1972). The fact that HK is targeted by the Trx family and can be glutathionylated indicates that cysteines might be important for *Pf*HK activity

The reversible modification of cysteine residues can significantly change activities and conformations of target proteins. In the process of oxidized glutathione-mediated *S*-glutathionylation, it can be considered an oxidation of the reduced thiols of hexokinase. The *S*-glutathionylation of hexokinases by oxidized glutathione, which leads to inhibition, was observed in different species. In our studies, anti-GSH antibodies were used to detect the added group of GS on *Pf*HK, and we showed that *S*-glutathionylation on *Pf*HK was increased with increasing time, temperature and glutathione concentration. Another direct evidence of *S*-glutathionylation was obtained from a MALDI-TOF analysis. A clear mass increase of ~305 Da was observed for different cysteine-containing peptides. Due to the efficacy of trypsin digestion and the resolution of MALDI-TOF, not all cysteine residues in *Pf*HK were detected. However, combined with the enzyme assay and the MALDI-TOF results of samples, which incubated in different concentrations of oxidized glutathione, some putative sites of *S*-glutathionylation could be concluded. $Cys^{236}$ and $Cys^{346}$ were found to be glutathionylated in most samples, indicating that these two glutathionylated sites did not contribute to the activity changes. Glutathionylated $Cys^{21}$ and $Cys^{249}$ were only observed in *Pf*HK treated with 0.1 mM and 0.5 mM GSSG. A tentative inference was that the glutathionylation of these two cysteine residues was random and did not affect activity. $Cys^{85}$, $Cys^{237}$, $Cys^{249}$, $Cys^{399}$, and $Cys^{431}$ were found to be not glutathionylated. The members in the undetected remainder ($Cys^{185}$, $Cys^{193}$, $Cys^{219}$, $Cys^{260}$, $Cys^{273}$, and $Cys^{445}$) might contribute to the enzyme inhibition by glutathionylation. To confirm which one or few of these cysteine residues play a vital role during this process, a more sensitive MALDI-TOF and further specific mutations are necessary.

From the studies, not only as the target of the thioredoxin superfamily but also regulated by *S*-glutathionylation, the cysteine residues in *Pf*HK have been proved to be capable of being regulated by redox events *in vitro*. Further studies are required to elucidate the mechanism and functional consequence of *Pf*HK regulation under physiological conditions.

# 6 References


Adachi T, Pimentel D R, Heibeck T, Hou X, Lee Y J, Jiang B, *et al.* (**2004**). S-glutathiolation of Ras mediates redox-sensitive signaling by angiotensin II in vascular smooth muscle cells. *J. Biol. Chem.*, 279, **29857-29862**.

Adachi T, Weisbrod R M, Pimentel D R, Ying J, Sharov V S, Schöneich C, *et al.* (**2004**). S-Glutathiolation by peroxynitrite activates SERCA during arterial relaxation by nitric oxide. *Nat. Med.*, 10, **1200-1207**.

Alberty R A. (**1958**). On the Determination of Rate Constants for Coenzyme Mechanisms1. *J. Am. Chem. Soc.*, 80, **1777-1782**.

Aleshin A E, Kirby C, Liu X, Bourenkov G P, Bartunik H D, Fromm H J, *et al.* (**2000**). Crystal structures of mutant monomeric hexokinase I reveal multiple ADP binding sites and conformational changes relevant to allosteric regulation. *J. Mol. Biol.*, 296, **1001-1015**.

Aleshin A E, Zeng C, Bartunik H D, Fromm H J, Honzatko R B. (**1998**). Regulation of hexokinase I: crystal structure of recombinant human brain hexokinase complexed with glucose and phosphate. *J. Mol. Biol.*, 282, **345-357**.

Aleshin A E, Zeng C, Bourenkov G P, Bartunik H D, Fromm H J, Honzatko R B. (**1998**). The mechanism of regulation of hexokinase: new insights from the crystal structure of recombinant human brain hexokinase complexed with glucose and glucose-6-phosphate. *Structure*, 6, **39-50**.

Anderson C M, Stenkamp R E, Steitz T A. (**1978**). Sequencing a protein by X-ray crystallography: II. Refinement of yeast hexokinase B Co-ordinates and sequence at 2.1 Å resolution. *J. Mol. Biol.*, 123, **15-33**.

Anderson T J, Nair S, Nkhoma S, Williams J T, Imwong M, Yi P, *et al.* (**2010**). High heritability of malaria parasite clearance rate indicates a genetic basis for artemisinin resistance in western Cambodia. *J. Infect. Dis.*, 201, **1326-1330**.

Armstrong R L, Wilson J E, Shoemaker C B. (**1996**). Purification and Characterization of the Hexokinase from Schistosoma mansoni, Expressed in Escherichia coli. *Protein Expres. Purif*, 8, **374-380**.

Arzoine L, Zilberberg N, Ben-Romano R, Shoshan-Barmatz V. (**2009**). Voltage-dependent anion channel 1-based peptides interact with hexokinase to prevent its anti-apoptotic activity. *J. Biol. Chem.*, 284, **3946-3955**.

Ashley M V, Stefan H K. (**2012**). Malaria vaccine development: persistent challenges. *Curr. Opin. Immun.*, 24, **324-331**.

Atamna H, Pascarmona G, Ginsburg H. (**1994**). Hexose-monophosphate shunt activity in intact Plasmodium falciparum-infected erythrocytes and in free parasites. *Mol. Biochem. Parasitol.*, 67, **79-89**.

Babbitt S E, Altenhofen L, Cobbold S A, Istvan E S, Fennell C, Doerig C, *et al.* (**2012**). Plasmodium falciparum responds to amino acid starvation by entering into a hibernatory state. *Proc Natl Acad Sci U S A*, 109, **E3278-3287**.

Bakker B M, Mensonides F I, Teusink B, van Hoek P, Michels P A, Westerhoff H V. (**2000**). Compartmentation protects trypanosomes from the dangerous design of glycolysis. *Proc Natl*

*Acad Sci U S A*, 97, **2087-2092**.

Bebernitz G R, Beaulieu V, Dale B A, Deacon R, Duttaroy A, Gao J, *et al.* (**2009**). Investigation of functionally liver selective glucokinase activators for the treatment of type 2 diabetes. *J. Med. Chem.*, 52, **6142-6152**.

Becker K, Kanzok S M, Iozef R, Fischer M, Schirmer R H, Rahlfs S. (**2003**). Plasmoredoxin, a novel redox-active protein unique for malarial parasites. *Eur. J. Biochem.*, 270, **1057-1064**.

Becker K, Tilley L, Vennerstrom J L, Roberts D, Rogerson S, Ginsburg H. (**2004**). Oxidative stress in malaria parasite-infected erythrocytes: host-parasite interactions. *Int. J. Parasitol.*, 34, **163-189**.

BeltrandelRio H, Wilson J E. (**1992**). Interaction of mitochondrially bound rat brain hexokinase with intramitochondrial compartments of ATP generated by oxidative phosphorylation and creatine kinase. *Arch. Biochem. Biophys.*, 299, **116-124**.

Beulter E. (**1984**). *Red cell metabolism: A manual of biochemical methods* ( 3rd ed. ed.): Grune and Stratton New York.

Beutler E, Duparc S. (**2007**). Glucose-6-phosphate dehydrogenase deficiency and antimalarial drug development. *Am. J. Trop. Med. Hyg.*, 77, **779-789**.

Bissati K, Zufferey R, Witola W H, Carter N S, Ullman B, Ben Mamoun C. (**2006**). The plasma membrane permease PfNT1 is essential for purine salvage in the human malaria parasite Plasmodium falciparum. *Proc Natl Acad Sci U S A*, 103, **9286-9291**.

Bradford M M. (**1976**). A rapid and sensitive method for the quantitation of microgram quantities of protein utilizing the principle of protein-dye binding. *Anal. Biochem.*, 72, **248-254**.

Brito I. (**2001**). Eradicating malaria: high hopes or a tangible goal? *Health Policy at Harvard*, 2, **61-66**.

Brown J, Miller D M, Holloway M T, Leve G D. (**1967**). Hexokinase isoenzymes in liver and adipose tissue of man and dog. *Science (New York, N.Y.)*, 155, **205-207**.

Cáceres A J, Portillo R, Acosta H, Rosales D, Quiñones W, Avilan L, *et al.* (**2003**). Molecular and biochemical characterization of hexokinase from Trypanosoma cruzi. *Mol. Biochem. Parasitol.*, 126, **251-262**.

Cárdenas M L, Rabajille E, Niemeyer H. (**1978**). Maintenance of the monomeric structure of glucokinase under reacting conditions. *Arch. Biochem. Biophys.*, 190, **142-148**.

Calvo-Calle J M, Oliveira G A, Nardin E H. (**2005**). Human CD4+ T cells induced by synthetic peptide malaria vaccine are comparable to cells elicited by attenuated Plasmodium falciparum sporozoites. *J. Immunol.*, 175, **7575-7585**.

Capano M, Crompton M. (**2002**). Biphasic translocation of Bax to mitochondria. *Biochem. J.*, 367, **169**.

Cardenas M L, Cornish-Bowden A, Ureta T. (**1998**). Evolution and regulatory role of the hexokinases. *Biochim Biophys Acta*, 1401, **242-264**.

Carter R, Mendis K N. (**2002**). Evolutionary and historical aspects of the burden of malaria. *Clin. Microbiol. Rev.*, 15, **564-594**.

Chen Y R, Chen C L, Pfeiffer D R, Zweier J L. (**2007**). Mitochondrial Complex II in the Post-ischemic heart oxidative injury and the role of protein S-glutathionylation. *J. Biol. Chem.*, 282, **32640-32654**.

Christofk H R, Vander Heiden M G, Harris M H, Ramanathan A, Gerszten R E, Wei R, *et al.* (**2008**). The M2 splice isoform of pyruvate kinase is important for cancer metabolism and tumour growth. *Nature*, 452, **230-233**.

Clarke D D, Sokoloff L. (**1999**). Circulation and energy metabolism of the brain. *Basic neurochemistry:*

*molecular, cellular and medical aspects*, 6, **637-669**.

Clavreul N, Adachi T, Pimental D R, Ido Y, Schöneich C, Cohen R A. (**2006**). S-glutathiolation by peroxynitrite of p21ras at cysteine-118 mediates its direct activation and downstream signaling in endothelial cells. *Faseb. J.*, 20, **518-520**.

Clayton A M, Cirimotich C M, Dong Y, Dimopoulos G. (**2013**). Caudal is a negative regulator of the Anopheles IMD Pathway that controls resistance to Plasmodium falciparum infection. *Dev. Comp. Immunol.*, 39, **323-332**.

Collins W E. (**2012**). *Plasmodium knowlesi*: a malaria parasite of monkeys and humans. *Annu. Rev. Entomol.*, 57, **107-121**.

Colowick S P. (**1973**). The Hexokinases. *The enzymes*, 9, **1-48**.

Coulson R M, Hall N, Ouzounis C A. (**2004**). Comparative genomics of transcriptional control in the human malaria parasite Plasmodium falciparum. *Genome Res.*, 14, **1548-1554**.

Crabb B S, Rug M, Gilberger T W, Thompson J K, Triglia T, Maier A G, *et al.* (**2004**). Transfection of the human malaria parasite *Plasmodium falciparum*. *Methods Mol Biol*, 270, **263-276**.

Crosnier C, Bustamante L Y, Bartholdson S J, Bei A K, Theron M, Uchikawa M, *et al.* (**2011**). Basigin is a receptor essential for erythrocyte invasion by *Plasmodium falciparum*. *Nature*, 480, **534-U158**.

Cross J V, Templeton D J. (**2004**). Oxidative stress inhibits MEKK1 by site-specific glutathionylation in the ATP-binding domain. *Biochem. J.*, 381, **675**.

Dalle-Donne I, Rossi R, Colombo G, Giustarini D, Milzani A. (**2009**). Protein S-glutathionylation: a regulatory device from bacteria to humans. *Trends Biochem. Sci.*, 34, **85-96**.

Dalle-Donne I, Rossi R, Giustarini D, Colombo R, Milzani A. (**2007**). S-glutathionylation in protein redox regulation. *Free. Radical. Biol. Med.*, 43, **883-898**.

Danenberg K D, Cleland W. (**1975**). Use of chromium-adenosine triphosphate and lyxose to elucidate the kinetic mechanism and coordination state of the nucleotide substrate for yeast hexokinase. *Biochemistry-us*, 14, **28-39**.

Dixon D P, Skipsey M, Grundy N M, Edwards R. (**2005**). Stress-induced protein S-glutathionylation in Arabidopsis. *Plant Physiol.*, 138, **2233-2244**.

Dorfman J R, Bejon P, Ndungu F M, Langhorne J, Kortok M M, Lowe B S, *et al.* (**2005**). B cell memory to 3 Plasmodium falciparum blood-stage antigens in a malaria-endemic area. *J. Infect. Dis.*, 191, **1623-1630**.

Du T, Xu Z, Aronin N, Zamore P D. (**2003**). Asymmetry in the assembly of the RNAi enzyme complex. *Cell*, 115, **199-208**.

Feachem R, Sabot O. (**2008**). A new global malaria eradication strategy. *The Lancet*, 371, **1633-1635**.

Fidock D A, Rosenthal P J, Croft S L, Brun R, Nwaka S. (**2004**). Antimalarial drug discovery: efficacy models for compound screening. *Nat Rev Drug Discov*, 3, **509-520**.

Findlay V J, Townsend D M, Morris T E, Fraser J P, He L, Tew K D. (**2006**). A novel role for human sulfiredoxin in the reversal of glutathionylation. *Cancer Res.*, 66, **6800-6806**.

Fitch C D. (**2004**). Ferriprotoporphyrin IX, phospholipids, and the antimalarial actions of quinoline drugs. *Life Sci.*, 74, **1957-1972**.

Fratelli M, Demol H, Puype M, Casagrande S, Eberini I, Salmona M, *et al.* (**2002**). Identification by redox proteomics of glutathionylated proteins in oxidatively stressed human T lymphocytes. *Proc. Natl. Acad. Sci.*, 99, **3505-3510**.

Fratelli M, Demol H, Puype M, Casagrande S, Villa P, Eberini I, *et al.* (**2003**). Identification of proteins

undergoing glutathionylation in oxidatively stressed hepatocytes and hepatoma cells. *Proteomics*, 3, **1154-1161**.

Fukuda Y, Yamaguchi S, Shimosaka M, Murata K, Kimura A G. (**1984**). Purification and characterization of glucokinase in Escherichia coli B (Vol. 48). Tokyo, JAPON: Agricultural Chemical Society of Japan.

Gallogly M M, Mieyal J J. (**2007**). Mechanisms of reversible protein glutathionylation in redox signaling and oxidative stress. *Curr Opin Pharmacol*, 7, **381-391**.

Gardner M J, Hall N, Fung E, White O, Berriman M, Hyman R W, *et al*. (**2002**). Genome sequence of the human malaria parasite Plasmodium falciparum. *Nature*, 419, **498-511**.

Gatto M T, Tita B, Artico M, Saso L. (**2002**). Recent studies on lonidamine, the lead compound of the antispermatogenic indazol-carboxylic acids. *Contraception*, 65, **277-278**.

Gauthier T, Denis-Pouxviel C, Murat J. (**1990**). Respiration of mitochondria isolated from differentiated and undifferentiated HT29 colon cancer cells in the presence of various substrates and ADP generating systems. *Int J Biochem Cell B*, 22, **411-417**.

Geary T G, Divo A A, Bonanni L C, Jensen J B. (**1985**). Nutritional requirements of Plasmodium falciparum in culture. III. Further observations on essential nutrients and antimetabolites. *J Protozool*, 32, **608-613**.

Gelb B D, Adams V, Jones S N, Griffin L D, MacGregor G R, McCabe E. (**1992**). Targeting of hexokinase 1 to liver and hepatoma mitochondria. *Proc. Natl. Acad. Sci.*, 89, **202-206**.

Gilbert H F. (**1984**). Redox control of enzyme activities by thiol/disulfide exchange. *Method. Enzymol.*, 107, **330**.

Ginsburg H, Krugliak M, Eidelman O, Ioav Cabantchik Z. (**1983**). New permeability pathways induced in membranes of Plasmodium falciparum infected erythrocytes. *Mol. Biochem. Parasitol.*, 8, **177-190**.

Giustarini D, Milzani A, Aldini G, Carini M, Rossi R, Dalle-Donne I. (**2005**). S-nitrosation versus S-glutathionylation of protein sulfhydryl groups by S-nitrosoglutathione. *Antioxid Redox Sign*, 7, **930-939**.

Goel A, Mathupala S P, Pedersen P L. (**2003**). Glucose metabolism in cancer Evidence that demethylation events play a role in activating type II hexokinase gene expression. *J. Biol. Chem.*, 278, **15333-15340**.

González C, Ureta T, Sánchez R, Niemeyer H. (**1964**). Multiple molecular forms of ATP: hexose 6-phosphotransferase from rat liver. *Biochem. Biophys. Res. Commun.*, 16, **347**.

Goodman A L, Blagborough A M, Biswas S, Wu Y, Hill A V, Sinden R E, *et al*. (**2011**). A viral vectored prime-boost immunization regime targeting the malaria Pfs25 antigen induces transmission-blocking activity. *PLoS One*, 6, **e29428**.

Gottlob K, Majewski N, Kennedy S, Kandel E, Robey R B, Hay N. (**2001**). Inhibition of early apoptotic events by Akt/PKB is dependent on the first committed step of glycolysis and mitochondrial hexokinase. *Sci Signal*, 15, **1406**.

Graham J F, Cummins C J, Smith B H, Kornblith P L. (**1985**). Regulation of hexokinase in cultured gliomas. *Neurosurgery*, 17, **537-542**.

Gregoriou M, Trayer I P, Cornish-Bowden A. (**1981**). Isotope-exchange evidence for an ordered mechanism for rat-liver glucokinase, a monomeric cooperative enzyme. *Biochemistry-us*, 20, **499-506**.

Griffin L, Gelb B, Wheeler D, Davison D, Adams V, McCabe E. (**1991**). Mammalian hexokinase 1:

evolutionary conservation and structure to function analysis. *Genomics,* 11, **1014-1024**.

Grossbard L, Schimke R T. (**1966**). Multiple Hexokinases of Rat Tissues PURIFICATION AND COMPARISON OF SOLUBLE FORMS. *J. Biol. Chem.,* 241, **3546-3560**.

Hall N, Karras M, Raine J D, Carlton J M, Kooij T W, Berriman M, *et al.* (**2005**). A comprehensive survey of the Plasmodium life cycle by genomic, transcriptomic, and proteomic analyses. *Science,* 307, **82-86**.

Hammond S M. (**2005**). Dicing and slicing: the core machinery of the RNA interference pathway. *Febs. Lett.,* 579, **5822-5829**.

Hay S I, Guerra C A, Tatem A J, Noor A M, Snow R W. (**2004**). The global distribution and population at risk of malaria: past, present, and future. *Lancet Infect Dis,* 4, **327-336**.

Heikkinen S, Pietilä M, Halmekytö M, Suppola S, Pirinen E, Deeb S S, *et al.* (**1999**). Hexokinase II-deficient Mice prenatal death of homoyzgotes without disturbances in glucose tolerance in the heteroyzgotes. *J. Biol. Chem.,* 274, **22517-22523**.

Hengartner H, Zuber H. (**1973**). Isolation and characterization of a thermophilic glucokinase from Bacillus stearothermophilus. *Febs. Lett.,* 37, **212-216**.

Holroyde M J, Allen M, Storer A, Warsy A, Chesher J, Trayer I, *et al.* (**1976**). The purification in high yield and characterization of rat hepatic glucokinase. *Biochem. J.,* 153, **363**.

Hviid L. (**2007**). Development of vaccines against Plasmodium falciparum malaria: taking lessons from naturally acquired protective immunity. *Microbes Infect.,* 9, **772-776**.

Jang J C, Leon P, Zhou L, Sheen J. (**1997**). Hexokinase as a sugar sensor in higher plants. *Plant Cell,* 9, **5-19**.

Jensen M D, Conley M, Helstowski L D. (**1983**). Culture of Plasmodium falciparum: the role of pH, glucose, and lactate. *J Parasitol,* 69, **1060-1067**.

Joet T, Morin C, Fischbarg J, Louw A I, Eckstein-Ludwig U, Woodrow C, *et al.* (**2003**). Why is the Plasmodium falciparum hexose transporter a promising new drug target? *Expert Opin Ther Targets,* 7, **593-602**.

Johnson J H, Zimniak A, Racker E. (**1982**). Inhibition of hexokinase and protein kinase activities of tumor cells by a chloromethyl ketone derivative of lactic acid. *Biochemistry-us,* 21, **2984-2989**.

Jortzik E, Mailu M B, Preuss J, Fischer M, Bode L, Rahlfs S, *et al.* (**2011**). Glucose-6-phosphate dehydrogenase-6-phosphogluconolactonase: a unique bifunctional enzyme from Plasmodium falciparum. *Biochem. J.,* 436, **641-650**.

Kaji A, Trayser K A, Colowick S P. (**1961**). MULTIPLE FORMS OF YEAST HEXOKINASE. *Ann. Ny. Acad. Sci.,* 94, **798-811**.

Kanzok S M, Schirmer R H, Turbachova I, Iozef R, Becker K. (**2000**). The thioredoxin system of the malaria parasite Plasmodium falciparum. Glutathione reduction revisited. *J. Biol. Chem.,* 275, **40180-40186**.

Kaselonis G, McCabe E, Gray S. (**1999**). Expression of Hexokinase 1 and Hexokinase 2 in Mammary Tissue of Nonlactating and Lactating Rats: Evaluation by RT–PCR. *Mol. Genet. Metab.,* 68, **371-374**.

Katzen H M, Schimke R T. (**1965**). Multiple forms of hexokinase in the rat: tissue distribution, age dependency, and properties. *Proc. Natl. Acad. Sci.,* 54, **1218**.

Katzen H M, Soderman D D, Nitowsky H M. (**1965**). Kinetic and electrophoretic evidence for multiple forms of glucose-ATP phosphotransferase activity from human cell cultures and rat liver.

*Biochem. Biophys. Res. Commun.,* 19, **377-382**.

Ke H, Morrisey J M, Ganesan S M, Painter H J, Mather M W, Vaidya A B. (**2011**). Variation among Plasmodium falciparum strains in their reliance on mitochondrial electron transport chain function. *Eukaryotic cell,* 10, **1053-1061**.

Kehr S, Jortzik E, Delahunty C, Yates III J R, Rahlfs S, Becker K. (**2011**). Protein S-glutathionylation in malaria parasites. *Antioxid Redox Sign,* 15, **2855-2865**.

Kelley D E, He J, Menshikova E V, Ritov V B. (**2002**). Dysfunction of mitochondria in human skeletal muscle in type 2 diabetes. *Diabetes,* 51, **2944-2950**.

Kim W, Yoon J H, Jeong J M, Cheon G J, Lee T S, Yang J I, *et al.* (**2007**). Apoptosis-inducing antitumor efficacy of hexokinase II inhibitor in hepatocellular carcinoma. *Mol Cancer Ther,* 6, **2554-2562**.

Kirk K. (**2001**). Membrane transport in the malaria-infected erythrocyte. *Physiol. Rev.,* 81, **495-537**.

Kirk K, Horner H A, Kirk J. (**1996**). Glucose uptake in Plasmodium falciparum-infected erythrocytes is an equilibrative not an active process. *Mol. Biochem. Parasitol.,* 82, **195-205**.

Kropp E S, Wilson J E. (**1970**). Hexokinase binding sites on mitochondrial membranes. *Biochem. Biophys. Res. Commun.,* 38, **74-79**.

Lambros C, Vanderberg J P. (**1979**). Synchronization of Plasmodium falciparum erythrocytic stages in culture. *J Parasitol,* 65, **418-420**.

Lind C, Gerdes R, Schuppe-Koistinen I, Cotgreave I A. (**1998**). Studies on the mechanism of oxidative modification of human glyceraldehyde-3-phosphate dehydrogenase by glutathione: catalysis by glutaredoxin. *Biochem. Biophys. Res. Commun.,* 247, **481-486**.

Lindén M, Gellerfors P, Nelson B. (**1982**). Pore protein and the hexokinase-binding protein from the outer membrane of rat liver mitochondria are identical. *Febs. Lett.,* 141, **189**.

Liu H, Naismith J H. (**2008**). An efficient one-step site-directed deletion, insertion, single and multiple-site plasmid mutagenesis protocol. *BMC Biotechnol,* 8, **91**.

Liu S, Ammirati M J, Song X, Knafels J D, Zhang J, Greasley S E, *et al.* (**2012**). Insights into mechanism of glucokinase activation: observation of multiple distinct protein conformations. *J. Biol. Chem.,* 287, **13598-13610**.

Liu X, Kim C S, Kurbanov F T, Honzatko R B, Fromm H J. (**1999**). Dual mechanisms for glucose 6-phosphate inhibition of human brain hexokinase. *J. Biol. Chem.,* 274, **31155-31159**.

Magnani M, Bianchi M, Casabianca A, Stocchi V, Daniele A, Altruda F, *et al.* (**1992**). A recombinant human'mini'-hexokinase is catalytically active and regulated by hexose 6-phosphates. *Biochem. J.,* 285, **193**.

Majewski N, Nogueira V, Bhaskar P, Coy P E, Skeen J E, Gottlob K, *et al.* (**2004**). Hexokinase-mitochondria interaction mediated by Akt is required to inhibit apoptosis in the presence or absence of Bax and Bak. *Mol. Cell,* 16, **819-830**.

Martínez-Ruiz A, Lamas S. (**2007**). Signalling by NO-induced protein S-nitrosylation and S-glutathionylation: convergences and divergences. *Cardiovasc. Res.,* 75, **220-228**.

Marti M, Good R T, Rug M, Knuepfer E, Cowman A F. (**2004**). Targeting malaria virulence and remodeling proteins to the host erythrocyte. *Science,* 306, **1930-1933**.

Mathupala S P, Heese C, Pedersen P L. (**1997**). Glucose Catabolism in Cancer Cells the type II hexokinase promoter contains funcitionally active response element for the tumor suppressor p53. *J. Biol. Chem.,* 272, **22776-22780**.

Mathupala S P, Ko Y H, and, Pedersen P L. (**2006**). Hexokinase II: cancer's double-edged sword acting

as both facilitator and gatekeeper of malignancy when bound to mitochondria. *Oncogene,* 25, **4777-4786**.

Mathupala S P, Ko Y H, Pedersen P L. (**2009**). Hexokinase-2 bound to mitochondria: cancer's stygian link to the "Warburg Effect" and a pivotal target for effective therapy. Paper presented at the Seminars in cancer biology.

Mathupala S P, Rempel A, Pedersen P L. (**2001**). Glucose Catabolism in Cancer Cells identification and characterization of a marked activation response of the type II hexokinase gene to hypoxic conditions. *J. Biol. Chem.,* 276, **43407-43412**.

McRee D E. (**1993**). *Practical Protein Crystallography*. San Diego: Academic Press.

McRobert L, McConkey G A. (**2002**). RNA interference (RNAi) inhibits growth of Plasmodium falciparum. *Mol. Biochem. Parasitol.*, 119, **273-278**.

Mechai F, Loulergue P, Bouchaud O. (**2012**). [Immunization against malaria]. *Rev Prat,* 62, **605-610**.

Miccoli L, Oudard S, Sureau F, Poirson F, Dutrillaux B, Poupon M. (**1996**). Intracellular pH governs the subcellular distribution of hexokinase in a glioma cell line. *Biochem. J.,* 313, **957**.

Michelet L, Zaffagnini M, Vanacker H, Le Maréchal P, Marchand C, Schroda M, *et al.* (**2008**). In vivo targets of S-thiolation in Chlamydomonas reinhardtii. *J. Biol. Chem.,* 283, **21571-21578**.

Mochizuki Y. (**1981**). Evolutionary aspects of lower deuterostomian hexokinases. *Comp. Biochem. Phys. B,* 70, **745-751**.

Mochizuki Y, Hori S H. (**1980**). Immunological relationships of starfish hexokinases: phylogenetic implication. *Comp. Biochem. Phys. B,* 65, **119-125**.

Mulichak A M, Wilson J E, Padmanabhan K, Garavito R M. (**1998**). The structure of mammalian hexokinase-1. *Nat. Struct. Biol.,* 5, **555-560**.

Murray C J, Rosenfeld L C, Lim S S, Andrews K G, Foreman K J, Haring D, *et al.* (**2012**). Global malaria mortality between 1980 and 2010: a systematic analysis. *Lancet,* 379, **413-431**.

Ning J, Purich D L, Fromm H J. (**1969**). Studies on the kinetic mechanism and allosteric nature of bovine brain hexokinase. *J. Biol. Chem.,* 244, **3840-3846**.

Nkrumah L J, Muhle R A, Moura P A, Ghosh P, Hatfull G F, Jacobs W R, *et al.* (**2006**). Efficient site-specific integration in Plasmodium falciparum chromosomes mediated by mycobacteriophage Bxb1 integrase. *Nat. methods,* 3, **615-621**.

Nussenzweig V, Good M F, Hill A V. (**2011**). Mixed results for a malaria vaccine. *Nat. Med.,* 17, **1560-1561**.

O'Neill P M, Posner G H. (**2004**). A medicinal chemistry perspective on artemisinin and related endoperoxides. *J. Med. Chem.,* 47, **2945-2964**.

Olafsson P, Certa U. (**1994**). Expression and cellular localisation of hexokinase during the bloodstage development of Plasmodium falciparum. *Mol. Biochem. Parasitol.,* 63, **171-174**.

Olafsson P, Matile H, Certa U. (**1992**). Molecular analysis of Plasmodium falciparum hexokinase. *Mol. Biochem. Parasitol.,* 56, **89-101**.

Olszewski, Linás M. (**2011**). Central carbon metabolism of Plasmodium parasites. *Mol. Biochem. Parasitol.,* 175, **95-103**.

Pastorino J G, Hoek J B. (**2008**). Regulation of hexokinase binding to VDAC. *J. Bioenerg. Biomembr.,* 40, **171-182**.

Pastorino J G, Shulga N, Hoek J B. (**2002**). Mitochondrial binding of hexokinase II inhibits Bax-induced cytochrome c release and apoptosis. *J. Biol. Chem.,* 277, **7610-7618**.

Patterson L J, Robert-Guroff M. (**2008**). Replicating adenovirus vector prime/protein boost strategies

for HIV vaccine development. *Expert Opin Biol Ther,* 8, **1347-1363**.

Pedersen P. (**1978**). Tumor mitochondria and the bioenergetics of cancer cells. *Prog Exp Tumor Res,* 22, **190**.

Pedersen P L. (**2007**). Warburg, me and Hexokinase 2: Multiple discoveries of key molecular events underlying one of cancers' most common phenotypes, the "Warburg Effect", ie, elevated glycolysis in the presence of oxygen. *J. Bioenerg. Biomembr.,* 39, **211-222**.

Pedersen P L, Mathupala S, Rempel A, Geschwind J, Ko Y H. (**2002**). Mitochondrial bound type II hexokinase: a key player in the growth and survival of many cancers and an ideal prospect for therapeutic intervention. *BBA-Bioenergetics,* 1555, **14-20**.

Polakis P G, Wilson J E. (**1985**). An intact hydrophobic N-terminal sequence is critical for binding of rat brain hexokinase to mitochondria. *Arch. Biochem. Biophys.,* 236, **328-337**.

Postic C, Shiota M, Magnuson M A. (**2001**). Cell-specific roles of glucokinase in glucose homeostasis. *Recent. Prog. Horm. Res,* 56, **195-218**.

Preller A, Wilson J E. (**1992**). Localization of the type III isozyme of hexokinase at the nuclear periphery. *Arch. Biochem. Biophys.,* 294, **482-492**.

Purich D L, Fromm H J. (**1971**). The kinetics and regulation of rat brain hexokinase. *J. Biol. Chem.,* 246, **3456-3463**.

Qanungo S, Starke D W, Pai H V, Mieyal J J, Nieminen A-L. (**2007**). Glutathione supplementation potentiates hypoxic apoptosis by S-glutathionylation of p65-NFκB. *J. Biol. Chem.,* 282, **18427-18436**.

Rahlfs S, Fischer M, Becker K. (**2001**). Plasmodium falciparum possesses a classical glutaredoxin and a second, glutaredoxin-like protein with a PICOT homology domain. *J. Biol. Chem.,* 276, **37133-37140**.

Raj D K, Mu J, Jiang H, Kabat J, Singh S, Sullivan M, *et al.* (**2009**). Disruption of a *Plasmodium falciparum* multidrug resistance-associated protein (PfMRP) alters its fitness and transport of antimalarial drugs and glutathione. *J. Biol. Chem.,* 284, **7687-7696**.

Rathjen T, Nicol C, McConkey G, Dalmay T. (**2006**). Analysis of short RNAs in the malaria parasite and its red blood cell host. *Febs. Lett.,* 580, **5185-5188**.

Redkar V D, Kenkare U W. (**1972**). Bovine Brain Mitochondrial Hexokinase SOLUBILIZATION, PURIFICATION, AND ROLE OF SULFHYDRYL RESIDUES. *J. Biol. Chem.,* 247, **7576-7584**.

Reed M B, Saliba K J, Caruana S R, Kirk K, Cowman A F. (**2000**). Pgh1 modulates sensitivity and resistance to multiple antimalarials in *Plasmodium falciparum. Nature,* 403, **906-909**.

Rempel A, Bannasch P, Mayer D. (**1994**). Differences in expression and intracellular distribution of hexokinase isoenzymes in rat liver cells of different transformation stages. *BBA-Gene Struct Expr,* 1219, **660-668**.

Rhodes G. (**1993**). *Crystallography Made Crystal Clear.* San Diego: Academic Press.

Roberts R J. (**1976**). Restriction endonucleases. *CRC Crit Rev Biochem,* 4, **123-164**.

Rogers P, Fisher R, Harris H. (**1975**). An electrophoretic study of the distribution and properties of human hexokinases. *Biochem. Genet.,* 13, **857-866**.

Rosano C, Sabini E, Rizzi M, Deriu D, Murshudov G, Bianchi M, *et al.* (**1999**). Binding of non-catalytic ATP to human hexokinase I highlights the structural components for enzyme–membrane association control. *Structure,* 7, **1427-1437**.

Roth E. (**1987**). Malarial parasite hexokinase and hexokinase-dependent glutathione reduction in the

Plasmodium falciparum-infected human erythrocyte. *J. Biol. Chem.*, 262, **15678-15682**.

Roth E, Jr. (**1990**). *Plasmodium falciparum* carbohydrate metabolism: a connection between host cell and parasite. *Blood Cells*, 16, **453-460**.

Sa J M, Twu O, Hayton K, Reyes S, Fay M P, Ringwald P, *et al.* (**2009**). Geographic patterns of *Plasmodium falciparum* drug resistance distinguished by differential responses to amodiaquine and chloroquine. *Proc Natl Acad Sci U S A*, 106, **18883-18889**.

Saito T, Maeda T, Nakazawa M, Takeuchi T, Nozaki T, Asai T. (**2002**). Characterisation of hexokinase in Toxoplasma gondii tachyzoites. *Int. J. Parasitol.*, 32, **961-967**.

Sambrook J, Russell D W. (**2001**). *Molecular Cloning: A Laboratory Manual*. New York: Cold Spring Harbor Laboratory Press.

Sanchez C P, Dave A, Stein W D, Lanzer M. (**2010**). Transporters as mediators of drug resistance in Plasmodium falciparum. *Int. J. Parasitol.*, 40, **1109-1118**.

Schwab D A, Wilson J E. (**1989**). Complete amino acid sequence of rat brain hexokinase, deduced from the cloned cDNA, and proposed structure of a mammalian hexokinase. *Proc Natl Acad Sci*, 86, **2563-2567**.

Scopes R K, Testolin V, Stoter A, Griffiths-Smith K, Algar E M. (**1985**). Simultaneous purification and characterization of glucokinase, fructokinase and glucose-6-phosphate dehydrogenase from Zymomonas mobilis. *Biochem. J.*, 228, **627-634**.

Sebastian S, Horton J D, Wilson J E. (**2000**). Anabolic function of the type II isozyme of hexokinase in hepatic lipid synthesis. *Biochem. Biophys. Res. Commun.*, 270, **886-891**.

Sebastian S, Wilson J E, Mulichak A, Garavito R M. (**1999**). Allosteric regulation of type I hexokinase: A site-directed mutational study indicating location of the functional glucose 6-phosphate binding site in the N-terminal half of the enzyme. *Arch. Biochem. Biophys.*, 362, **203-210**.

Sharlow E R, Lyda T A, Dodson H C, Mustata G, Morris M T, Leimgruber S S, *et al.* (**2010**). A target-based high throughput screen yields Trypanosoma brucei hexokinase small molecule inhibitors with antiparasitic activity. *PLoS Negl Trop Dis*, 4, **e659**.

Shelton M D, Chock P B, Mieyal J J. (**2005**). Glutaredoxin: role in reversible protein s-glutathionylation and regulation of redox signal transduction and protein translocation. *Antioxid Redox Sign*, 7, **348-366**.

Shenton D, Grant C M. (**2003**). Protein S-thiolation targets glycolysis and protein synthesis in response to oxidative stress in the yeast Saccharomyces cerevisiae. *Biochem. J.*, 374, **513**.

Sherman I W. (**1998**). *Malaria*: Wiley Online Library.

Shimomura O, Johnson F H, Saiga Y. (**1962**). Extraction, purification and properties of aequorin, a bioluminescent protein from the luminous hydromedusan, Aequorea. *J Cell Comp Physiol*, 59, **223-239**.

Shoham M, Steitz T A. (**1980**). Crystallographic studies and model building of ATP at the active site of hexokinase. *J. Mol. Biol.*, 140, **1-14**.

Sidhu A B, Valderramos S G, Fidock D A. (**2005**). pfmdr1 mutations contribute to quinine resistance and enhance mefloquine and artemisinin sensitivity in *Plasmodium falciparum*. *Mol. Microbiol.*, 57, **913-926**.

Singh B, Kim Sung L, Matusop A, Radhakrishnan A, Shamsul S S, Cox-Singh J, *et al.* (**2004**). A large focus of naturally acquired *Plasmodium knowlesi* infections in human beings. *Lancet*, 363, **1017-1024**.

Smith T. (**2000**). Mammalian hexokinases and their abnormal expression in cancer. *Brit. J. Biomed. Sci.*,

57, **170**.

Sturm N, Jortzik E, Mailu B M, Koncarevic S, Deponte M, Forchhammer K, *et al.* (**2009**). Identification of proteins targeted by the thioredoxin superfamily in Plasmodium falciparum. *PLoS Pathog,* 5, **e1000383**.

Sui D, Wilson J E. (**1997**). Structural determinants for the intracellular localization of the isozymes of mammalian hexokinase: intracellular localization of fusion constructs incorporating structural elements from the hexokinase isozymes and the green fluorescent protein. *Arch. Biochem. Biophys.*, 345, **111-125**.

Tarun A S, Vaughan A M, Kappe S H I. (**2009**). Redefining the role of de novo fatty acid synthesis in Plasmodium parasites. *Trends Parasitol.*, 25, **545-550**.

Thailayil J, Magnusson K, Godfray H C, Crisanti A, Catteruccia F. (**2011**). Spermless males elicit large-scale female responses to mating in the malaria mosquito Anopheles gambiae. *Proc Natl Acad Sci U S A,* 108, **13677-13681**.

Tielens A, Van den Heuvel J, Van Mazijk H, Wilson J E, Shoemaker C B. (**1994**). The 50-kDa glucose 6-phosphate-sensitive hexokinase of Schistosoma mansoni. *J. Biol. Chem.,* 269, **24736-24741**.

Tonkin C J, van Dooren G G, Spurck T P, Struck N S, Good R T, Handman E, *et al.* (**2004**). Localization of organellar proteins in *Plasmodium falciparum* using a novel set of transfection vectors and a new immunofluorescence fixation method. *Mol. Biochem. Parasitol.,* 137, **13-21**.

Towbin H, Staehelin T, Gordon J. (**1979**). Electrophoretic transfer of proteins from polyacrylamide gels to nitrocellulose sheets: procedure and some applications. *Proc Natl Acad Sci U S A,* 76, **4350-4354**.

Trager W, Jensen J B. (**1976**). Human malaria parasites in continuous culture. *Science,* 193, **673-675**.

Trape J F, Pison G, Spiegel A, Enel C, Rogier C. (**2002**). Combating malaria in Africa. *Trends Parasitol.*, 18, **224-230**.

Trape J F. (**2001**). The public health impact of chloroquine resistance in Africa. *Am. J. Trop. Med. Hyg.*, 64, **12-17**.

Tsien R Y. (**1998**). The green fluorescent protein. *Annu. Rev. Biochem.,* 67, **509-544**.

Ureta T, Medina C, Preller A. (**1987**). The evolution of hexokinases. *Arch Bio Med Exp,* 20, **343-357**.

van Dooren G G, Stimmler L M, McFadden G I. (**2006**). Metabolic maps and functions of the Plasmodium mitochondrion. *Fems Microbiol. Rev.,* 30, **596-630**.

Vander Heiden M G, Cantley L C, Thompson C B. (**2009**). Understanding the Warburg effect: the metabolic requirements of cell proliferation. *Sci Signal,* 324, **1029**.

Viñuela E, Salas M, Sols A. (**1963**). Glucokinase and Hexokinase in Liver in Relation to Glycogen Synthesis. *J. Biol. Chem.,* 238, **PC1175-PC1177**.

Victoria Porter E, Chassy B M, Holmlund C E. (**1982**). Purification and kinetic characterization of a specific glucokinase from Streptococcus mutans OMZ70 cells. *BBA-Protein Struct M,* 709, **178-186**.

Walker D G. (**1963**). ON THE PRESENCE OF TWO SOLUBLE GLUCOSE-PHOSPHORYLATING ENZYMES IN ADULT LIVER AND THE DEVELOPMENT OF ONE OF THESE AFTER BIRTH. *Biochim Biophys Acta,* 77, **209-226**.

Wang J, Boja E S, Tan W, Tekle E, Fales H M, English S, *et al.* (**2001**). Reversible glutathionylation regulates actin polymerization in A431 cells. *J. Biol. Chem.,* 276, **47763-47766**.

Warburg O. (**1956**). On the origin of cancer cells. *Science,* 123, **309-314**.

Warburg O H, Dickens F. (**1930**). *The Metabolism of tumours: investigations from the Kaiser Wilhelm Institute for biology, Berlin-Dahlem*: Constable & Company Limited.

Wellems T E, Plowe C V. (**2001**). Chloroquine-resistant malaria. *J. Infect. Dis.*, 184, **770-776**.

White N, Marsh K, Turner R, Miller K, Berry C, Williamson D, *et al.* (**1987**). Hypoglycaemia in African children with severe malaria. *The Lancet*, 329, **708-711**.

White N J. (**1996**). The treatment of malaria. *N Engl J Med*, 335, **800-806**.

White T K, Wilson J E. (**1989**). Isolation and characterization of the discrete N-and C-terminal halves of rat brain hexokinase: retention of full catalytic activity in the isolated C-terminal half. *Arch. Biochem. Biophys.*, 274, **375-393**.

WHO. (**1999**). Making a difference. The World Health Report 1999. *Health Millions*, 25, **3-5**.

WHO. (**2010**). Global Report on Antimalarial Drug Efficacy and Drug Resistance 2000-2010. Geneva, Switzerland.

WHO. (**2011**). World Malaria Report 2011 (pp. 259). Geneva, Switzerland: WHO Press.

WHO. (**2012**). World Malaria Report 2012 (pp. 105). Geneva, Switzerland: WHO Press.

Willcox M L, Bodeker G. (**2004**). Traditional herbal medicines for malaria. *Bmj*, 329, **1156-1159**.

Wilson J. (**1995**). Hexokinases *Reviews of Physiology, Biochemistry and Pharmacology, Volume 126* (pp. 65-198): Springer.

Wilson J E. (**2003**). Isozymes of mammalian hexokinase: structure, subcellular localization and metabolic function. *J. Exp. Biol.*, 206, **2049-2057**.

Wolf A, Agnihotri S, Munoz D, Guha A. (**2011**). Developmental profile and regulation of the glycolytic enzyme hexokinase 2 in normal brain and glioblastoma multiforme. *Neurobiol. Dis.*, 44, **84-91**.

Woodrow C J, Burchmore R J, Krishna S. (**2000**). Hexose permeation pathways in Plasmodium falciparum-infected erythrocytes. *Proc Natl Acad Sci U S A*, 97, **9931-9936**.

Woodrow C J, Penny J I, Krishna S. (**1999**). Intraerythrocytic Plasmodium falciparum expresses a high affinity facilitative hexose transporter. *J. Biol. Chem.*, 274, **7272-7277**.

Wu R, Wyatt E, Chawla K, Tran M, Ghanefar M, Laakso M, *et al.* (**2012**). Hexokinase II knockdown results in exaggerated cardiac hypertrophy via increased ROS production. *EMBO Mol Med*, 4, **633-646**.

Ying J, Tong X, Pimentel D R, Weisbrod R M, Trucillo M P, Adachi T, *et al.* (**2007**). Cysteine-674 of the sarco/endoplasmic reticulum calcium ATPase is required for the inhibition of cell migration by nitric oxide. *Arterioscl. Throm. Vas.*, 27, **783-790**.

Zeng C, Aleshin A E, Hardie J B, Harrison R W, Fromm H J. (**1996**). ATP-binding site of human brain hexokinase as studied by molecular modeling and site-directed mutagenesis. *Biochemistry-us*, 35, **13157-13164**.

Zhou H, Hou Q, Chai Y, Hsu Y-T. (**2005**). Distinct domains of Bcl-X L are involved in Bax and Bad antagonism and in apoptosis inhibition. *Exp. Cell Res.*, 309, **316-328**.

Zocher K, Fritz-Wolf K, Kehr S, Fischer M, Rahlfs S, Becker K. (**2012**). Biochemical and structural characterization of Plasmodium falciparum glutamate dehydrogenase 2. *Mol. Biochem. Parasitol.*, 183, **52-62**.